# Electricity transition in a developing city

MSc Thesis

A case-study of Ulaanbaatar (Mongolia)

27 september 2019

Universiteit Utrecht

# Electricity transition in a developing city

A case-study of Ulaanbaatar (Mongolia)

R.O. Sanders
MSc Sustainable Development
Track: Energy & Materials
r.o.sanders@students.uu.nl
6232523

MSc Thesis (30 EC)
GEO4-2321

Supervisor: Wina Graus

Universiteit Utrecht

# Summary

It has become increasingly important to achieve renewable energy goals by implementing renewables on a local scale. This research aims to combine local electricity demand and supply-side analyses in order to be able to estimate costs and avoided emissions of implementing renewables. This study uses Ulaanbaatar as a case-study in order to answer the following research question: '*What is the renewable electricity potential in a developing city and what are the costs, emissions and barriers of achieving a high renewable electricity share before 2030?*'. In this study, two scenarios are constructed: a business-as-usual scenario and a maximum renewable scenario. The total electric capacity needed to meet demand is established in both scenarios, after which they are compared with respect to resulting costs and greenhouse gas emissions.

Ulaanbaatar's electricity demand is projected to grow alongside the city's electricity gross domestic product, from 1.4 TWh in 2010 to 6.4 TWh in 2030. According to the business-as-usual scenario, current capacity, which primarily contains old lignite-fired combined heat and power plants, is expanded with the new CHP Baganuur. Electricity generation costs 5.6 US$cts/kWh in 2030, which causes ~5 Mt $CO_2$-eq/yr (843 g $CO_2$-eq/kWh) of greenhouse gas emissions.

The southern part of the researched area is highly suitable for wind power (88-90%) and solar power (84-90%), whereas the area surrounding Ulaanbaatar is less suitable (56-78% for wind and 34-66% for solar power). The maximum rated power per grid cell is 11.4-41.3 GW (10.7 TWh/yr) for wind power and 134-1077 $GW_p$ (271-2264 TWh/yr) for solar PV, which exceeds projected demand. The maximum renewable electricity share in the alternative scenario (GREEN) is estimated to be 77% in Ulaanbaatar in 2030. New capacity consists of 1988 MW wind power, 482 MW utility PV and 1381 MW solar PV on the city's available roof area. The remaining electricity demand (23%) is supplied by CHP-4. Electricity generation costs 7.8 US$cts/kWh in 2030, which is 38% higher than the baseline, but reduces emissions by 54% between 2019 and 2030. By implementing this scenario, challenges arise, such as the low-capacity power grid, unfair competition with current CHPs, and involvement of the public.

This research is relevant to other developing cities surrounded by areas with moderate population density, vegetation and relief, as there may be enough renewable potential to meet demand in the future. They might also face similar challenges with respect to variable electricity output, grid capacity and subsidies.

**Key concepts**

Renewable electricity, scenario analysis, deployment potential, greenhouse gas emissions, barriers, energy policy

*Word count: 22024*

# Preface

During the writing of this thesis, the term for changing global atmospheric conditions changed from global change to global crisis. It is now, more than ever, relevant to investigate options in order to reduce greenhouse gas emissions on global, national and local scale. Modelling local energy and carbon systems is crucial for analyzing whether national or global climate targets are feasible. This document includes the case-study of Ulaanbaatar, capital of Mongolia: a developing city with growing population, gross domestic product and electricity demand. What if a city like this could transition from coal-based electricity generation to implementing maximum renewables? I asked myself this question when I visited this city in 2015 and took the picture on the front page.

This research is performed as a part of my thesis for the MSc Sustainable Development (track Energy and Materials). It aims to provide an answer to whether cities like Ulaanbaatar could replace their non-renewables within the foreseeable future if this would be more expensive compared to the current situation. I sincerely hope readers enjoy this research!

# Reading guide

This document consists of 11 chapters and an appendix. Chapter 1 includes the general introduction of this research and formulates the central research question and sub-questions. These sub-questions are answered in six corresponding chapters 2 to 7. In each chapter, the applied methodology is described first, after which the corresponding results are presented. In chapter 2, the electricity demand is projected between 2010 and 2030 in Ulaanbaatar. Chapter 3 described the business-as-usual scenario in detail and provides projections for current and future electric capacity, emissions and costs of electricity. Then, the potential of wind and solar power in the area surrounding Ulaanbaatar is established in chapter 4 by analysis of hourly wind speeds, solar irradiation and suitable area for renewables. In chapter 5, the resulting capacity factors for both technologies are assessed and the optimal electricity mix is established, which contains renewable capacity on one hand and capacity which provides non-variable baseload of electricity on the other hand. Chapter 6 continues by describing the GREEN scenario and projecting its costs and emissions compared to the baseline. Furthermore, chapter 7 gives a concise overview of important barriers which derive from implementing a high share of renewable electricity. Lastly, chapter 8 discusses the performed methodology and its results and concludes the study in chapter 9. Cited sources, acknowledgements and a yearly scenario comparison are found in the remaining chapters.

# Glossary

| | |
|---|---|
| ADB | Asian Development Bank |
| AFM | Asia Foundation's Masterplan |
| BAU | business-as-usual |
| C | carbon |
| °C | degrees Celcius |
| cap | capita |
| CES | Central Energy System |
| $CH_4$ | methane |
| CHP | combined heat and power plant |
| $CO_2$(-eq) | carbon dioxide (equivalent) |
| cos | cosine |
| g | gram |
| GDP | gross domestic product |
| GHG | greenhouse gas emissions |
| GIS | Geographical Information System |
| GMT | Greenwhich Mean Time |
| GoM | Government of Mongolia |
| IEA | International Energy Agency |
| IF | International Futures forecasting system |
| IMF | International Monetary Fund |
| IPCC | Intergovernmental Panel on Climate Change |
| J | Joule |
| JCM | Joint Crediting System |
| LCOE | Levelized cost of electricity |
| m | meter |
| MNT | Tugruk |
| MoE | Ministry of Energy |
| $N_2O$ | nitrous oxide |
| NSO | National Statistical Office |
| O&M | operations and maintenance |
| OECD | Organisation for Economic Co-operation and Development |
| OFAT | one-factor-at-a-time |
| PV | photovoltaics |
| SDG | Sustainable Development Goal |
| SDU | Statistical Department of Ulaanbaatar |
| sin | sine |
| t | ton |
| UB | Ulaanbaatar |
| UNFCCC | United Nations Framework Convention on Climate Change |
| US$ | United States Dollar |
| V1-V13 | grid cell 1-13 |
| W(h) | Watt(-hour) |
| yr | year |

# Table of contents


Summary 3

Preface 4

Reading guide 4

Glossary 5

1. Introduction 7

- 1.1 General introduction 7
- 1.2 Research objective 10
- 1.3 Research framework 10
- 1.4 Key concepts and definitions 11

2. Electricity demand 14

- 2.1 Methodology 14
- 2.2 Projections 15

3. Business-as-usual scenario 19

- 3.1 Methodology 19
- 3.2 Scenario projections 25

4. Deployment potential of solar and wind energy 30

- 4.1 Methodology 30
- 4.2 Renewable potential 42

5. Balancing supply and demand 47

- 5.1 Methodology 47
- 5.2 Electricity mix 48

6. GREEN scenario 50

- 6.1 Methodology 50
- 6.2 Scenario projections 51
- 6.3 Comparison BAU and GREEN 56

7. Barriers and policy 60

8. Discussion 63

- 8.1 Sensitivity analysis 63
- 8.2 Limitations 65
- 8.3 Implications 66

9. Conclusions 67

10. References 69

11. Acknowledgments 77

12. Appendix 78

Detailed scenario comparison 79

# 1. Introduction

## 1.1 General introduction

The concept of sustainable development is gaining more and more attention by citizens, companies and governments around the world. Its most common used definition – "*meeting the needs of the present without compromising the ability of future generations to meet their own needs*" (Brundtland, 1987) – is becoming more relevant as issues with food supply, urbanization and greenhouse gas (GHG) emissions are becoming evident (United Nations, 2017). The United Nations defined a set of seventeen Sustainable Development Goals (SDGs), one of which is *"to ensure access to affordable, reliable, sustainable and modern energy for all*" by 2030 (United Nations, 2017a). This is an important SDG, as transitioning to renewable energy could limit the problem of climate change (IPCC, 2014). In developed countries the share of people with access to electricity is high and the share of renewable energy is increasing in their fuel mix (IPCC, 2014a).

However, electricity reliability, affordability and sustainability all have much room for improvement in developing countries (United Nations, 2017). The current share of people without access to electricity in developing countries is 28% (fig. 1.1; WHO, 2009). Developing countries show no decarbonization but an increase in GHG emissions per capita (IPCC, 2014). For instance, the GHG emissions of Middle-East and Africa have increased from 0.54 to 1.83 Gt $CO_2$-eq/yr since 1970, which is mainly due to providing electricity and heating (IPCC, 2014a). Although these emissions are still much lower than industrialized countries, developing countries may still have a big influence on GHG emissions in the future if this trend continues (IPCC, 2014a). Additionally, as many developing countries and regions are presently lacking reliable energy systems, the potential of low-carbon systems increases, which may reduce future worldwide emissions (IPCC, 2014a).

Therefore, it is important to look at providing renewable energy for developing countries, the costs and how this could be implemented. Limiting the global temperature rise to 2 degrees, compared to pre-industrial levels, is an often-proposed scenario in order to avoid hazardous consequences of climate change (Crijns-Graus, 2016; IEA, 2017b). In these 2 degrees (2D) scenarios, renewables play an important part in developing countries' future energy supply (fig. 1.2). For instance, Africa, the Americas and non-OECD-Asia are expected to increase their renewable energy supply to more than half by 2050 according to the 2D scenarios (fig. 1.2; Crijns-Graus, 2016). However, it is unclear how to achieve these goals on a local scale.


Figure 1.1 Share of people with access to electricity. Source: World Bank (2014)

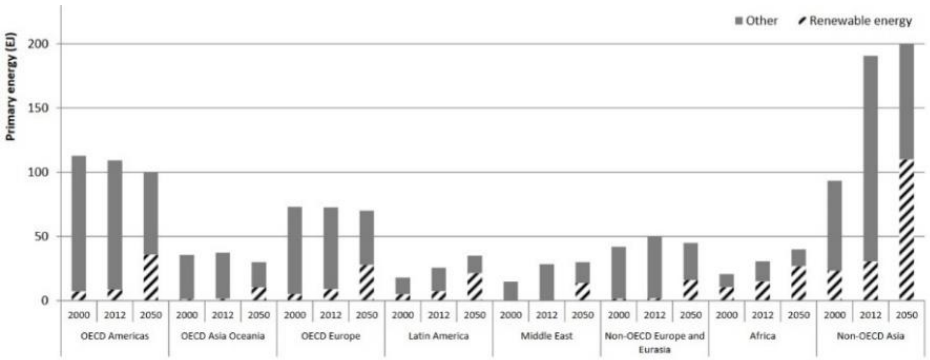


Figure 1.2 Projected primary energy supply in EJ according to 2 degrees scenario per region. Source: Crijns-Graus (2016)

For this reason, it is vital to look at how renewables can be implemented regionally in developing countries. In developing cities and other regions, increasing electricity demand is a major cause of rising GHG emissions and other air pollutants, like $SO_2$, $NO_x$ and PMs (particulate matter; IPCC, 2014). Therefore, it is important to review electricity supply and demand on a regional scale and how regions could implement - and benefit from - renewable electricity.

Many studies have been dedicated to electricity demand side and supply side analysis on a national scale (McPherson, 2014; Perwez, 2015; Nie, 2016;) and regional scale (Phdungsilp, 2010; Feng, 2013; Dhakal, 2010; Kale, 2014; Winkler, 2017) and many also include renewable capacity in order to meet demand (Kalashnikov, 2011; Amirnekooei, 2012). However, these studies do not include detailed renewable potential studies on a local scale or include local data on land-use, insulation or wind-speeds. Likewise, many renewable potential studies have been conducted (Hofierka, 2009; Mondal, 2010; Millward-Hopkins, 2013), but they do not include (projections of) electricity demand or look at weather variability or other constraints.

As mentioned above, scholars have investigated many components of (renewable) electricity on different scales, but a detailed, small-scale example is missing, together with local complications and costs. Research is currently missing, in which multiple components are combined into a detailed scenario and renewables meet future electricity demand. In order to fill this knowledge gap, Ulaanbaatar, the capital of Mongolia, is used as a case-study.

Mongolia is a developing country in central Asia with a population of around 3 million people and a land surface area of 1.5 million $km^2$ (World Bank, 2017). Half of Mongolia's population lives in Ulaanbaatar (1.4 million people; NSOM, 2016), the remaining people live (a nomadic life) in the extensive rural areas of the country. The government has attempted to supply electricity to all people, but still approximately 15% of the Mongolian population does not have access to electricity (World Bank, 2014). In Ulaanbaatar many households do not have access to basic services due to expansive growth of ger settlements around the city without proper spatial planning (Sumiya, 2016). In Ulaanbaatar it is estimated only 38% used electricity for cooking and 40% were affected by the impacts of energy poverty in 2016 (Sumiya, 2016).

Ulaanbaatar depends on the so-called Central Energy System (CES) for its heat and electricity supply (fig. 1.4; GoM, 2017), which generates 80% of the country's electricity (CEE Bankwatch Network, 2017). The Central System consists of three CHP plants with a total capacity of 1163 MW of which CHP 4 is the biggest (705 MW, fig. 1.3) and is located in Ulaanbaatar (CEE Bankwatch Network, 2017). Three of the CHP plants are located in Ulaanbaatar and an additional CHP plant (Baganuur) is planned to go in operation in the near future (GoM, 2017). The CHP plants have low efficiencies because of 1) the use of other bituminous coal and lignite for electricity generation (IEA, 2016; IPCC, 1996) and 2) high age of the plants and infrastructure, which struggles with high distribution and transmission losses (GoM, 2017).

At the same time, because of recent economic development, Mongolia experienced rapid growth in electricity and heat demand, which could not be supplied by national electricity sector and was imported from Russia and China (GoM, 2017). To meet this growing energy demand, new coal-fired CHP plants have been planned for the coming years (CEE Bankwatch Network, 2017). As a result, Ulaanbaatar's GHG emissions are growing yearly (World Bank, 2014) and will continue to grow if these CHP plants are realized.

Mongolia has enormous potential of renewable energy because of the large amount of available space and extremely low population density. Mongolia has an average yearly solar insolation of 1.4 MWh/m$^2$ and 270-300 sunny days per year (Sovacool, 2011; GoM, 2017) Mongolia's wind potential is large with a technical potential of 370 GW (Sovacool, 2011). Although Mongolia has deployed some wind-energy (Salkhit Wind project), it only constitutes 3% of the Central System's electricity supply (fig. 1.3; CEE Bankwatch Network, 2017). Therefore, this research focuses on using this renewable potential in order to fit Ulaanbaatar's current and future electricity gaps.

Previous research on Mongolia has been primarily focused on pollution (Huang, 2013; Guttikunda, 2008), rural electricity or management (Sovacool 2011, Kamata, 2010), renewable energy investments (Detert, 2013), electricity consumption (Enkthuul, 2013), nuclear energy (Liodakis, 2011), municipal waste energy recovery (Toshiki, 2015) and ideal tilt of solar PV (Adiyasuren, 2013).

This research's contribution to the sustainability problem is bifold: 1) it offers a thoroughly developed alternative to the electricity sector in Ulaanbaatar, which could help this city establish a sustainable electricity sector without being dependent on neighboring countries, 2) it combines a thorough potential study with a supply-demand analysis on a local scale.

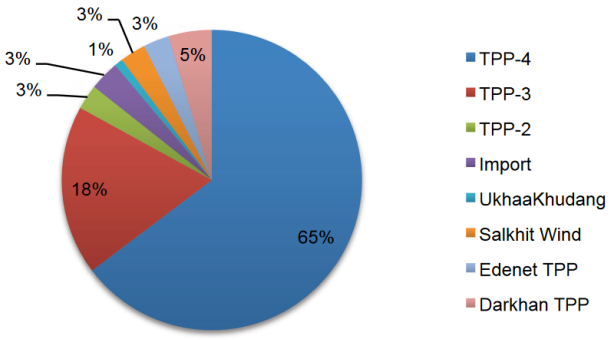


Figure 1.3 Power source mix of the Central System in percentages. Source: CEE Bankwatch Network, 2017

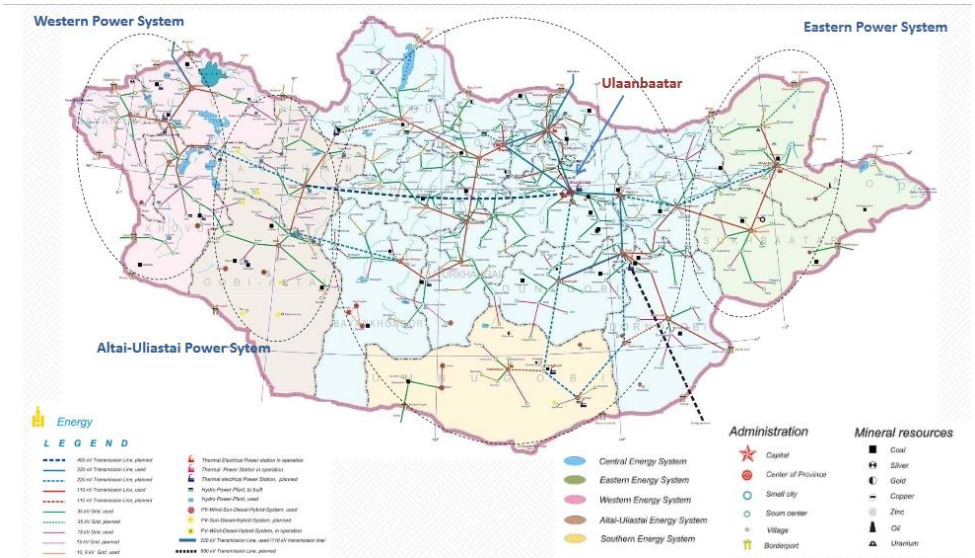


Figure 1.4 Map of Mongolian electricity system. Source: GoM (2017)

## 1.2 Research objective

This research aims at filling the aforementioned knowledge gap by determining the precise renewable electricity potential in a developing city, providing a cost-analysis of implementing these renewables, determining suitable non-variable sources for electricity mix completion and suggesting needed policies in order to meet future electricity demand. Ulaanbaatar, the capital of Mongolia, is used as a case-study to reach this aim. This research aims at answering the following research question and sub-questions:

**What is the renewable electricity potential in a developing city and what are the costs, emissions and barriers of achieving a high renewable electricity share before 2030?**

*Sub-question 1: What is the projected electricity demand of the Ulaanbaatar region until 2030?*

*Sub-question 2: What is the needed capacity and are the costs and emissions in the business-as-usual scenario in order to meet projected electricity demand until 2030?*

*Sub-question 3: What is the deployment potential of renewable electricity sources in the Ulaanbaatar region?*

*Sub-question 4: How can variable renewable electricity output be compensated in the Ulaanbaatar region?*

*Sub-question 5: What are the resulting costs and indirect emissions of implementing a high share of renewable electricity, compared to the business-as-usual scenario?*

*Sub-question 6: What barriers exist to implementing renewable electricity in the Ulaanbaatar region and which policy instruments are needed to overcome them?*

## 1.3 Research framework

This research has an intervention-oriented perspective. It investigates the current (problematic) situation according to some criterions and proposes an alternative solution (Verschuren, 2010). Also, it has a very practical approach, as the outcome of this research could be used by the Mongolian government and be used by other developing cities to implement renewable electricity.

In the first step of this research Ulaanbaatar's electricity demand until 2030 is determined. Secondly, business as usual power capacity until 2030 is investigated with corresponding costs and emissions. Then, the amount of new solar and wind capacity that is needed to replace or supplement current capacity until 2030 is calculated, based on solar irradiance, wind speeds and suitable area for renewable capacity in the Ulaanbaatar area. Two scenarios are compared with respect to greenhouse gas intensity and costs. Lastly, the challenges originating from the alternative scenario are described together with policies to counter these. A schematic representation of the research framework is shown in figure 1.5.

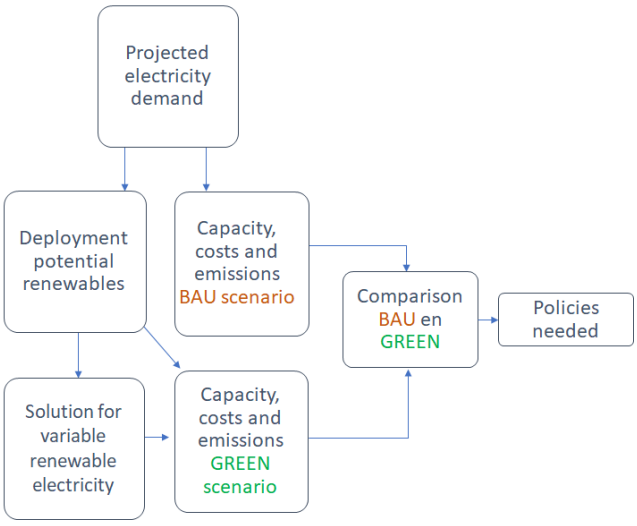


Figure 1.5. Research framework for this study. Source: own figure.

## 1.4 Key concepts and definitions

### 1.4.1 Renewable electricity

The term renewable energy is defined as a natural energy source for which the rate of consumption is slower than the rate of depletion (IEA, 2017a). The most common used renewable electricity sources are wind-energy, solar PV, geothermal energy, biomass and hydro-electricity (IEA, 2017a). According to Mongolia's energy department, there is a theoretical potential of around 6.2 GW of hydro-electricity (GoM, 2017). However, high potential-areas are more located to the west of Ulaanbaatar, in the provinces Hövsgöl and Arhangay (GoM, 2017). Recent research on geothermal potential in Mongolia is limited, but there is some research on applying geothermal space heating (Hahn, 2012; Sohn, 2015). Since there are limited examples of power generation from geothermal energy in Mongolia and there are no (planned) drilling sites (Dorj, 2015), this study neglects power use from geothermal energy.

Additionally, Mongolia's natural vegetation includes desert and (forest)-steppe (Farukh, 2009), which, combined with the harsh continental climate, does not support fast growing crops for biomass electricity generation. Wind speeds, on the other hand, vary across Mongolia but the wind-energy potential in rural areas is overall high (fig. 1.7; US Department of Energy, 2000).

As electricity from wind-energy and solar PV have the highest potential for this case-study (fig. 1.6-1.7), due to Mongolia's extremely low population density and extensive rural areas, this research focuses on these two sources of electricity. Currently, the combined wind- and solar energy only provide around 5% of Mongolia's electricity generation (GoM, 2017).

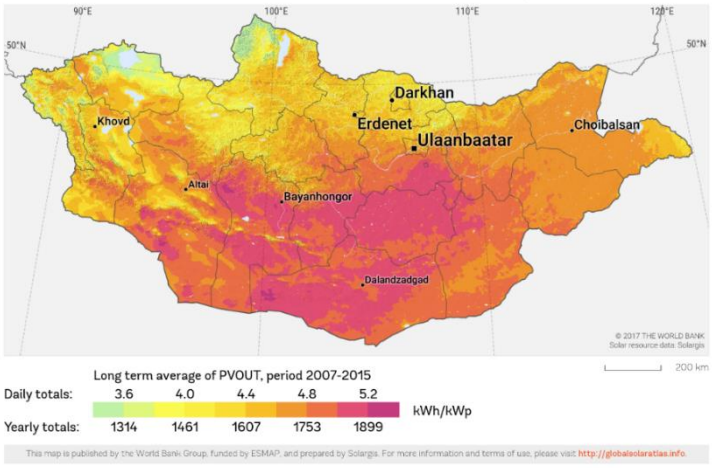


Figure 1.6 Solar energy potential in Mongolia. Source: SolarGIS (Worldbank, 2017).

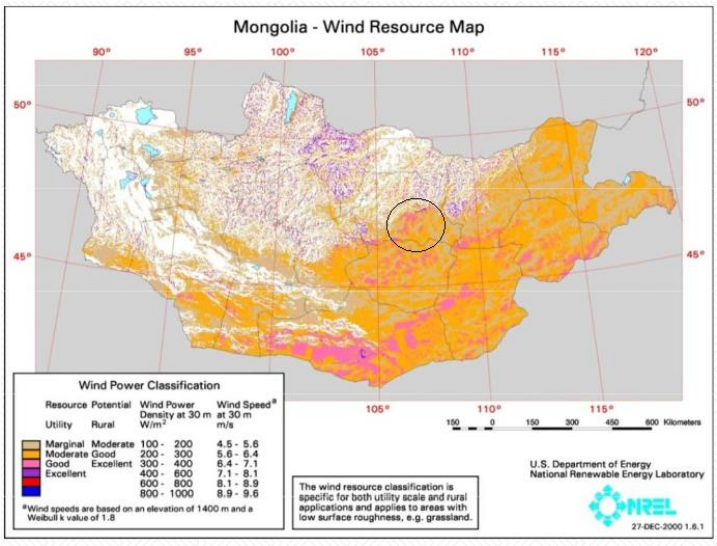


Figure 1.7 Wind-energy potential in Mongolia. Circle indicates area surrounding Ulaanbaatar. Source: WERAM, 2001

### 1.4.2 Scenario analysis

The construction of scenarios is an often-accepted tool for environmental policy making (IEA, 2017b). A scenario is defined as*: "a disciplined method for imaging possible futures in which organizational decisions may be played out"* (Schoemaker, 1995). For this research, two technical scenarios are constructed, which focus on the potential of different technologies rather than needed policies (Blok, 2009): a business-as-usual (*BAU*) scenario and a maximum renewable electricity scenario *(GREEN).* Both scenarios are internally consistent and transparent, as similar assumptions are made for each and they are described thoroughly in this study (Blok, 2009). Another important requirement for both scenarios is that projected electricity demand until 2030 is met with local capacity so that importing of electricity is kept at an imperative minimum.

The term business-as-usual (BAU) scenario is used in this study for a scenario that includes existing capacity, current plans for expansion and closure of existing capacity and for constructing new capacity by GoM. Information on these capacities and plans are retrieved from various sources (GoM, 2017; CEE Bankwatch, 2017; UNFCCC, 2018). BAU is used as a baseline, which is compared to an alternative scenario (Blok, 2009).

The alternative renewable scenario, from here on called GREEN, does not incorporate efforts for reducing electricity demand, despite the Trias Energetica (Antvorskov, 2008), since it regards a fully developing city and the probability that demand could be lowered in reality is considered small. Instead, this scenario includes the implementation of a maximum renewable electricity share until 2030. This scenario includes the retirement of the plants CHP-2 and CHP-3 and the construction of new wind power and solar PV capacity. Both scenarios are described more in detail in chapter 3 and 5.

### 1.4.3 Deployment potential

Potential analysis is a tool used for technical scenarios in order to explore possible future technological systems and to assess their feasibility and implications (Blok, 2009). This study focuses on the deployment potential of solar and wind energy, which includes the technical potential of these technologies and takes into account stock-turnover and market growth (Blok, 2009). The resulting (investment) costs do not limit the deployment potential. In this research, stock-turnover is taken into account in the form of replacing old CHPs with new capacity, but neglects changes in the global or regional renewable energy market as it is assumed to have low influence on local demand and supply.

### 1.4.4 Greenhouse gas emissions

Only greenhouse gas emissions (GHG) originating from electricity generation are considered in this scenario. They are both directly caused by electricity production, but indirect emissions are also included in this study. Emissions are divided into three scopes, of which scope 1 is the source of emissions that physically are caused inside the city (GHGP, 2013). In this research, emissions from electricity generation by CHPs and construction of new plants that are located inside the city are included in this scope. Scope 2 are emissions that occur *"from the use of electricity, steam, and/or heating/cooling supplied by grids which may or may not cross city boundaries"* (GHGP, 2013). Emissions from CHPs outside the city that provide energy for Ulaanbaatar or imported electricity from other countries are included in this scope. Scope 3 consists of GHGs emitted outside the city's boundaries but by activities that take place inside the city. In this research only GHGs deriving from the construction of solar panels, wind turbines and CHPs outside the city are included in this scope, whereas emissions due to mining and transportation are neglected.

### 1.4.5 Barriers

Many barriers arise when countries or cities replace non-renewable sources of electricity production with renewable capacity. This research focuses on two types of barriers: technical barriers and financial barriers. Technical barriers are linked to the previously described technical potential, but also include other technological

problems, such as distribution and transmission and seasonal or daily variable electricity output. Financial barriers include high investment costs, discount rates, risk and payback periods (Painuly, 2001).

### 1.4.6 Energy policy

This research focuses on top-down policies from cities or national governments in order to stimulate or discourage people or companies to use certain sources of energy. Three types of policy instruments are included (Sterner, 2013): economic (Helm, 2005), normative (Keohane, 1998) and communicative. Economic policies are market-based, such as the stimulation of renewables by feed-in tariffs (Sterner, 2013). Examples of normative or regulatory policies are prohibition of coal-firing plants or setting standards for emissions from factories. Communicative measures include information campaigns or tv-commercials to raise awareness.

In this research the analytical framework shown schematically in figure 1.8 will be used. This framework will be further explained in the methodology section.

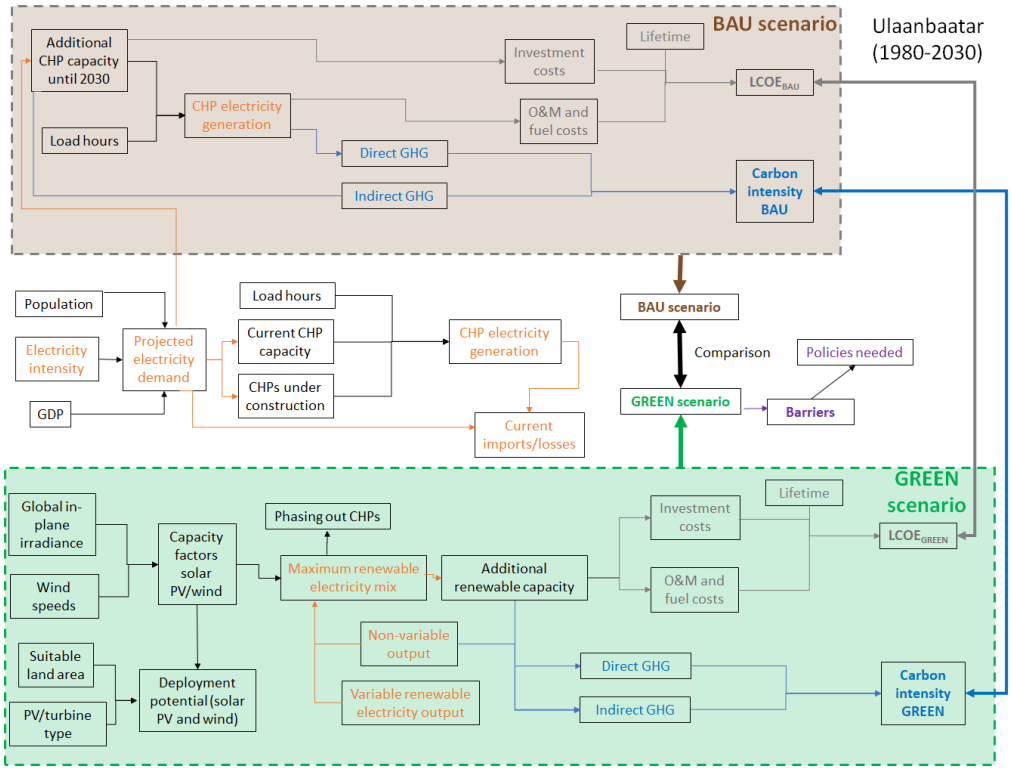


Figure 1.8. Technical framework used in this study. Source: own figure.

# 2. Electricity demand

In this chapter the electricity demand for Ulaanbaatar between 2010 and 2030 is projected and described in detail. It therefore aims to answer research sub-question 1: *What is the projected electricity demand of the Ulaanbaatar region until 2030?* First, the applied methods are described, after which GDP, population, electricity consumption and demand are projected.

## 2.1 Methodology

In order to estimate Ulaanbaatar's demand until 2030, the yearly needed electricity generation has to be determined. There are no existing scenarios for the development of electricity demand for Ulaanbaatar or Mongolia in general. Therefore, projecting demand in this research is performed by using the projected gross domestic product of Ulaanbaatar ($GDP_{city}$), the electricity intensity and percentages for electricity losses and import (eq. 2.1). Consequently, it is assumed that the main driver of electricity demand is the city's GDP.

(2.1) $$E_{generation} = \frac{E_{consumption}}{GDP_{national}} * GDP_{city} + E_{losses} - E_{import}$$

$E_{generation}$ = Electricity generation per year (GWh)
$E_{consumption}$ = Electricity consumption per year (GWh)
$GDP_{national}$ = GDP of Mongolia (million US$)
$GDP_{city}$ = GDP of Ulaanbaatar (million US$)
$E_{losses}$ = Transmission and distribution electricity losses per year (GWh)
$E_{import}$ = Imported electricity to Ulaanbaatar per year (GWh)

All costs or prices from Mongolian literature are converted from national currency (Tugruk, MNT) to United States Dollar (US$) using the exchange rate at time of writing (1 US$ = 2594 MNT). The electricity intensity ($\frac{E_{consumption}}{GDP_{national}}$) until 2016 is derived from the International Energy Agency (IEA, 2016a and b) and extrapolated until 2030, assuming a linear decline of -0.97% per year. Data of Ulaanbaatar's GDP originates from the Statistical Department of Ulaanbaatar (SDU), which provides an online statistics index. The SDU shows data on either city-, district- or khoroo-level (sub-district) (SDU, n.d.). The city's GDP is available until 2016, which is thereafter projected using scenarios from the Asian Development Bank (2013-2019; ADB, 2018), the International Monetary Fund (2020-2023; IMF, n.d.) and the International Futures forecasting system from the University of Denver (2024-2030; IF, n.d). These three scenarios were developed for Mongolia as a whole, but, due to limited data availability and the city's high contribution to national GDP, their rates are also used for projecting UB's needed electricity generation. Electricity losses and imports are derived from the Mongolian Statistical Information Service (MSIS, n.d.). Again, due to limited data availability for Ulaanbaatar, national percentages of losses and import are downsized to city-scale.

In order to determine an uncertainty margin, two other methods and sources are applied. First, electricity generation is calculated according to eq. 2.2 with consumption per capita from Asia Foundation's Masterplan (AFM) for Ulaanbaatar city (Asia Foundation, 2014), combined with projected population until 2030. The latter is constructed using Ulaanbaatar's population statistics from SDU until 2016, which are extrapolated using the UN World Population Prospect's growth rate for Mongolia (UN, 2017b). Equation 2.2 calculates electricity generation for the years 2010, 2020 and 2030, since AFM only estimates consumption per capita for these years, and the data is not interpolated in between.

(2.2) $E_{generation} = \frac{E_{consumption}}{POP_{national}} * POP_{city} + E_{losses} - E_{import}$

$E_{generation}$ = Electricity generation per year (GWh)
$E_{consumption}$ = Electricity consumption per year (GWh)
$POP_{national}$ = Population of Mongolia (million persons)
$POP_{city}$ = Population of Ulaanbaatar (million persons)
$E_{losses}$ = Transmission and distribution electricity losses per year (GWh)
$E_{import}$ = Imported electricity to Ulaanbaatar per year (GWh)

As SDU provides historic population numbers on district- and khoroo-level, a second alternative way of projecting the city's population until 2030 is to analyze growth rates in Ulaanbaatar's individual districts and by extrapolating and summing these rates.

A third way of estimating electricity generation until 2030, ADB provides three scenarios for electricity consumption in Mongolia (GoM, 2017; fig. 2.1). The linear growth rates of the organic growth- and bear market scenario are taken and applied to projecting electricity generation in Ulaanbaatar. These scenarios are included in the error margin.

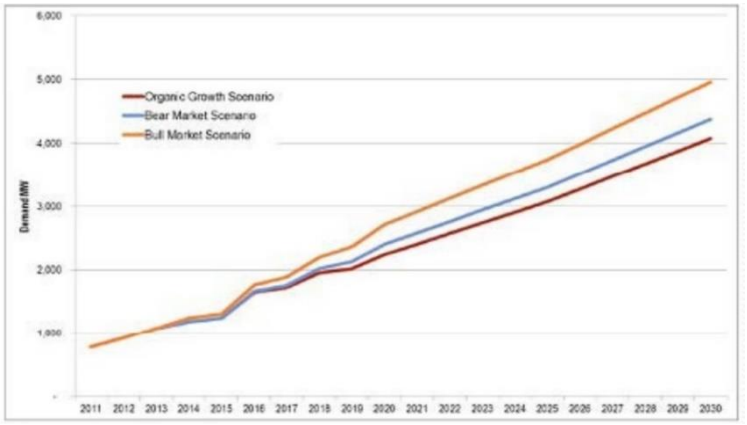


Figure 2.1. Three electricity demand scenarios (MW) by Asian Development Bank. Source: GoM, 2017.

## 2.2 Projections

Using the equations and data sources described in section 2.1, the GDP, population, electricity consumption and generation are projected for Ulaanbaatar between 2010 (base year) and 2030 (target year). An overview of essential results in this research step is shown in table 2.1 and is further elaborated in subsections 2.2.1-2.2.3.

Table 2.1. Overview of all variables for Ulaanbaatar calculated in chapter 2. Source: own table.

| | | Year | | | | |
|---|---|---|---|---|---|---|
| **Parameter** | **Unit** | 2010 | 2015 | 2020 | 2025 | 2030 |
| $GDP_{city}$ | billion US$ | 2.4 | 5.7 | 7.2 | 9.3 | 12.1 |
| $POP_{city}$ | million persons | 1.16 | 1.34 | 1.50 | 1.66 | 1.84 |
| $E_{consumption}$ | GWh | 1336 | 3000 | 3688 | 4495 | 5531 |
| $El_{osses}$ | GWh | 200 | 444 | 553 | 674 | 830 |
| $E_{import}$ | GWh | 95 | 270 | 0 | 0 | 0 |
| $E_{generation}$ | GWh | 1440 | 3175 | 4241 | 5169 | 6361 |

### 2.2.1 GDP and population

The gross domestic product (GDP) is projected to grow from 0.7 billion US$ in 2005 to 12.1 billion US$ in 2030 (fig. 2.2). Currently UB's GDP is already ~7.5 billion US$, because of enormous growth during the past fifteen years. In this study it is assumes it may double again until 2030.

Ulaanbaatar's population will also grow significantly until 2030 (fig. 2.2). According to this scenario, it may almost double between 2005 and 2030 (0.9 to 1.8 million inhabitants). If this increase in city population is compared to an extrapolation of current trends on khoroo-level, it results in a comparable population in 2030 (fig. 2.3). The Bayanzurkh and Songinokhairkhandistricts are experiencing and exceptionally rapid growth.

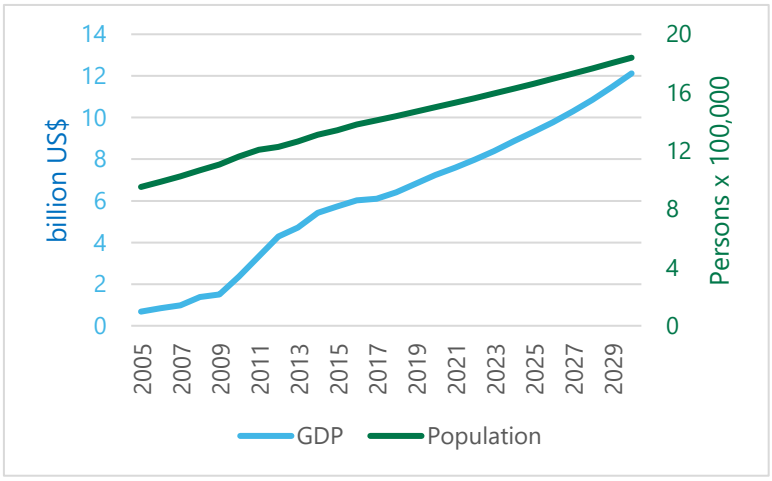


Figure 2.2 Projected population and gross domestic product scenario 2005-2030 for Ulaanbaatar. Source: own figure.

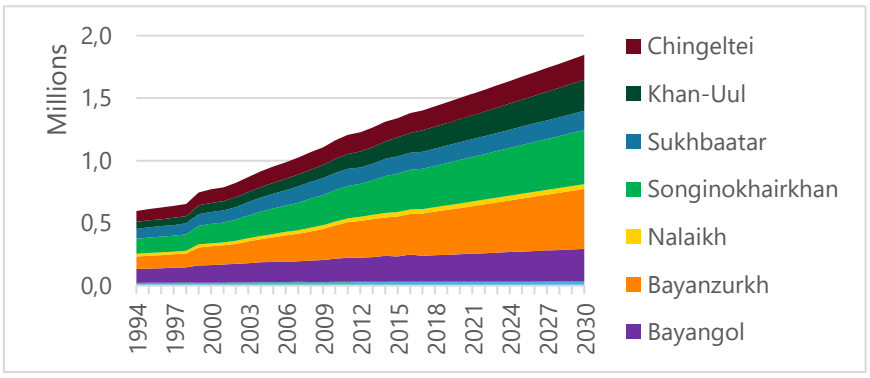


Figure 2.3 Extrapolated population per khoroo (district) for Ulaanbaatar 1994-2030 on district-level. Source: own figure.

### 2.2.2 Electricity consumption

Electricity consumption per GDP is decreasing significantly and is extrapolated to decline to 0.46 kWh/US$ in 2030 (fig. 2.4), as GDP is growing more rapidly than electricity consumption. Both consumption and consumption per capita endure a minor dip in 2016 after which they continue to grow until 2030 (fig. 2.5). Rapid GDP growth results in an increase of electricity consumption from 1.34 TWh in 2010 to 5.53 TWh in 2030.

The share of losses has increased from 10% in 1989 to 30% in 2000, after which it decreased again to 15% in 2016. This share is assumed to remain constant that year onwards, since current information does no give reason to

assume that existing transmission lines will be improved. Imports have varied yearly (5-20%), but is reduced to 0% from 2020, as total electricity supply exceeds demand at the time of writing (section 3.1.1).

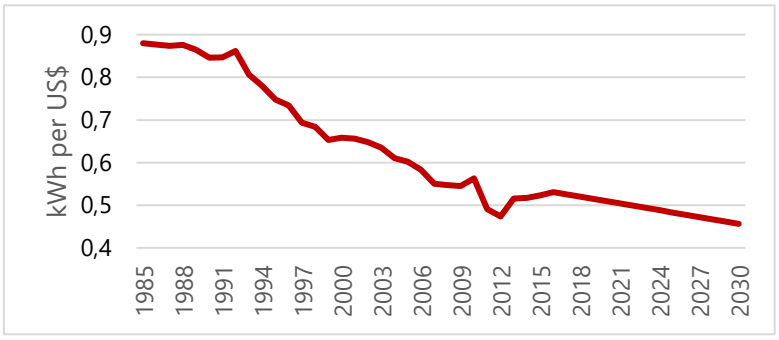


Figure 2.4 Projected electricity consumption per GDP in Ulaanbaatar 1985-2030. Source: own figure.

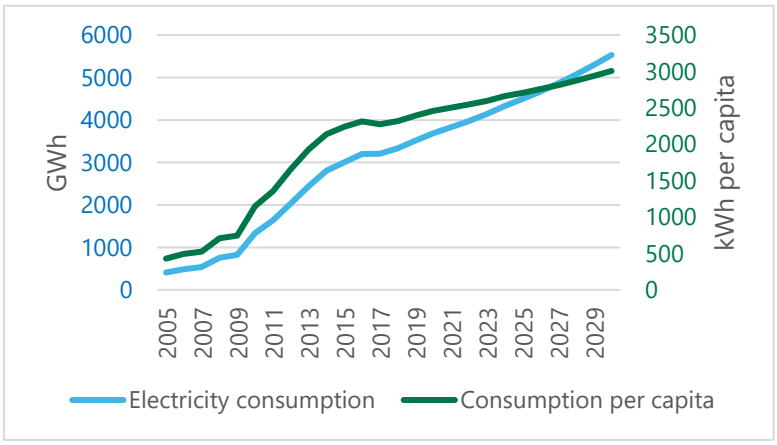


Figure 2.5 Projected electricity consumption and consumption per capita in Ulaanbaatar 2005-2030. Source: own figure.

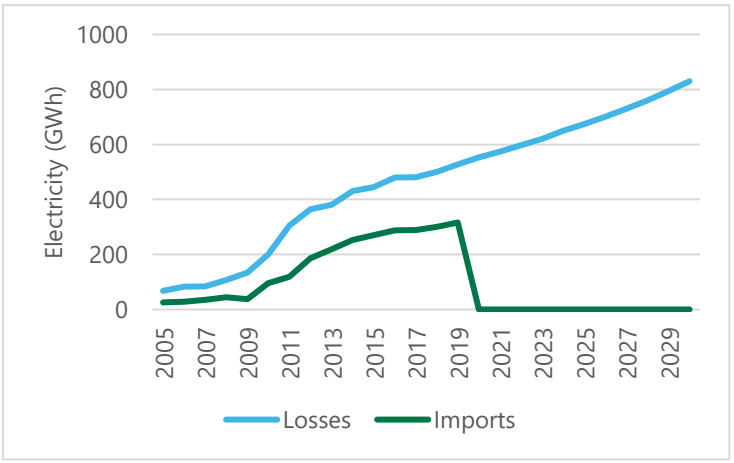


Figure 2.6. Projected electricity losses and imports in Ulaanbaatar 2005-2030. Source: own figure.

### 2.2.3 Electricity generation

In order to estimate the total needed electricity capacity in both BAU and GREEN, Ulaanbaatar's total electricity demand has to be established. The needed electricity generation between 2005 and 2030 is shown in figure 3.6, which includes an error margin containing two aforementioned ADB scenarios and AFM. Generation grows with a mean rate of 7.7% per year from 1.44 TWh in 2010 to 6.36 TWh in 2030. AFM estimates consumption per capita of 3339 kWh/cap in 2030, resulting in a generation of 7062 GWh, which is 11% higher than the GDP-driven scenario. The ADB scenarios also estimate higher needed generations of 7323 GWh (organic growth) and 7727 GWh (Bear market) in 2030. The GDP-driven electricity demand is adopted in BAU and GREEN, although, since ADB and AFM both calculate demand to be higher, this might be an underestimation. In order to quantify the impact of demand to costs and emissions in both scenarios, it is included in the sensitivity analysis (8.1).

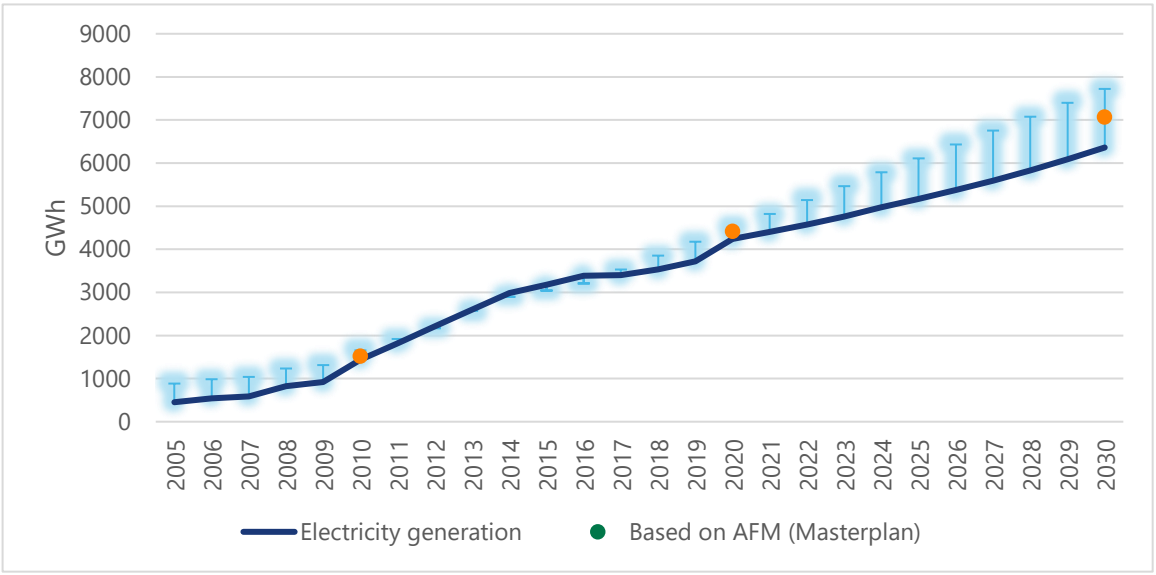


Figure 3.6. Projected needed electricity generation in Ulaanbaatar 2005-2030 with error margin and dots (section 2.2.1). Source: own figure.

# 3. Business-as-usual scenario

In order to answer sub-question 2 *'What is the needed capacity and are the costs and emissions in the business-as-usual scenario in order to meet projected electricity demand until 2030?'*, the methods and assumptions described section 3.1 are used. Subsequently, electricity consumption, generation, capacity, emissions and costs in Ulaanbaatar are projected for BAU between 2010 (base year) and 2030 (target year) in section 3.2.

## 3.1 Methodology

### 3.1.1 Electricity capacity

Three combined heat and power plants (CHP-2, CHP-3 and CHP-4) and Mongolia's only wind farm (Salkhit) all currently deliver electricity to Ulaanbaatar. Therefore, as there are no current plans for closing these plants, they are all included in the BAU scenario. Although Darkhan CHP and Erdenet CHP (fig. 3.1) deliver electricity to the CES, they are not included in BAU, because of their remote geographical locations from Ulaanbaatar. A fourth planned CHP (Baganuur) is to be built in 2021 and is also included in this scenario. Although in earlier reports CHP-5 is often mentioned as new project to cover Ulaanbaatar's growing electricity demand (AFM, 2014; CEE Bankwatch, 2017), the project is currently on hold and therefore is not added to Ulaanbaatar's future capacity.

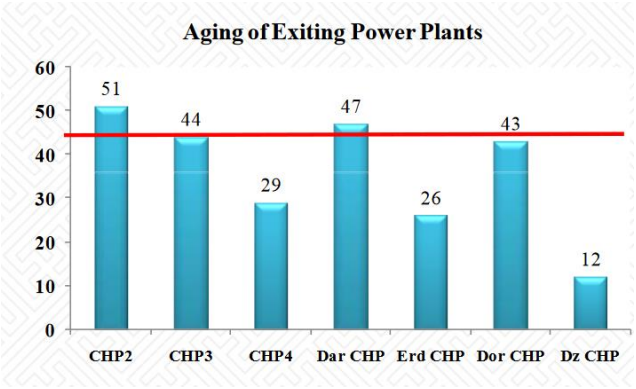


Figure 3.1. The age of existing CHPs in Mongolia. Source: GoM, 2017.

Electric capacity between 2010 and 2030 for CHP-2 to CHP-4 and Baganuur is taken from Mongolia's Third National Communication under the United Nations Framework Convention on Climate Change (UNFCCC, 2018). Salkhit wind farm consists of 31 1.6 MW turbines (The Wind power, n.d.). As there are no current plans for closing CHP-2 and CHP-3 despite their old age (fig. 3.1), they are included in UNFCCC (2018) and in the BAU scenario.

Table 3.1 Electricity capacity in Ulaanbaatar 2010-2030. Source: UNFCCC (2018).

| Name of facility | 2010 (base year) | 2030 | Comments and assumptions |
|---|---|---|---|
| CHP-2 | 21.5 | 0 | Assumed to be closed in 2026 |
| CHP-3 | 136 | 436 | Expansion of 50 MW in 2015, and 250 MW in 2021 |
| CHP-4 | 580 | 705 | Expansion of 125 MW in 2015 |
| Baganuur | 0 | 700 | Is built in 2021 to a 350 MW facility, expanded to 700 MW until 2030 |
| Salkhit | 0 | 49.6 | Fully operational from 2012, 31x1.6MW turbines |
| Total | 738 | 1891 | |

However, for BAU it is assumed CHP-2 closes in 2026, as an age of 60 years is then reached and the plant's operations cannot be economically feasible. The total capacity which supplies UB increases from 738 MW in 2010 to 1891 MW in 2030 (table 3.1).

Yearly electricity generation by CHP-3, CHP-4 and Baganuur is also derived from UNFCCC (2018). For CHP-2, the CHP-3's load factor is applied, as it is similar in fuel and combustion type and age (table 3.2). Baganuur has a relatively low load factor, but this is expected to increase beyond 2030 after the closure of CHP-3 and CHP-4 in order to become economically feasible. For Salkhit wind farm, a monitoring report is used, which shows that electricity supply with actual weather conditions of 90.1 GWh/yr is significantly smaller than the estimated yearly supply of 168.5 GWh/yr (UNFCCC, 2017). Ulaanbaatar's total electricity supply between 2010 and 2030 is shown in table 3.2. For transmission and distribution losses, the same percentages are used as in step 1 (section 2.1).

In the previous section, projected demand was determined between 2010 and 2030. According to expected output by current and future powerplants, total supply exceeds the city's demand by ~1 TWh in 2016 and by ~3 TWh in 2030. This oversupply of electricity is assumed to be distributed to other regions in the CES. In this study, the share of a facility to the CES is applied to UB's demand to determine its contribution to meeting the city's demand. For instance, CHP-4 is projected to supply 4.6 TWh to the CES in 2030, of which 3 TWh is allocated to UB and 1.6 elsewhere (table 3.2).

The maximum capacity of transmission lines for import to and export from the CES to Russia is currently 100-180 MW (CEE Bankwatch, 2017), whereas exact local capacity is unknown. There are plans to expand both the national and international electricity grid (Asian Super Grid), but they are in their initial stages (Batmunkh, 2018). Therefore, for both BAU and GREEN, the capacity of transmission lines is estimated to grow to 415 MW, which is a minimum in order to achieve significant renewable electricity supply given projected demand in Ulaanbaatar in 2030 (chapter 5). Because of the excess of supply, it is assumed that no net import of electricity has to occur from the time of writing (2019).

Table 3.2 Electricity supply before losses in Ulaanbaatar 2010-2030. Source: various.

| | Total electricity supply (GWh, before losses) | | Allocated electricity supply to Ulaanbaatar (GWh, before losses) | | |
|---|---|---|---|---|---|
| Name of facility | 2010 | 2030 | 2030 | Load hours | Comments and assumptions |
| CHP-2 | 136 | 0 | 0 | 6307 | Closes in 2026, same assumed load hours as CHP-3 |
| CHP-3 | 750 | 2750 | 1805 | 6307 | UNFCCC (2018) |
| CHP-4 | 3000 | 4600 | 3020 | 6383 | |
| Baganuur | 0 | 2250 | 1477 | 3214 | |
| Salkhit | 1 | 90 | 59 | 1810 | UNFCCC (2017) |
| Total | 3887 | 9690 | 6361 | | |

### 3.1.2 Greenhouse gas emissions

As mentioned in section 1.4.4, in order to calculate the total amount of greenhouse gas (GHG) emissions in UB, various types of (in)direct emissions are summed. Emission types that are included are summed in equation 3.1. Greenhouse gas intensity is calculated by dividing the total amount of emissions by the total electricity demand (eq. 3.2). The individual parts of these equations are further described below.

(3.1) $GHG_{BAU} = GHG_{direct} + GHG_{indirect} = CO_{2\ direct} + GHG_{other\ direct} + GHG_{construction} + CO_{2\ import}$

$GHG_{BAU}$ = Total yearly greenhouse gas emissions in BAU scenario (kt $CO_2$-eq)
$GHG_{direct}$ = Total yearly direct greenhouse gas emissions (kt $CO_2$-eq)
$GHG_{indirect}$ = Total yearly indirect greenhouse gas emissions (kt $CO_2$-eq)
$CO_{2\ direct}$ = Direct $CO_2$ emissions (kt $CO_2$)
$GHG_{other\ direct}$ = Direct other greenhouse gas emissions (kt $CO_2$-eq)
$GHG_{construction}$ = Greenhouse gas emissions from construction or expansion power plants, wind parks or solar parks (kt $CO_2$-eq)
$CO_{2\ import}$ = $CO_2$ emission from importing electricity to Ulaanbaatar (kt $CO_2$)

(3.2) $GHGI = \frac{GHG_{total}}{E_{generation}}$

GHGI = Greenhouse gas intensity (g $CO_2$-eq/kWh)
$GHG_{total}$ = Total yearly greenhouse gas emissions (kt $CO_2$-eq)
$E_{generation}$ = Electricity generation per year (GWh)

#### 3.1.2.1 Direct $CO_2$ emissions

For calculating direct $CO_2$ emissions, the emission factors of the CHP plants are multiplied by the plants' estimated electricity generation until 2030 (eq. 3.3).

(3.3) $CO_{2\ direct} = E_{generation} * \%_{plant} * \varepsilon_{plant}$

$CO_{2\ direct}$ = Direct $CO_2$ emissions (t $CO_2$)
$E_{generation}$ = Electricity generation per year (MWh)
$\%_{plant}$ = Percentage of plant's power production of total electricity supply (%)
$E_{plant}$ = Emission factor of individual CHP plant (t $CO_2$/MWh)

Specific $CO_2$ emissions for CHP-2, 3, 4 and Baganuur are taken from Joint Crediting Mechanism (JCM, n.d.) and UNFCCC (2018) (table 3.3). The plant emission factors range from 0.797 t$CO_2$/MWh for CHP-4 and 1.666 t$CO_2$/MWh for CHP-2. With these factors the individual plants' efficiencies are calculated, which range between 20% (CHP-2) and 41% (CHP-4/Baganuur). CHP-2's efficiency is extremely low due to lignite combustion and high age. For the BAU scenario, it is assumed the plant emission factors remain constant until 2030, as there is no reliable data to assume efficiency or fuel type will change or improve. As Baganuur is not operational yet, the plant's GHG emission factor is estimated from UNFCCC (2018) (0.889 t$CO_2$-eq /MWh).

Table 3.3 Emission factors of electric capacity in Ulaanbaatar. Source: various.

| | | Source | | Name of facility | Emission factor (t $CO_2$/MWh) | Electric efficiency | Source |
|---|---|---|---|---|---|---|---|
| Lignite emission factor (t $CO_2$/TJ) | 90.9 | JCM (n.d.) | | CHP-2 | 1.666 | 20% | JCM (n.d.) |
| Net calorific value for lignite coal (TJ/Gg) | 29.33 | JCM (n.d.) | | CHP-3 | 0.896 | 37% | JCM (n.d.) |
| | | | | CHP-4 | 0.797 | 41% | JCM (n.d.) |
| | | | | Baganuur | 0.889 | 41% | UNFCCC (2018) |

### 3.1.2.2 Other direct greenhouse gas emissions

For including other GHGs in the total direct emissions from UB's power plants, data from CCPIU (2017) is used. In 2014, 9.2 Tg $CO_2$ is emitted by CHP power generation by solid fuels. This type of generation also emits 2.3 Gg $CO_2$-eq $CH_4$ (0.03%) and 51.4 Gg $CO_2$-eq $N_2O$ (0.56%). Using these ratios, the amount of $CH_4$ and $N_2O$ emissions is calculated for UB's CHP plants.

### 3.1.2.3 Indirect emissions

The construction and expansion of current and new power plants is negligible in both scenarios compared to direct emissions from fuel combustion (Weisser, 2007; Pacca, 2002; Yu, 2014). However, the construction of wind turbines and solar panels do affect total emissions. Emissions from the construction of wind turbines (11 g $CO_2$-eq/kWh) and solar panels (46 g $CO_2$-eq/kWh) are included in both scenarios (IPCC, 2011). Both scenarios do not account for transportation or mining of coal.

The CES and Ulaanbaatar have imported electricity from Russia for some years now (MSIS, n.d.; figure 3.2). By combining Russia's electricity mix and average efficiency per fuel type from IEA statistics (IEA, 2016a) and the standard emission factors for other bituminous coal, lignite, natural gas and fuel oil (IPCC, 1996; fig. 3.3; table 3.4), the emissions from imported electricity are calculated (eq. 3.4). This results in the Russian emission factor of 525 g$CO_2$/kWh. As mentioned before, because of oversupply, import of electricity stops in 2020.

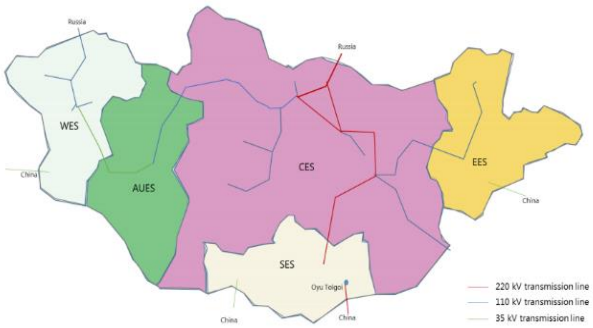


Figure 3.2. Mongolia's electricity grid and connections to neighboring countries. Source: JCM (n.d)

(3.4) $$CO_{2\ import} = \frac{E_{import}}{\eta_{Russia}} * \varepsilon_{Russian} * \frac{44}{12}$$

$CO_{2\ import}$ = Total indirect $CO_2$ from imported electricity
$E_{import}$ = Net imported electricity to Ulaanbaatar per year (TJ)
$\varepsilon_{Russian}$ = Russian Emission factor from electricity production (tC/TJ)

(3.5) $$\varepsilon_{Russian} = \varepsilon_{other\ bituminous} * \%_{other\ bituminous} + \varepsilon_{lignite} * \%_{lignite} + \varepsilon_{nat\ gas} * \%_{nat\ gas} + \varepsilon_{fuel\ oil} * \%_{fuel\ oil}$$

$\varepsilon_{Russian}$ = Russian emission factor from electricity production (tC/TJ)
$\varepsilon_{other\ bituminous}$ = Other bituminous coal emission factor production (tC/TJ)
$\varepsilon_{lignite}$ = Lignite emission factor production (tC/TJ)
$\varepsilon_{nat\ gas}$ = Natural gas emission factor production (tC/TJ)
$\varepsilon_{fuel\ oil}$ = Other bituminous coal emission factor production (tC/TJ)
$\%_{fuel}$ = Percentage of electricity production in Russia (%)

Table 3.4 Russian average efficiency of electricity generation and emission factors per fuel type. Source: various.

| | Other bituminous coal | Lignite | Natural gas | Fuel oil | Source |
|---|---|---|---|---|---|
| Share of electricity mix | 8% | 7% | 49% | 1% | IEA (2016a) |
| National electric efficiency in 2016 | 26% | 33% | 29% | 30% | |
| Emission factors (t C/TJ) | 26 | 28 | 15 | 21.1 | IPCC, 1996 |
| Emission factors (t $CO_2$/TJ) | 95 | 101 | 56 | 77.4 | |

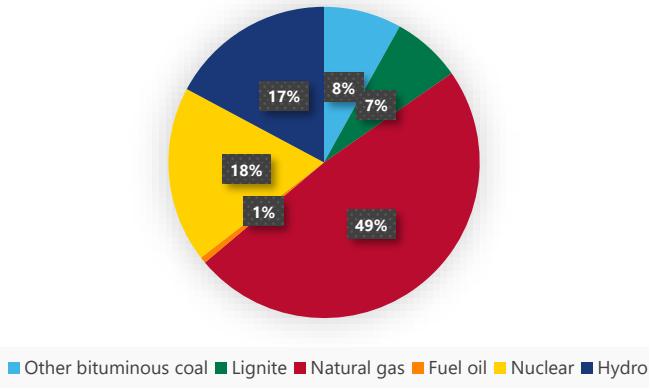


Figure 3.3. Russian electricity mix. Source: IEA (2016a).

### 3.1.3 Costs

In order to compare individual electricity suppliers, the investment (I), operations and maintenance (O&M) and fuel (F) costs per power source are determined and used to calculate the levelized cost of electricity for each facility and is shown in a cost curve (LCOE, eq. 3.6; fig. 3.4; Branker, 2011; HOMER, n.d.). For calculating levelized costs of electricity for the BAU scenario as a whole ($LCOE_{BAU}$), the weighted average of LCOEs per technology is calculated (eq. 3.7). One-time investment costs are annualized over the lifetime of the technology (table 3.5). A social discount rate from China is assumed (r=8%; Zhuang, 2007) for all production technologies, but changing this discount rate is included in the sensitivity analysis (section 8.1). Costs before 2010 or after 2030 and residual value of technologies are not taken into account when calculating $LCOE_{BAU}$, although the addition of initial investments of CHP-2, 3 and 4 to the scenarios is also included in the sensitivity analysis. The following investments are retrieved from literature and are used in the analysis:

- Construction of Salkhit wind farm in 2012: 122 million US$ (Mott Macdonald, n.d.).
- Expansion of CHP-4 in 2015: 45 million US$ (JICA, 2013)
- Expansion of CHP-3 in 2019: 77,000 US$[1] (Shillendans, 2015b)
- Construction of Baganuur in 2021: 3.5 billion US$ (CEE Bankwatch, 2017)

(3.6) $$LCOE = \frac{\alpha * I + M + F}{E_{generation}}$$

LCOE = Levelized cost of electricity for specific technology (US$/kWh)
α = Capital recovery factor (-)
I = Total investment costs for technology (US$)
M = Yearly operations and maintenance costs for technology (US$/yr)
F = Yearly fuel costs (US$/yr)
$E_{generation}$ = Electricity generation by technology per year (kWh/yr)

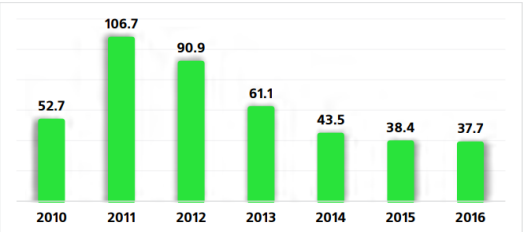


Figure 3.3. The average coal price in Mongolia (US$ per tonne, 2010-2016). Source: ERI, 2017

[1] This price seems too low for a 250MW expansion, but a more realistic price cannot be retrieved from literature.

(3.7) $$\mathrm{LCOE_{BAU}} = \frac{\sum \alpha_a * I_a + \sum M_a + \sum F_a}{\sum E_a}$$

$LCOE_{BAU}$ = Average levelized cost of electricity for business-as-usual scenario (US$/kWh)
α = Capital recovery factor for power source a (-)
$I_a$ = Total investment costs for power source a (US$)
$M_a$ = Yearly operations and maintenance costs for power source a (US$/yr)
$F_a$ = Yearly fuel costs for power source a (US$/yr)
$E_a$ = Electricity generation per year by power source a (kWh)

(3.8) $$\alpha = \frac{r(1+r)^t}{(1+r)^t - 1}$$

α = Capital recovery factor (-)
r = Discount rate (-)
t = Lifetime of technology (yr)

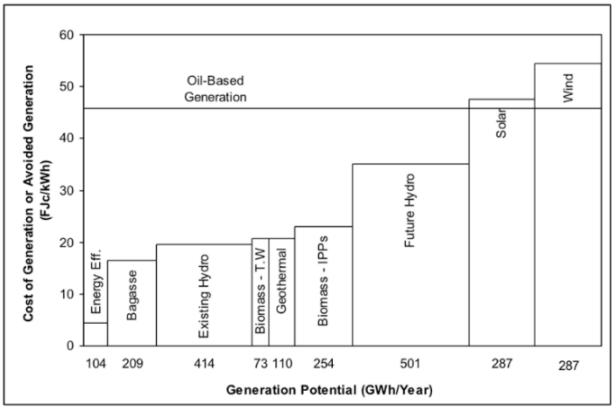


Figure 3.4. Example of cost curve with different LCOEs and generation potentials. Source: The conversation, 2012.

Most yearly O&M costs are derived from government website Shilendans (2015), as most power suppliers in UB are owned by the state. For CHP-2, 3, and 4 it contains annual accounts with expenses between 2015 and 2018. For earlier years, the average of these years is assumed. For future years, the 2018 value is assumed until 2026 for CHP-2 and 2030 for CHP-3 and 4. For estimating O&M costs for Baganuur from 2021, the amount of O&M dollars per MW from CHP-4 is calculated (26 US$/kW) and multiplied by Baganuur's capacity, which results in ~19 million US$ in 2030. For Salkhit's O&M costs, assumption from IEA's New Policies Scenario assumptions for China in 2020 (30 US$/kW) is assumed (table 5.1; IEA, 2016c).

Fuel costs are not included in the financial disclosures of Shilendans (2015). The average Mongolian coal price for the last seven years is 61.6 US$/ton (ERI, 2017, fig. 3.3) and it is assumed this contains mostly lignite. By using the Mongolian net calorific value for lignite (table 3.3) together with the CHP's individual efficiencies, the fuel price per plant is calculated, ranging from 18.5 US$/MWh and 38.5 US$/MWh (table 3.5).

As mentioned in section 3.1, UB's CHPs are very old. Because of this, the lifetimes of these powerplants are significantly higher than the average values for CHP plants, but for Baganuur a shorter lifetime is expected (table 3.5). These lifetimes are included in the sensitivity analysis (8.1). Lastly, for imported electricity from Russia a price of 5.47 rouble/kWh (Moscow price; TACC, 2018) and exchange rate of 0.015 rouble/US$ are used.

Table 3.5. Estimated lifetimes for various power suppliers in Ulaanbaatar 2010-2030

| Name of facility | Fuel price (US$/MWh) | Estimated lifetime (end of operation year) |
|---|---|---|
| CHP-2 | 38.5 | 60 (2026) |
| CHP-3 | 20.7 | 60 (2033) |
| CHP-4 | 18.4 | 45 (2033) |
| Baganuur | 18.5 | 40 (2051) |
| Salkhit | - | 20 (2030) |

## 3.2 Scenario projections

An overview of the most important projections in the business-as-usual scenario is shown in table 3.6. Individual parts of this table are further elaborated in the following sections, including projected electricity generation, greenhouse gas emissions and levelized costs of electricity. Note: this table includes $CO_2$ emissions, fuel costs and electricity generation based on Ulaanbaatar generation, while it shows load hours, O&M costs and LCOEs for the total facilities as a whole.

Table 3.6. Overview of yearly electricity generation and various types of GHG emissions and costs per electricity supplier in the BAU scenario for Ulaanbaatar 2010-2030. Source: own table.

| | | Year | | | | |
|---|---|---|---|---|---|---|
| **Parameter (unit)** | **Facility** | 2010 | 2015 | 2020 | 2025 | 2030 |
| $E_{generation}$ per facility to Ulaanbaatar (GWh) | CHP-2 | 50 | 87 | 92 | 75 | 0 |
| | CHP-3 | 278 | 478 | 1521 | 1524 | 1805 |
| | CHP-4 | 1112 | 2552 | 2568 | 2550 | 3020 |
| | Baganuur | 0 | 0 | 0 | 970 | 1477 |
| | Salkhit | 0 | 58 | 61 | 50 | 59 |
| | **Total** | **1440** | **3175** | **4241** | **5372** | **6361** |
| Load hours per facility (hours) | CHP-2 | 6307 | 6307 | 6307 | 6307 | 0 |
| | CHP-3 | 5515 | 4032 | 5161 | 6307 | 6307 |
| | CHP-4 | 5172 | 5674 | 5390 | 6525 | 6525 |
| | Baganuur | 0 | 0 | 0 | 2500 | 3214 |
| | Salkhit | 0 | 1825 | 1825 | 1825 | 1825 |
| | **Average** | 5665 | 4460 | 4671 | 4693 | 4468 |
| $CO_{2\ direct}$ based on Ulaanbaatar generation (kt) | CHP-2 | 84 | 144 | 153 | 125 | 0 |
| | CHP-3 | 249 | 429 | 1362 | 1366 | 1617 |
| | CHP-4 | 886 | 2034 | 2047 | 2032 | 2407 |
| | Baganuur | 0 | 0 | 0 | 862 | 1313 |
| | Salkhit | 0 | 0 | 0 | 0 | 0 |
| | **Total** | **1219** | **2607** | **3562** | **4385** | **5337** |
| $GHG_{other\ direct}$ based on Ulaanbaatar generation (kt $CO_2$-eq) | CHP-2 | 0.49 | 0.84 | 0.89 | 0.73 | 0.00 |
| | CHP-3 | 1.46 | 2.51 | 7.98 | 8.9 | 9.42 |
| | CHP-4 | 5.19 | 11.9 | 11.99 | 11.91 | 14.1 |
| | Baganuur | - | - | - | - | - |
| | Salkhit | 0 | 0 | 0 | 0 | 0 |
| | **Total** | **7.1** | **15.3** | **20.9** | **20.6** | **23.6** |
| $CO_{2\ import}$ (kt $CO_2$) | **Total** | **50** | **142** | **0** | **0** | **0** |
| Annual O&M costs per facility (million US$/yr) | CHP-2 | 9.9 | 9.9 | 11.3 | 11.3 | 0 |
| | CHP-3 | 11.8 | 9.3 | 14 | 14 | 14 |
| | CHP-4 | 17 | 17 | 18.5 | 18.5 | 18.5 |
| | Baganuur | 0 | 0 | 0 | 18.4 | 18.4 |
| | Salkhit | 0 | 1.5 | 1.5 | 1.5 | 1.5 |
| | **Total** | **38.7** | **37.7** | **45.3** | **63.7** | **52.4** |

| | | | | | | |
|---|---|---|---|---|---|---|
| Annual fuel costs based on Ulaanbaatar generation (million US$/yr) | CHP-2 | 2 | 3 | 4 | 3 | 0 |
| | CHP-3 | 6 | 10 | 31 | 32 | 37 |
| | CHP-4 | 20 | 47 | 47 | 47 | 56 |
| | Baganuur | 0 | 0 | 0 | 18 | 27 |
| | Salkhit | 0 | 0 | 0 | 0 | 0 |
| | **Total** | **28** | **60** | **82** | **99** | **120** |
| Import costs (million US$) | Total | 7.8 | 22.1 | 0 | 0 | 0 |
| LCOE based on total generation to CES (US$cts/kWh) | CHP-2 | 11 | 12 | 12 | 12 | 0 |
| | CHP-3 | 4 | 2.7 | 2.7 | 2.6 | 2.6 |
| | CHP-4 | 2.5 | 2.4 | 2.4 | 2.3 | 2.3 |
| | Baganuur | 0 | 0 | 0 | 19.7 | 15.7 |
| | Salkhit | 0 | 15.4 | 15.4 | 15.4 | 15.4 |

### 3.2.1 Electricity capacity and generation

The existing and additional future capacity described in section 3.1. is used to estimate the amount of electricity supply to Ulaanbaatar's electricity grid in the BAU scenario between 2010 and 2030. The expected electricity supply to Ulaanbaatar by each CHP and Salkhit in order to meet demand, is shown in figure 3.5. CHP-2 and Salkhit only generate 0-4% of demand, whereas CHP-4 is the biggest contributor to the city's power grid. Baganuur is operational from the year 2021 and adds ~1-1.5 TWh to UB's electricity mix. Despite the high ages of CHP-3 and CHP-4, they remain operational and even increase their supply between 2010 and 2030. Imports are included in this scenario, since Mongolia is currently still importing electricity, but due to expected overcapacity, net imports are brought back to zero from 2020 onwards.

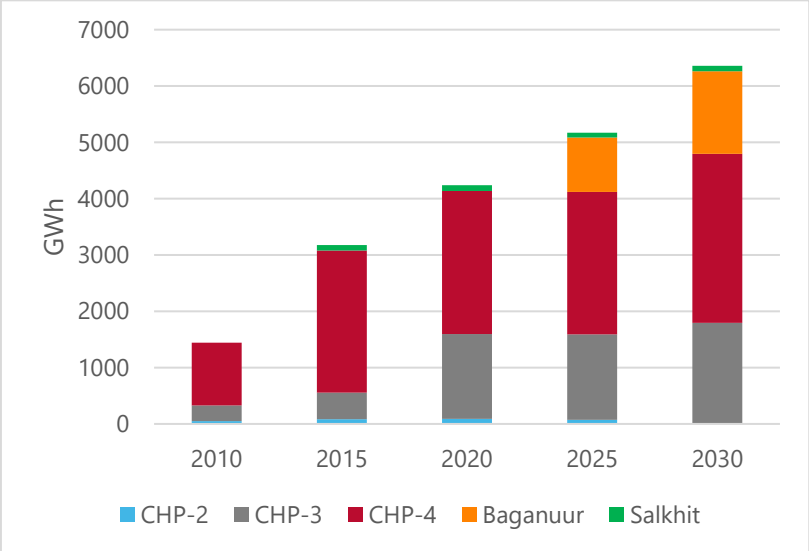


Figure 3.5. Projected needed electricity generation in Ulaanbaatar per facility in BAU 2010-2030

### 3.2.2 Greenhouse gas emissions

GHG emissions due to electricity generation in UB will increase in the BAU scenario alongside growing demand. According to this scenario, UB emitted a total of 1.28 Mt $CO_2$-eq in 2010 which will increase to 5.36 Mt $CO_2$-eq per year in 2030 (fig. 3.6). This results in cumulative greenhouse gas emissions of 73 Mt $CO_2$-eq between 2010-2030. A

small fraction of this originates from $N_2O$ and $CH_4$ emissions (7-24 kt $CO_2$-eq/yr) and constructing Salkhit wind turbines (1 kt $CO_2$-eq/yr). Imports from Russia, which mainly relies on natural gas, lignite and nuclear energy for its electricity generation, have caused indirect emissions between 50 kt $CO_2$ in 2010 and 167 kt $CO_2$ in 2019. In 2014, emissions originating from electricity generation in Ulaanbaatar contributed ~12% of total $CO_2$ emissions in Mongolia (20.8 Mt; Worldbank, n.d.).

The greenhouse gas intensity of Ulaanbaatar's electricity is expected to decline slightly from 0.89 in 2010 to 0.84 kg $CO_2$-eq/kWh in 2030 (fig. 3.8). Also, emissions per GDP decrease slightly between 2010 and 2030 (0.5-0.4 kg /US$; fig. 3.6). This contains ~26% of emissions per GDP for Mongolia in 2014 (Worldbank, n.d.). On the other hand, GHG emissions from electricity generation per person increases rapidly (1.1-2.9 t $CO_2$-eq/capita) according to the BAU scenario. In 2014, this constitutes about 29% of total emissions per capita for Mongolia (Worldbank, n.d.).

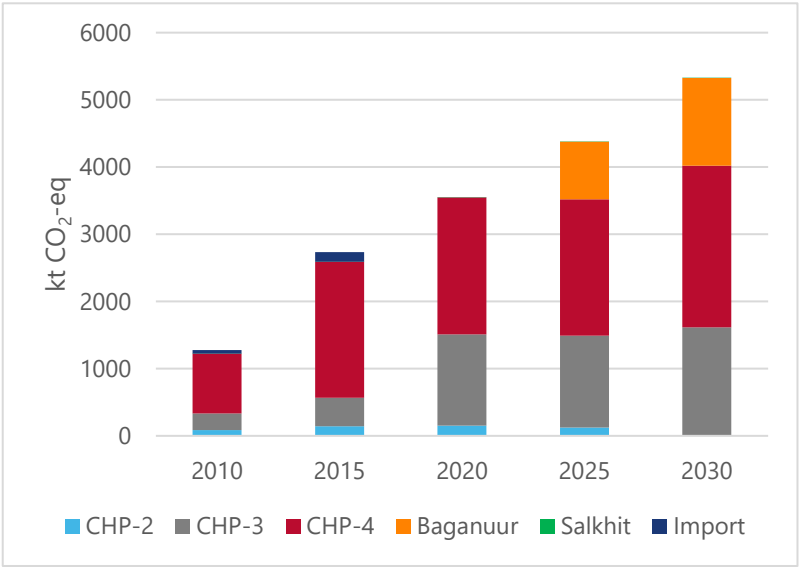


Figure 3.7. Total yearly GHG emissions for the BAU scenario per supplier 2010-2030, included direct $CO_2$, direct $N_2O$ and $CH_4$ and indirect construction and import emissions. Source: own figure.

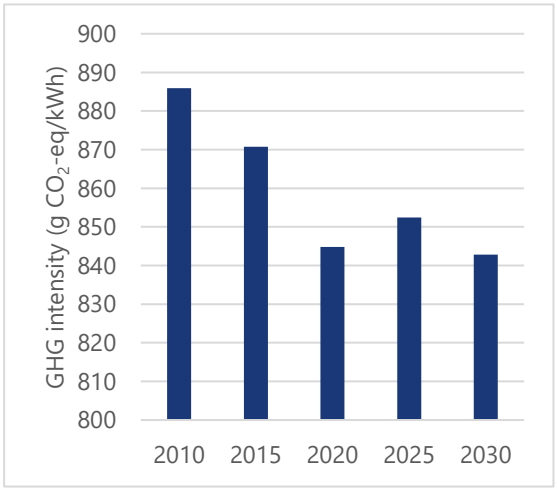


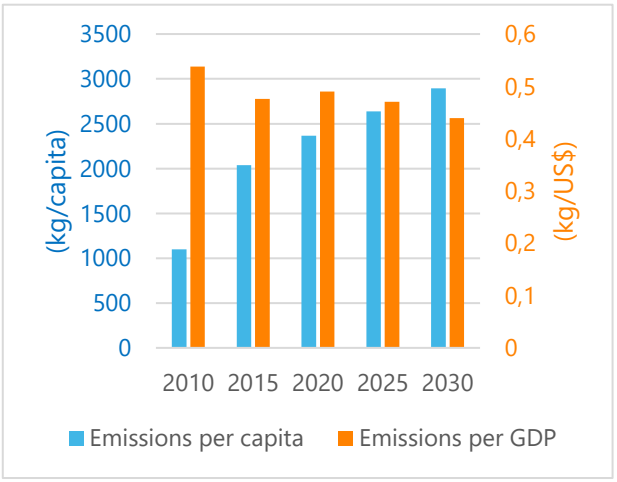


Figure 3.8. Carbon intensity (left) and total GHG emissions per $POP_{city}$ and per $GDP_{city}$. (right) for BAU scenario in Ulaanbaatar 2010-2030. Source: own figure.

### 3.2.3 Costs

Figure 3.9 shows an overview of total yearly O&M costs per facility as a whole and fuel costs per plant based on its supply to Ulaanbaatar. These costs made by CHP-2 remain rather stable, but the plant contains the highest share of total O&M costs until operation is stopped in 2026. CHP-3's costs increase until 2020 after which they remain constant until 2030. CHP-4's costs rise dramatically between 2010 and 2015 due to rapid increase of fuel use, after which they continue to grow more slowly towards 2030. In total, yearly costs for this CHP may almost double in this scenario (40-75 million US$/yr). Baganuur's costs are estimated to increase to 45 million US$, which also mainly contains fuel costs. The costs of import from Russia are between 8 million US$ in 2010 and 26 million US$ in 2019, which accommodates 14.8% of total yearly costs in 2019. Despite growing fuel costs, the resulting yearly costs (excluding annualized investments) decrease from 0.19 billion US$/yr in 2010 to 0.17 billion US$/yr in 2030 because of the closure of CHP-2 in 2026 and the discontinuance of net import from 2020. Cumulative costs (including investments such as the 2021 Baganuur investment visible in figure 3.10) increase to 6.5 billion US$.

By combining the annualized investment costs, total O&M costs and total fuel costs made by these facilities with the total electricity supply to the CES per plant, the LCOE for each power source is calculated (fig. 3.11), resulting in CHP-4 being the most cost-effective and Baganuur the most expensive technology. The reason for this is the absence of initial investments for CHP-4 and the high investments for Baganuur, together with a low projected load factor. CHP-2 is also particularly expensive because of low plant efficiency (20%) resulting in high fuel price (table 3.5). Although figure 3.11 shows LCOEs for the technologies in 2030, it includes CHP-2's LCOE during last year of operation (2026).

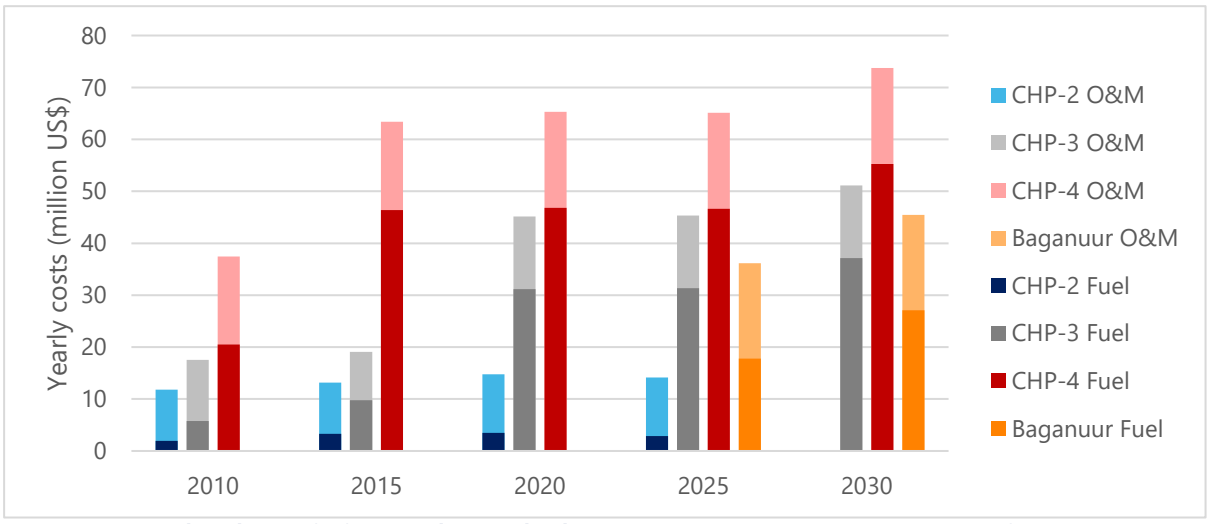


Figure 3.9. Projected yearly costs for four CHP plants in Ulaanbaatar in BAU scenario 2010-2030. Source: own figure.

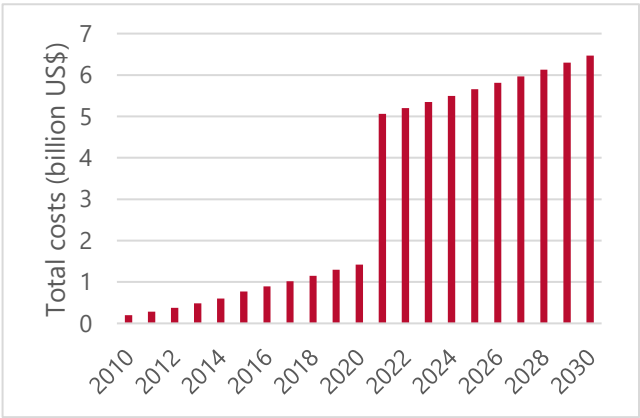


Figure 3.10. Total cumulative costs for electricity in the BAU scenario 2010-2030. Source: own figure.

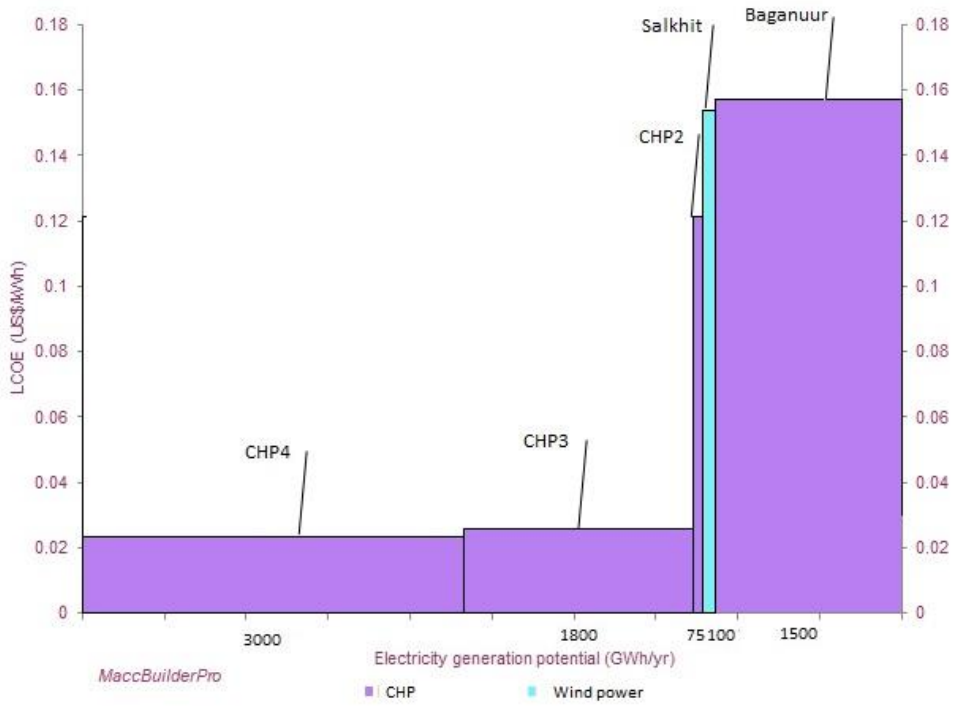


Figure 3.11. Cost curve showing levelized cost of electricity (US$/kWh) and average electricity generation (GWh/yr) for all BAU electricity suppliers. Source: own figure using MaccBuilderPro.

# 4. Deployment potential of solar and wind energy

This chapter describes the applied methods (4.1) and corresponding results (4.2) for answering sub-question 3: *What is the deployment potential of renewable electricity sources in the Ulaanbaatar region?* It includes the approach for acquiring potential of solar PV and wind energy by determining average wind speeds, solar irradiation and share of suitable land for renewables in the area surrounding Ulaanbaatar.

## 4.1 Methodology

The research area was established by estimating the highest wind and solar potential in the area surrounding Ulaanbaatar by using SolarGIS, World Bank's Global Wind Atlas (GWA, n.d.) and WERAM (2001). SolarGIS contains rough global data on horizontal irradiation, diffuse horizontal irradiation, optimal tilt and PV power potential (Worldbank, 2017), while the atlases contain global and national data on wind speeds. As a result, the research area is oriented towards the southeast from Ulaanbaatar (fig. 4.1). It contains parts of the aimags (provinces) Ulaanbaatar, Töv, Khentii, Govisumber, and Dundgovi.

Secondly, a more detailed analysis was conducted using data sets from the Goddard Earth Sciences Data and Information Services Centre by NASA (GMAO, 2008a&b). These datasets, also called MERRA, provide hourly reanalysis data on solar irradiation and wind speeds data with a resolution of 0.667 degree longitude x 0.5 degree latitude.

MAT1NXSLV provides atmospheric data of which the following variables were relevant for determining wind-energy potential (GMAO, 2008a):

- Displacement height (m)
- Eastward wind at 50 meter above surface (m/s)
- Northward wind at 50 meters above surface (m/s)

Additionally, MAT1NXRAD (GMAO, 2008b) provides hourly data on solar irradiation of which the following variables were used:

- Global surface incident shortwave flux ($W/m^2$)
- Surface incident shortwave flux assuming clear sky ($W/m^2$)
- Surface albedo (-)

In figure 4.1 the geographical orientation of the 16 (4x4) grid cells are visible, which have the same dimensions as the GMAO resolution (0.667x0.5°) and are named V1 (46.40N, 106.232E in the southwest) to V16 (48.40N, 108.90E in the northeast).

The temporal resolution of these datasets is high, which lends for a detailed analysis. For this research, one year of hourly data (1-1-2015 until 31-12-2015) is extracted for the aforementioned variables from both datasets for all 16 grid cells (a total of 840,960 data points). Data from the two MERRA datasets are used to estimate solar and wind potential.

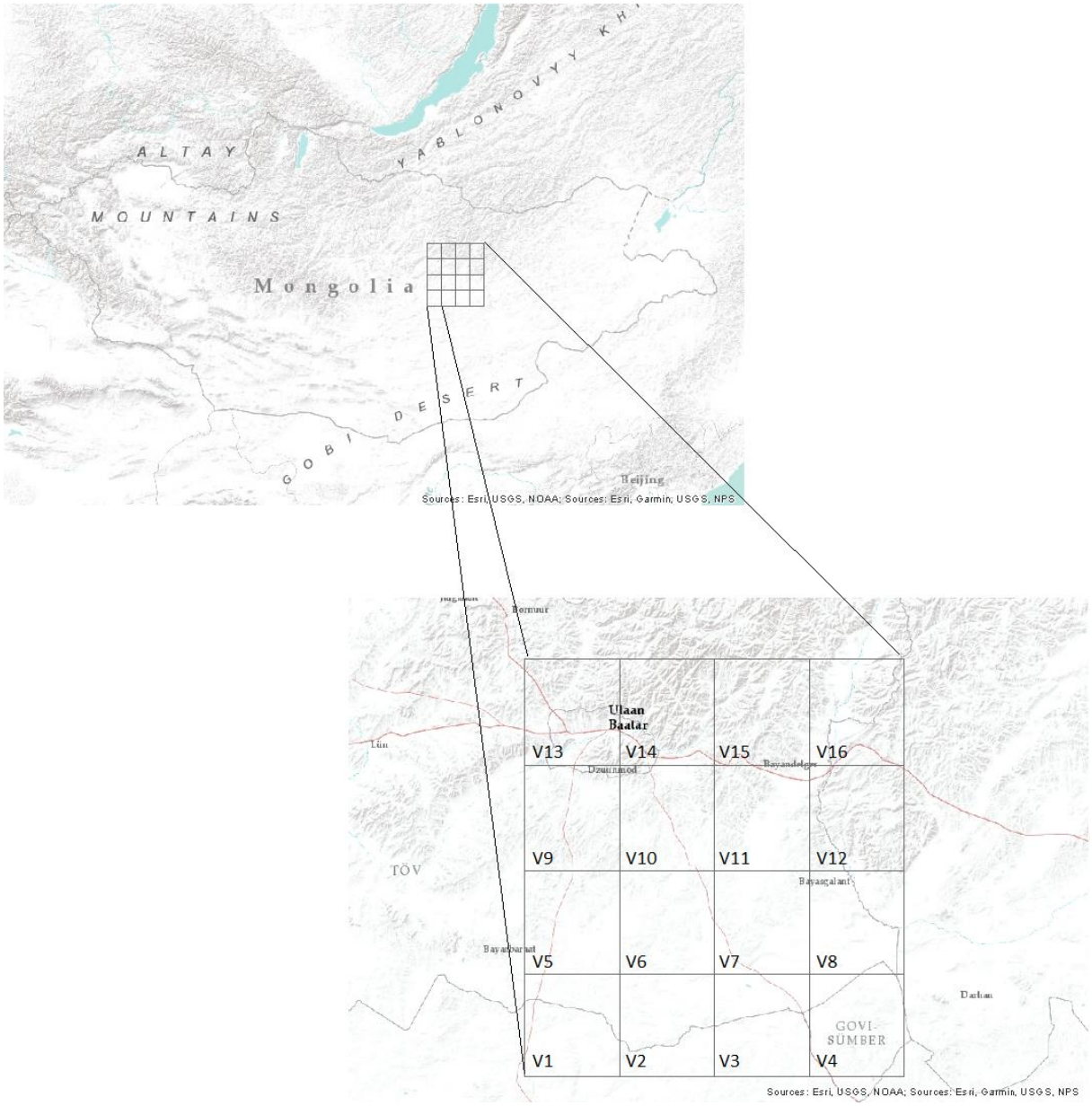


Figure 4.1: Geographical orientation of research area in Mongolia with grid cells named. Source: ESRI, retrieved with ArcMAP.

### 4.1.1 Solar power potential

In this research, it is assumed that solar PV panels are tilted and oriented towards the south in order to maximize potential. Therefore, the global irradiance on a tilted surface must be derived by summing the in-plane direct irradiance, the diffuse irradiance and the reflected irradiation from the surface (eq. 4.1; Yang, 2016).

(4.1) $G_c = I_c + D_c + D_g$

$G_c$ = Global irradiance (W/m$^2$)
$I_c$ = In-plane direct irradiance (W/m$^2$)
$D_c$ = Diffuse irradiance (W/m$^2$)
$D_g$ = Reflected irradiance from surface (W/m$^2$)

In order to calculate the in-plane direct irradiance on any surface at any time, the horizontal direct irradiance is multiplied by the cosine of the incidence angle, divided by the cosine of the solar zenith angle (eq. 4.2; fig. 4.2; Yang, 2017; Maatallah, 2011; Duffie, 2013; Reindl, 1990).

(4.2) $I_c = I_h * \frac{\cos\theta}{\cos z}$

$I_c$ = In-plane direct irradiance (W/m$^2$)
$I_h$ = Direct irradiation on horizontal surface (W/m$^2$)
θ = Incidence angle (degrees)
z = Solar zenith angle (degrees)

The zenith angle and incidence angle are dependent of a grid cell's latitude (46.5°≤φ≤48.0°), the earth's declination (-23.45°≤ $\delta$ ≤23.45°), the sun's hour angle (ω, 15 degrees per hour, 0° at noon), the slope of the solar panel (β) and the azimuth angle of the surface (γ). In order to maximize the solar irradiance on the solar panels, the slope is assumed to be equal to a grid cell's latitude, which means φ = β (Maatallah, 2011). The azimuth angle is zero in this model, as the solar panels face directly to the south, resulting in the last term of eq. 4.4 to drop out (Duffie, 2013). The executed formulae for calculating the zenith and incidence angle are shown in eq. 4.3 and 4.4. An overview of relation between zenith, incidence and declination angle is shown in figure 4.3.

(4.3) $\cos z = \cos\varphi * \cos\delta * \cos\omega + \sin\varphi * \sin\delta$

z = Solar zenith angle (degrees)
$\varphi$ = The grid cell's latitude (degrees)
$\delta$ = Declination (degrees)
ω = Hour angle (degrees)

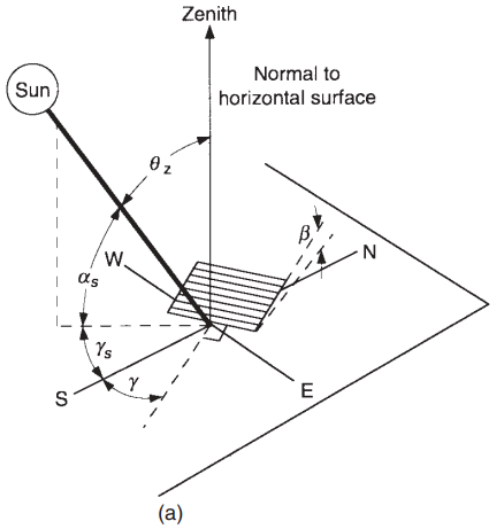


Figure 4.2. Orientation of zenith, incidence and azimuth angles during solar irradiation. Source: Duffie, 2013

(4.4) $\cos\theta = \sin\varphi * \sin\delta * \sin\beta - \cos\varphi * \sin\delta * \sin\beta * \cos\gamma + \cos\varphi * \cos\delta * \cos\beta * \cos\omega + \sin\varphi * \cos\delta * \sin\beta * \cos\gamma * \cos\omega + \cos\delta * \sin\beta * \sin\gamma * \sin\omega$

θ = Incidence angle (degrees)
φ = Grid cell's latitude (degrees)
δ = Declination (degrees)
β = Surface inclination or slope (degrees)
γ = Surface azimuth angle (degrees)
ω = Hour angle (degrees)

(4.5) $\delta = 23.45 * \sin\left(\frac{284+n}{365}\right)$

δ = Declination (degrees)
n = Number of days since the beginning of the year (n=1 on January 1st).

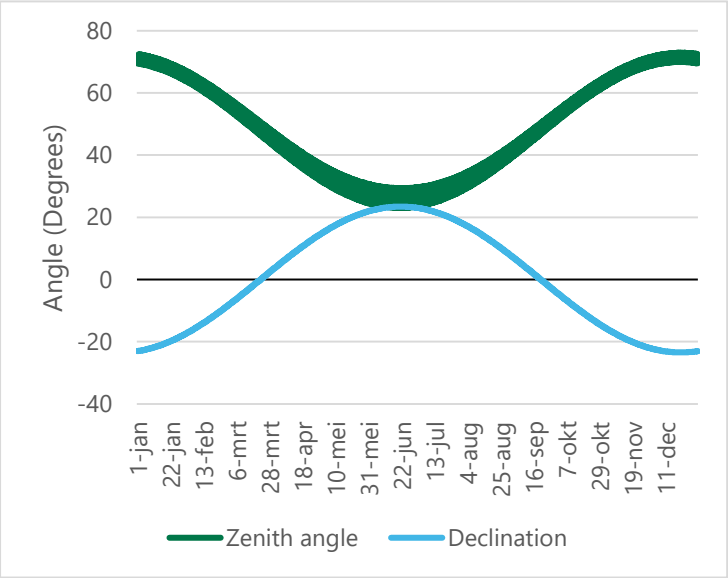


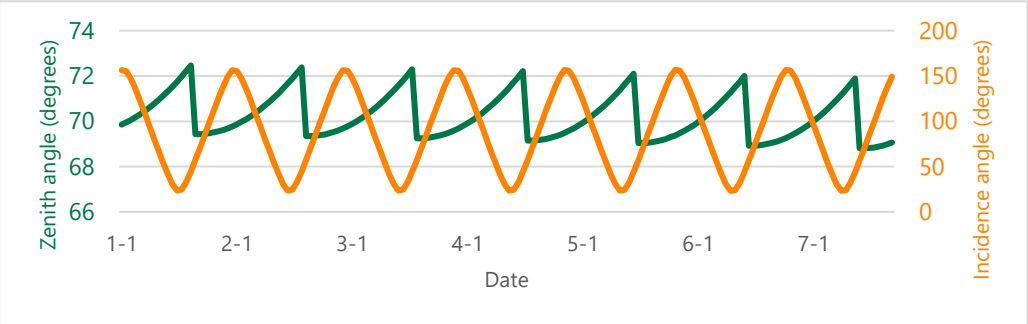


Figure 4.3. Upper: yearly variation of zenith and declination angles for grid cell V1. Lower: weekly variation of zenith and incidence angles for grid cell V1 in first week of January. Source: own figures.

For calculating the hour angle, local time has to be converted to solar time, which accounts for the difference in longitude between location of a grid cell and the standard meridian of the local time zone (eq. 4.6, 4.7). It is important to include solar time in this research, as grid cells range from λ=106.232E-108.90E while the nearest meridian is at 120E (+8 GMT). Since V1, V5, V8 and V13 are aligned towards the south, they have the same longitude, just like V2, V6, V11 and V14, etc. This results in a significant difference between local time and solar time of minus 53 to 45 minutes (fig. 4.4).

The equation of time (E) is also included in equation 4.7, which is the difference between mean time and true time and depends on the so-called 'mean anomaly' (B, eq. 4.8; Maatallah, 2011).

(4.6) $\omega = 15 * (t_s - 12)$

ω = Hour angle (degrees)
Ts = Solar time (hours)

(4.7) $t_s = t_{local} + \frac{\lambda}{15} - Z_{local} + E$

$t_s$ = Solar time (h)
$t_{local}$ = Local time (+8 GMT)
λ = Longitude of the grid cell (degrees)
$Z_{local}$ = Time zone east of GMT (h)
E = Difference between mean time and true time (h)

(4.8) $E = 3.8210^{-6}(75 + 1868 * \cos B - 32077 * \sin B - 14619 * \cos 2B - 40890 * \sin 2B$

E = Equation of time (-)
B = 360*(n-1)/365, with n is number of days since the beginning of the year (-)

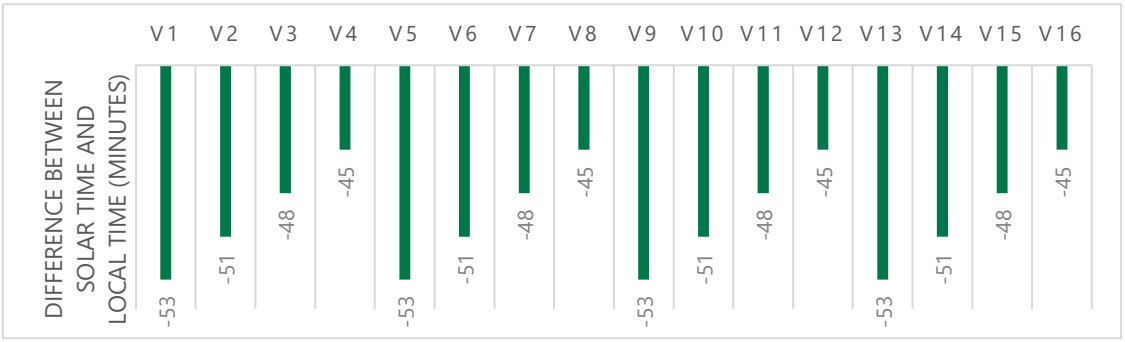


Figure 4.4. Difference between local time ($t_{local}$) and solar time ($t_s$) per grid cell in minutes. Source: own figure.

The hourly extraterrestrial radiation ($H_0$) on a horizontal surface is the amount of solar radiation that would reach the surface without a functioning atmosphere (Duffie, 2013). In reality, this amount is often lower because of the occurrence of atmospheric layers and clouds. Therefore, the total radiation on a horizontal surface is defined as global horizontal radiation ($I_{global}$), which is the sum of direct ($I_h$) and diffuse radiation ($I_{diffuse}$). Both the hourly extraterrestrial and global horizontal radiation are provided by the MERRA database (GMAO, 2008b) and their ratio results in the hourly cloudiness index ($k_t$, eq. 4.9). This index implies how much of the global radiation reaches the surface, compared to the amount with a clear sky.

The diffuse fraction (d), which is the ratio of diffuse horizontal radiation to the global horizontal radiation, depends on the cloudiness index (eq. 4.10, 4.11; Duffie, 2013; Ridley, 2010; McPherson, 2017). In order to estimate the amount of diffuse radiation to a tilted PV panel, an isotropic model after Hottel-Woertz-Liu-Jordan is applied, which means the intensity of diffuse radiation is assumed to be uniform along the hemisphere (eq. 4.12; Maatallah, 2011; Duffie, 2013).

(4.9) $k_t = \frac{I_{global}}{H_0}$

$k_t$ = hourly cloudiness index (-)
$I_{global}$ = Global radiation on horizontal surface (W/m2)
$H_0$ = Extraterrestrial radiation on a horizontal surface (W/m2)

(4.10) $d = \begin{cases} 1.0 - 0.09k_t & \text{if } k_t \leq 0.22, \\ 0.9511 - 0.1604k_t + 4.388{k_t}^2 - 16.638{k_t}^3 + 12.336{k_t}^4 & \text{if } 0.22 < k_t \leq 0.80, \\ 0.165 & \text{if } k_t > 0.8 \end{cases}$

d = Diffuse fraction (-)
$k_t$ = hourly cloudiness index (-)

(4.11) $d = \frac{I_{diffuse}}{I_{global}} = \frac{I_{diffuse}}{I_{diffuse}+I_h}$

d = Diffuse fraction (-)
$I_{diffuse}$ = Diffuse radiation on a horizontal surface (W/m$^2$)
$I_{global}$ = Global radiation on horizontal surface (W/m$^2$)
$I_h$ = Direct radiation on horizontal surface (W/m$^2$)

(4.12) $D_c = I_{diffuse} * \left(\frac{1+\cos\beta}{2}\right)$

$D_c$ = Diffuse irradiance (W/m$^2$)
$I_{diffuse}$ = Diffuse radiation on a horizontal surface (W/m$^2$)
β = Surface inclination or slope (degrees)

Lastly, a small part of in-plane radiation is reflected from the surface onto the solar panels. The level of reflectance depends on the surface's albedo (ρ, eq. 4.13; Yang, 2016; Maatallah, 2013; Duffie, 2013), which is higher in winter in Mongolia.

(4.13) $D_g = \rho * I_{global} * R_r$

$D_g$ = Reflected irradiance from surface (W/m$^2$)
P = surface albedo coefficient (-)
$I_{global}$ = Global radiation on horizontal surface (W/m$^2$)
$R_r$= (1-cos β /2), with β = slope of the solar panel (degrees)

An overview of in-plane direct, diffuse, reflected and global irradiance for grid cell V1 is shown in figure 4.5 and 4.6. Global irradiance seems to be highest during the vernal and autumnal equinox (end of March and September), which is mainly caused by higher direct irradiation. In summer direct radiation is lower, when diffuse radiation is highest and skies are cloudy. This agrees with the fact that summers in Mongolia behold more precipitation due to lower pressures (fig. 4.5; Climate-data, n.d.). Reflected irradiance is highest in winter and spring when snow does not melt and albedo is increased (fig. 4.5).

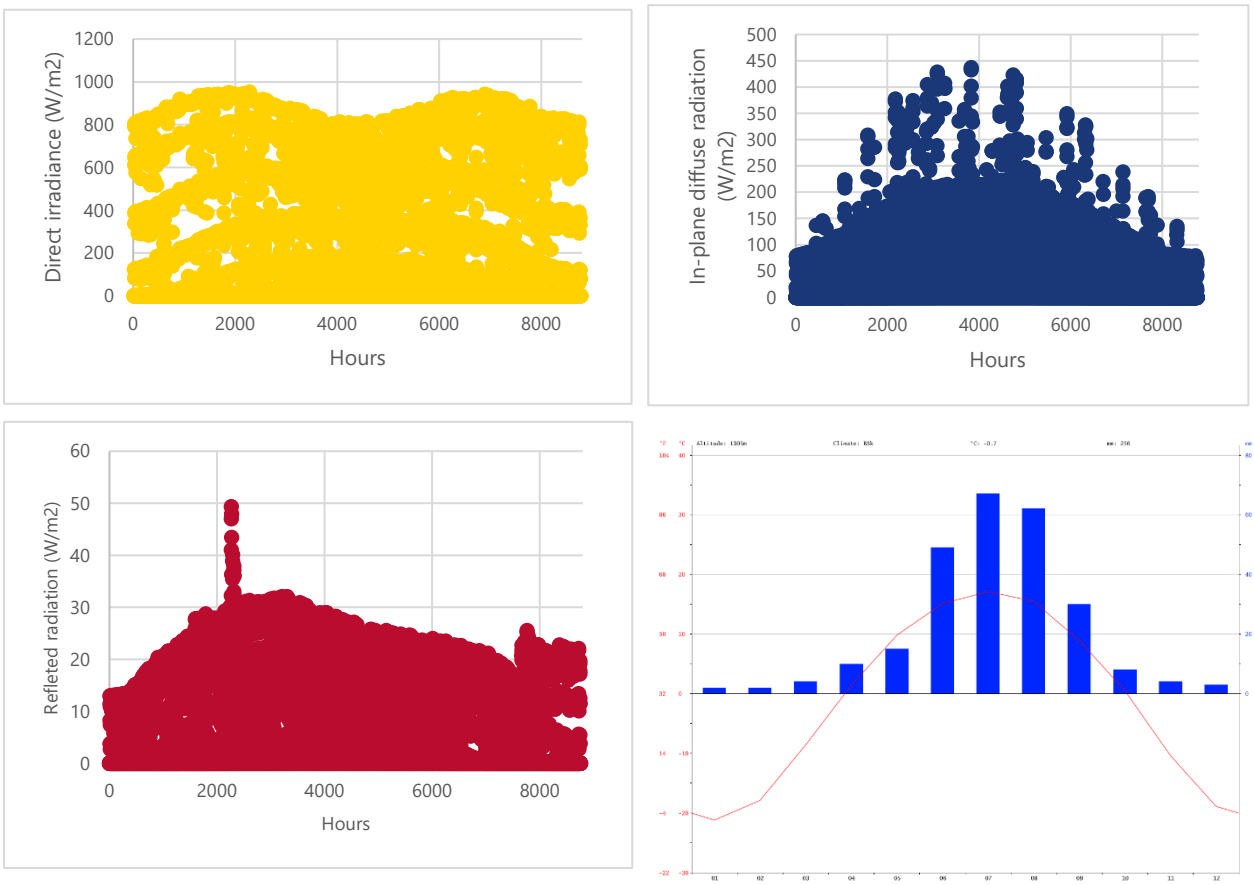


4.5. Upper and lower left: Scatter plots of hourly in-plane direct, diffuse and reflected radiation for grid cell V1 in the year 2015. Source: own figures, derived from MERRA data. Lower right: Climate graph for Ulaanbaatar. Source: Climate-data (n.d.)

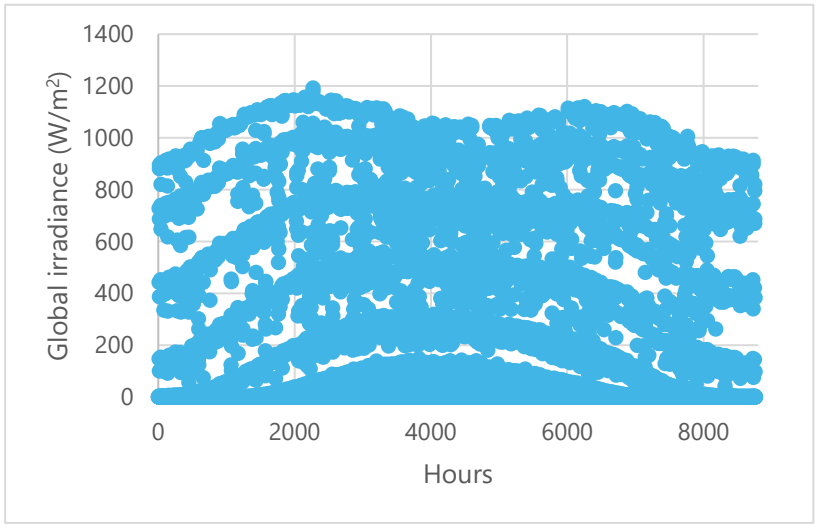


Figure 4.6. Scatter plot of hourly global tilted irradiance for grid cell V1 in 2015. Source: own figure derived from MERRA data.

The amount of power that is produced with the aforementioned radiation depends on the type and performance of these panels, which in turn are influenced by day temperature and wind speeds. In this study, constants for standard monocrystalline silicon cells are applied. The solar power potential ($PV_{pot}$) is calculated for each hour by using equation 4.14-4.17. (Van der Wiel, 2019; Jerez, 2015).

(4.14) $$PV_{pot} = P_r * \frac{G_c}{G_{stc}}$$

$PV_{pot}$ = Solar power potential (-)
$P_r$ = Performance ratio (-)
$G_c$ = Global irradiance (W/m$^2$)
$G_{stc}$ = Global radiation under standard test conditions (W/m$^2$)

(4.15) $$P_r = 1 + \gamma\,(T_{cell} - T_{ref})$$

$P_r$ = Performance ratio (-)
γ = Constant (-0.005)
$T_{cell}$ = Solar cell temperature (°C)
$T_{ref}$ = Constant (25 °C)

The cell temperature relates to the average day temperature in each grid cell. Data for monthly mean temperatures in 2015 is extracted for each grid cell's coordinates from the Climate Change Knowledge Portal by Worldbank (Harris, 2014). Monthly data for maximum temperatures is derived from regional statistics by MSIS (n.d.) for the regions Mandalgobi (V1, V2), Choir (V3-V8), Zuunmod (V9-V12) and Ulaanbaatar (V13-V16) for the same year, which result in a range of minus 20 degrees Celcius in winter and 55 degrees in summer (fig. 4.7). Wind speeds at 50-meter altitude for each grid cell are provided by the MERRA database and is converted to wind speeds at 10-meter height by using equation 4.19.

(4.16) $$T_{cell} = c1 + c2 * T_{day} - c3 * I_{global} + c4 * v(10)$$

$T_{cell}$ = Solar cell temperature (°C)
c1 = Constant (4.3 ◦C)
c2 = Constant (0.943)
c3 = Constant (0.028 degrees m$^2$/W)
c4 = Constant (-1.528 degrees s/m)
$T_{day}$ = ($T_{mean}$+$T_{max}$) / 2
v(10) = Wind speed at 10 meters above displacement height

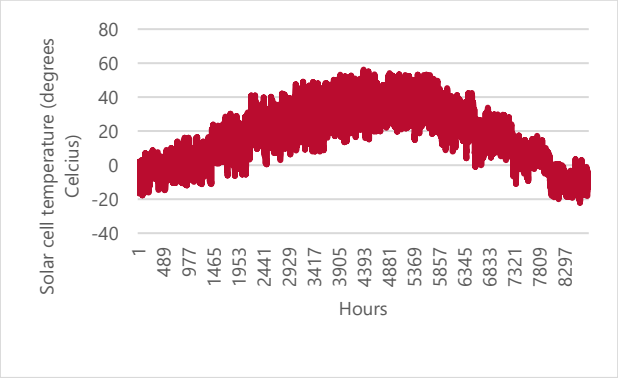


Figure 4.7. Yearly variation of solar cell temperature for grid cell V1. Source: own figure.

Finally, the average yearly $PV_{pot,\ year}$ is calculated, which is taken as the capacity factor for solar PV for each grid cell. Subsequently, this is multiplied by the suitable area for solar PV per grid cell and the efficiency of 20% (200 $W_p/m^2$) to estimate a grid cells maximum yearly electricity generation by solar PV (eq. 2.25).

(4.17) $E_{PV} = P_{panel} * PV_{pot\ year} * A_{pv} * h/yr$

$E_{pv}$ = Maximum yearly electricity generation by solar PV per grid cell (Wh)
$P_{panel}$ = Nominal power of solar cell per square meter (200 $W_p/m^2$)
$PV_{pot\ year}$ = Average yearly solar power potential (-)
$A_{pv}$ = Suitable area for solar PV per grid cell ($m^2$)
h/yr = Hours per year (8760)

The methodology for determining the suitable area for solar PV and wind turbines ($A_{pv}$ and $A_{wind}$) is further described in section 4.1.3.

### 4.1.2 Wind power potential

The three aforementioned variables provided by MERRA – displacement height and east- and northward wind at 50 meters above the surface – are combined into calculating the wind energy potential ($W_{pot}$, eq. 4.21). First, the east- and northward wind speeds are combined into the actual wind speed at 50 meters height using the Pythagorean Theorem (eq. 4.18; NASA, n.d.). The wind direction can also be derived from this calculation (fig. 4.8).

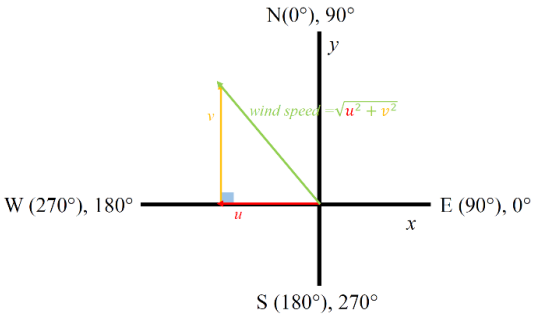


Figure 4.8. Orientation of u ($v_{east}$) and v ($v_{north}$) and the resulting wind direction and speed. Source: NASA, n.d.

(4.18) $v(50) = \sqrt{{v_{east}}^2 + {v_{north}}^2}$

v(50) = Wind speed at 50 meters (m/s)
$v_{east}$ = Eastward wind speed at 50 meter above surface (m/s)
$v_{north}$ = Northward wind speed at 50 meter above surface (m/s)

Additionally, the wind speeds at hub height has to be determined. In this thesis, a hub height of 80 meters is assumed as input for the wind potential analysis. This is done by using the wind profile power law, using the wind shear coefficient which varies for each type of surface (eq. 4.19, 4.20; Andrews, 2017). For each grid cell the same surface roughness of 0.143 is used, comparable with previous studies on wind potential of Mongolia (Elliot, 2001).

(4.19) $v(z_2) = v(z_1) * (\frac{z_2 - d}{z_1 - d})^{\alpha}$

v (z) = Wind speed at a specific height (m/s)
z = Height from surface (m)
d = Displacement height (m)
α = Wind shear coefficient (-)

(4.20) $\alpha\,(z_2) = \frac{1}{2}(\frac{z_0}{z_2})^{0.2}$

α (z) = Wind shear coefficient at a specific height (-)
$z_0$ = surface roughness (-)
z = Specific height from surface (m)

An overview of hourly wind speeds at 80 meter is shown in figure 4.9. Wind speeds do not seem to hold any seasonal variability (fig. 4.16). Grid cells V1, V2 and V4 have the highest yearly averaged wind speeds (5.6 m/s; table 3.5) and V13 the lowest (4.2 m/s) perhaps due to disturbance of wind flows by urban area. The maximum wind speed for V1 (19.5 m/s) is still well below cut-out wind speed.

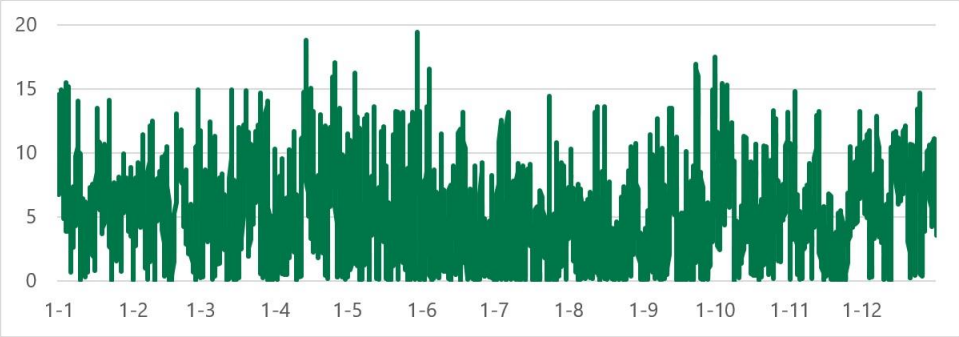


Figure 4.9. Yearly wind speeds at 80 meters altitude for grid cell V1 in 2015. Source: own figure derived from MERRA data.

The wind energy potential, or capacity factor for wind power, is determined by a wind power curve, which depends on cut-in wind speed (3.5 m/s), rated wind speed (13 m/s) and cut-out wind speed (25 m/s) (fig. 4.10; Andrews, 2017). Wind speeds below the cut-in speed and above the cut-out speeds result in a $W_{pot}$ of zero. Between the cut-in speed and rated wind speed, the power output increases according to figure 4.10 and equation 4.21 (Van der Wiel, 2019; Jerez, 2015). Between the rated and cut-out wind speed, wind turbines have maximum power output ($W_{pot}$=1).

(4.21) $$W_{pot} = \begin{cases} 0 & \text{if} \quad v(t) < v_{cut\text{-}in}, \\ \frac{v(t)^3 - v_{cut-in}{}^3}{v_{rated}{}^3 - v_{cut-in}{}^3} & \text{if } v_{cut\text{-}in} \leq v\,(t) < V_{rated}, \\ 1 & \text{if } v_{rated} \leq v(t) < V_{cut\text{-}out}, \\ 0 & \text{if } v_{cut\text{-}out} \leq v(t), \end{cases}$$

Figure 4.10. Example of typical wind power curve. Source: Wind power program (n.d)

$W_{pot}$ = Hourly wind energy potential (-)
v(t) = Hourly wind speed (m/s)
$v_{cut\text{-}in}$ = Standard onshore turbine cut-in speed (3.5 m/s)
$v_{rated}$ = Standard onshore turbine rated speed (13 m/s)
$v_{cut\text{-}out}$ = Standard onshore turbine cut-out speed (25 m/s)

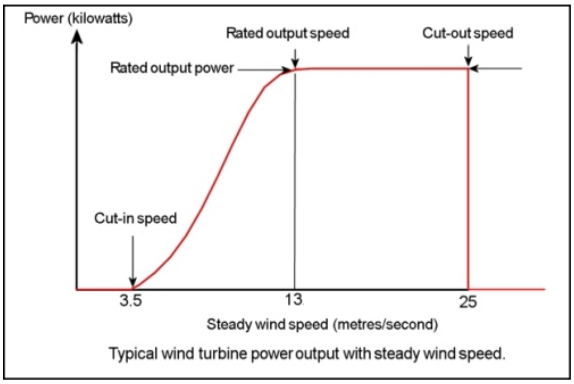


The yearly maximum electricity production by wind energy per grid cell is calculated by using the rated wind power per turbine (2.5 MW), a surface area per wind turbine of 0.32 $km^2$ (assuming 5D crosswind-8D

downwind spacing and a turbine diameter of 90 meters), the wind energy potential and the amount of suitable area per grid cell for wind energy (eq. 4.22). This equation includes the reductions in power output due to array losses (10% is assumed). The methodology for determining the suitable area for wind turbines is further described in section 4.1.3.

(4.22) $E_{wind} = P_{wind\ rated} * W_{pot} * a * \frac{A_{wind}}{A_{turbine}} * h/yr$

$E_{wind}$ = Yearly maximum electricity production by wind energy (Wh)
$P_{rated}$ = Rated wind power per turbine (W)
$W_{pot}$ =Wind energy potential (-)
$A_{wind}$ = Suitable area for wind turbines per grid cell ($m^2$)
$A_{turbine}$ = Surface area per wind turbine ($m^2$)
h/yr = Hours per year (8760)
a = Array loss factor (0.9)

### 4.1.3 Available space for renewable energy

The suitable area per grid cell for solar PV and wind energy is identified by using ArcGIS software. For both renewable technologies specific exclusions or conditions apply to the extent of possible implementation (Hoogwijk, 2004).

The required data to calculate suitable areas in every grid cell, are found in different databases (Hu, 2018). In order to estimate the total suitable area for both technologies, the following maps are used:

- Protected areas: Protected Planet (UNEP, 2009)
- Land cover classification (GlobCover 2009; Arino, 2009)
- Elevation: Global 30 Arc-Second Elevation (GTOPO30; EROS, n.d.)
- Permafrost: Global Permafrost Zonation Index Map (Gruber, 2012)

For both separate technologies their suitability is described in section 4.1.3.1 and 4.1.3.2.

#### 4.1.3.1 Onshore wind

Several areas are excluded for onshore wind, such as terrestrial protected areas, surfaces with common occurrence of permafrost and high elevations (Hu, 2018). The following areas are excluded from installing wind turbines:

- Protected areas
- Areas with slopes higher than 20% (or 11.31 degrees)
- Areas with elevation higher than 2600 meters

In order to remove these areas from the available space in each grid cell, the Protected Planet map and GTOPO30, in combination with the 'Slope'-tool in ArcMAP, are analyzed. Additionally, for certain types of land cover, implementing wind turbines is suboptimal but not impossible. In this research, they are quantified in suitability factors, ranging from 0 to 1 (Hu, 2018; NREL, 2016). The suitability factors for onshore wind from NREL (2016) are used for analysis (fig. 4.11).

Lastly, the permafrost zonation index map by Gruber (2012) is adapted into a second series of suitability factors, ranging from 1 (no permafrost) to 0 (always permafrost) by using the 'Reclassification'-tool in ArcMAP. In short, if the area is not protected, higher than 2600 meters or tilted more than 20%, the available space for wind turbines per grid cell is calculated by using equation 4.23.

| GlobCover Value | GlobCover Category | Suitability Factor [a] |
|---|---|---|
| 11 | Post-flooding or irrigated croplands | 0 |
| 14 | Rainfed croplands | 0.7 |
| 20 | Mosaic Cropland (50-70%) / Vegetation (grassland, shrubland, forest) (20-50%) | 0.7 |
| 30 | Mosaic Vegetation (grassland, shrubland, forest) (50-70%) / Cropland (20-50%) | 0.7 |
| 40 | Closed to open (>15%) broadleaved evergreen and/or semi-deciduous forest (>5m) | 0.1 |
| 50 | Closed (>40%) broadleaved deciduous forest (>5m) | 0.1 |
| 60 | Open (15-40%) broadleaved deciduous forest (>5m) | 0.1 |
| 70 | Closed (>40%) needleleaved evergreen forest (>5m) | 0.1 |
| 90 | Open (15-40%) needleleaved deciduous or evergreen forest (>5m) | 0.1 |
| 100 | Closed to open (>15%) mixed broadleaved and needleleaved forest (>5m) | 0.1 |
| 110 | Mosaic Forest/Shrubland (50-70%) / Grassland (20-50%) | 0.5 |
| 120 | Mosaic Grassland (50-70%) / Forest/Shrubland (20-50%) | 0.65 |
| 130 | Closed to open (>15%) shrubland (<5m) | 0.5 |
| 140 | Closed to open (>15%) grassland | 0.8 |
| 150 | Sparse (>15%) vegetation (woody vegetation, shrubs, grassland) | 0.9 |
| 160 | Closed (>40%) broadleaved forest regularly flooded - Fresh water | 0 |
| 170 | Closed (>40%) broadleaved semi-deciduous and/or evergreen forest regularly flooded - Saline water | 0 |
| 180 | Closed to open (>15%) vegetation (grassland, shrubland, woody vegetation) on regularly flooded or waterlogged soil - Fresh, brackish or saline water | 0 |
| 190 | Artificial surfaces and associated areas (urban areas >50%) | 0 |
| 200 | Bare areas | 0.9 |
| 210 | Water bodies | 0 |
| 220 | Permanent snow and ice | 0 |

Figure 4.11. Onshore wind suitability factors for each GlobCover category. Source: NREL (2016).

(4.23) $A_{wind} = A_{total} * f_{wind} * f_{permafrost}$

$A_{wind}$ = Suitable area for wind turbines per grid cell ($m^2$)
$A_{total}$ = Surface area per grid cell ($m^2$)
$f_{wind}$ = Land cover suitability factor for wind turbines (-)
$f_{permafrost}$ = Permafrost suitability factor (-)

### 4.1.3.2 Solar PV

Next, the area fit for solar PV needs to be established, for which rooftop PV and utility PV are distinguished. For utility PV the following areas are excluded (Hu, 2018):

- Protected areas
- Areas with slopes higher than 4 degrees
- Urban, forest and water bodies

A new set of land cover suitability factors for utility PV is based on Hoogwijk (2004). The land types that exist in Mongolia with their corresponding suitability factors are shown in table 2.6. The permafrost suitability factors are the same for both wind energy and solar PV, resulting in a comparable model for suitable area shown in equation 4.24.

(4.24) $A_{solar} = A_{total} * f_{solar} * f_{permafrost}$

$A_{wind}$ = Suitable area for wind turbines per grid cell ($m^2$)
$A_{total}$ = Surface area per grid cell ($m^2$)
$F_{wind}$ = Land cover suitability factor for wind turbines (-)
$f_{permafrost}$ = Permafrost suitability factor (-)

The applied methodology for establishing available space for rooftop PV in Ulaanbaatar also originates from Hoogwijk (2004), in which the roof area per capita depends on GDP per capita (eq. 4.25). The added 'utilization factor' for roofs of 0.40 accounts for architectural suitability and roof shading (Hoogwijk, 2004). Population and GDP data originate from sources mentioned in section 2.1. In order to apply an additional error margin, it is

assumed a maximum of 80% of remaining roof area can be covered with solar cells. The only possibility for solar PV on roof area in the research area is in Ulaanbaatar city (V13) The estimated rooftop area per person in 2030 is 11.7 $m^2$/cap, which would result in a yearly maximum power output of 3.5 TWh (fig. 4.12; 55% of electricity demand).

(4.25) $$\frac{A_{roof\ PV}}{POP_{city}} = 0.06 * GDP_{capita}{}^{0.6} * 0.40$$

$A_{roof\ PV}$ = Total available roof area for solar PV ($m^2$)
$POP_{city}$ = Population of Ulaanbaatar (persons)
$GDP_{capita}$ = GDP per capita of Ulaanbaatar (US$/capita)

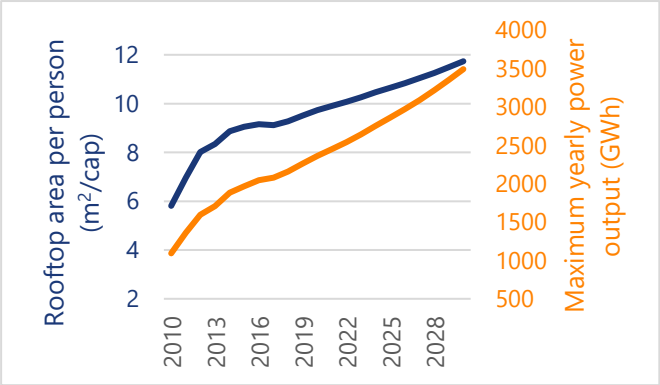


Figure 4.12. Development of rooftop area per person and corresponding maximum yearly power roof PV output. Source: own figure.

Table 2.6. Solar PV suitability factors for existing land covers in the research area. Source: Hoogwijk (2004)

* For these land types, a higher suitability factor is assumed than described in Hoogwijk (2004), as the research area generally contains these land covers with limited competition with other land uses

| GlobCover Value | Suitability factor solar PV |
|---|---|
| 11 | 0 |
| 14 | 0.01 |
| 20 | 0.01 |
| 30 | 0.01 |
| 90 | 0 |
| 100 | 0 |
| 110 | 0 |
| 120 | 0.01 |
| 140 | 0.9* |
| 150 | 0.9* |
| 200 | 0.9* |
| 210 | 0 |
| 220 | 0 |

## 4.2 Renewable potential

This section includes the results from the potential analysis for wind power and solar PV in the area surrounding Ulaanbaatar. An overview of decisive parameters is shown in table 3.3.

Table 3.3. Overview of solar and wind power potential per grid cell in Mongolia. Source: own table.

| Grid cell | Average wind speed at 80m (m/s) | Capacity factor wind ($W_{pot}$) | Rated wind power (GW) | Wind power output $E_{wind}$ (TWh/ year) | Average global irradiance (W/m2) | Capacity factor solar ($PV_{pot}$) | Rated solar power ($GW_p$) | Solar PV power output $E_{PV}$ (TWh/year) |
|---|---|---|---|---|---|---|---|---|
| V1 | 5.5 | 0.165 | 41.3 | 53.1 | 241.6 | 0.240 | 1074 | 2254 |
| V2 | 5.6 | 0.168 | 41.3 | 54.2 | 242.1 | 0.240 | 1074 | 2259 |
| V3 | 5.5 | 0.160 | 41.2 | 51.6 | 241.8 | 0.240 | 1077 | 2264 |
| V4 | 5.6 | 0.166 | 40.2 | 52.0 | 240.5 | 0.239 | 1051 | 2199 |
| V5 | 5.3 | 0.147 | 41.2 | 47.3 | 237.8 | 0.237 | 1045 | 2166 |
| V6 | 5.6 | 0.166 | 41.3 | 53.6 | 239.2 | 0.239 | 1042 | 2176 |
| V7 | 5.4 | 0.158 | 40.7 | 50.0 | 239.3 | 0.239 | 1023 | 2134 |
| V8 | 5.5 | 0.159 | 41.0 | 50.8 | 238.0 | 0.237 | 1020 | 2117 |
| V9 | 4.8 | 0.115 | 36.3 | 32.6 | 234.8 | 0.236 | 791 | 1631 |
| V10 | 5.4 | 0.153 | 33.7 | 40.3 | 235.8 | 0.238 | 749 | 1555 |
| V11 | 5.4 | 0.156 | 35.6 | 43.3 | 236.8 | 0.238 | 748 | 1561 |
| V12 | 5.3 | 0.146 | 31.6 | 35.9 | 234.7 | 0.236 | 540 | 1114 |
| V13 | 4.2 | 0.081 | 28.9 | 18.3 | 231.3 | 0.231 | 490 | 992 |
| V14 | 5.0 | 0.120 | 11.4 | 10.7 | 230.3 | 0.232 | 134 | 271 |
| V15 | 5.6 | 0.164 | 17.5 | 22.4 | 233.9 | 0.236 | 238 | 491 |
| V16 | 5.5 | 0.155 | 26.5 | 31.9 | 233.7 | 0.236 | 396 | 817 |

### 4.2.1 Available space for renewable technology

The research area's 4x4 grid cells have been analyzed by using the previously described methods. First, the amount of area per land cover was determined for each grid cell (fig. 4.8). Closed to open grassland, sparse vegetation and bare areas are most common (140, 150, 200) in the center and south of the research area, which have high suitability for both solar and wind power. In the north, landscape includes vegetation like mosaic croplands and open forests (20, 30, 90), containing lower suitability for both technologies. The artificial area in grid cell 13 is Ulaanbaatar city.

The second criterium for suitability of renewable technologies is the occurrence of permafrost (fig. 3.15). The majority of the research area does not contain permafrost, but the likelihood increases in parts with higher altitudes up north (fig. 4.9).

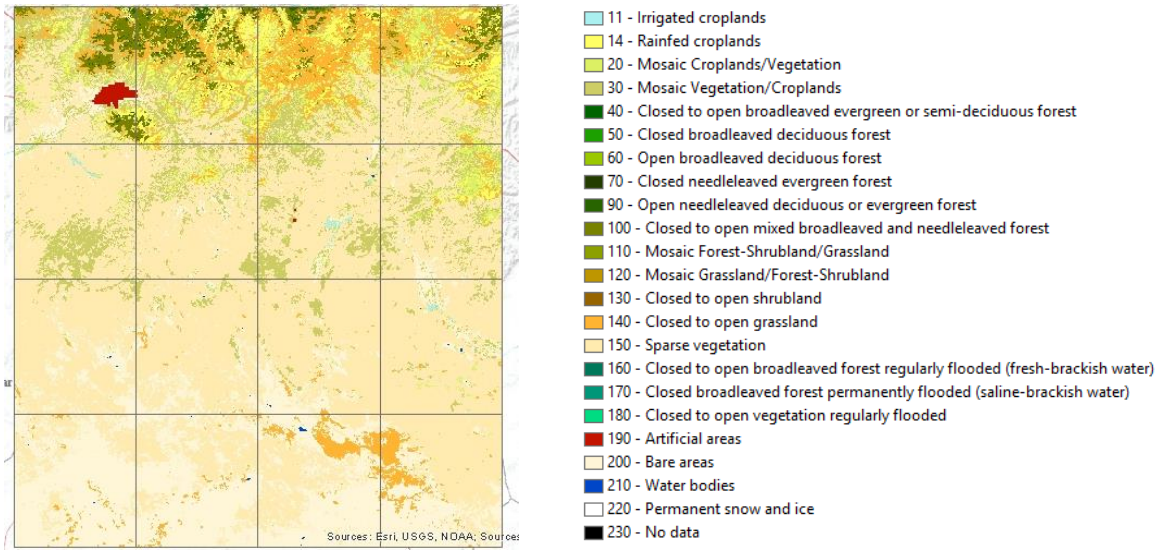


Figure 4.8. Land cover per grid cell. Source: own figure using ArcMAP and GlobCover 2009.

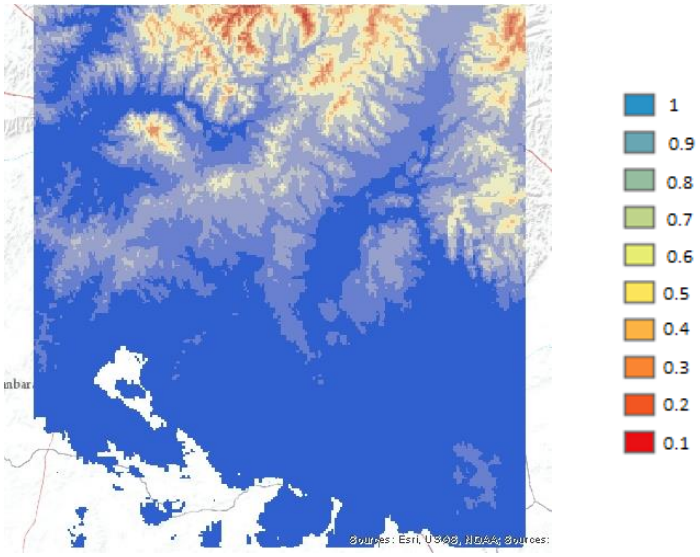


Figure 4.9. Permafrost suitability in the research area. Source: own figure using ArcMAP and the Permafrost Zonation index.

Figure 4.10 shows the research area without protected areas, as they are excluded for implementing renewable technologies. They mostly occur up north, where they take up big chunks of potential area in V13-V15 (fig. 3.16). That part of the research area also contains some relief, whereas the south is flatter. For wind power, areas with slopes higher than 11.3 degrees are excluded, but these areas do not occur in the research area (fig. 4.10). However, slopes of 4 degrees or more can be found in the grid cells, which exclude solar power.

The total amount of suitable area for solar PV and wind power per grid cell is shown in table 3.4. The shown percentages are shares suitable area of total non-protected area. In general, the research area contains a larger area available to wind turbines than solar panels. The grid cells in the south have the largest area available for renewable technologies (90%) due to limited protected areas, relief, vegetation and permafrost.

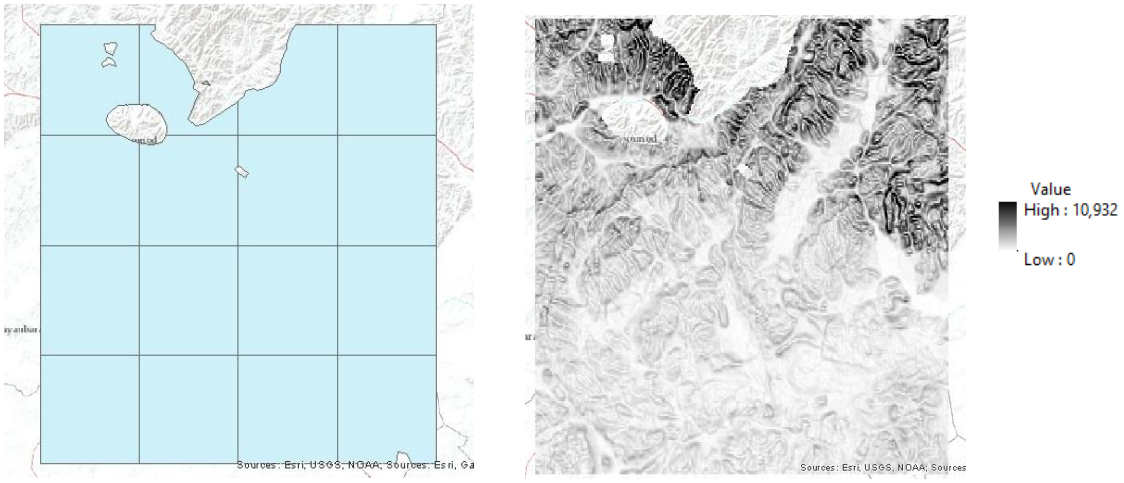


Figure 4.10. Left: research area (blue) without protected areas. Right: research area showing slopes (degree) without protected areas. Source: own figure using ArcMAP and GTOPO30 and Protected Planet maps.

Table 3.4. Total amount of suitable area per grid cell for large-scale PV and wind energy. Source: own table.

| Grid cell | Suitable area for utility scale PV per grid cell (km$^2$) | Share of suitable area (%) | Suitable area for wind turbines per grid cell (km$^2$) | Share of suitable area (%) |
|---|---|---|---|---|
| V1 | 5371 | 90% | 5358 | 90% |
| V2 | 5369 | 90% | 5356 | 90% |
| V3 | 5383 | 90% | 5344 | 89% |
| V4 | 5254 | 89% | 5204 | 88% |
| V5 | 5224 | 86% | 5335 | 88% |
| V6 | 5208 | 86% | 5349 | 89% |
| V7 | 5113 | 84% | 5275 | 87% |
| V8 | 5098 | 84% | 5309 | 88% |
| V9 | 3955 | 66% | 4706 | 78% |
| V10 | 3743 | 64% | 4369 | 73% |
| V11 | 3742 | 63% | 4607 | 75% |
| V12 | 2699 | 53% | 4099 | 67% |
| V13 | 2451 | 51% | 3751 | 67% |
| V14 | 668 | 38% | 1474 | 52% |
| V15 | 1188 | 34% | 2273 | 50% |
| V16 | 1982 | 40% | 3429 | 56% |

### 4.2.2 Solar and wind power potential

The previously described methodology for estimating capacity factors for solar PV ($PV_{pot}$) result in values between 0.231 (V13) and 0.240 (V1-V3). Combining these values with the maximum amount of suitable land area per grid cell, large-scale solar PV installations could yield power outputs between 271 TWh per grid cell per year (V13) and 2264 TWh per grid cell per year (V3) (fig. 4.11, table 3.3). These theoretically enormous power outputs are 35-376 times higher than projected demand in 2030. If UB's electricity demand in 2030 were only to be met with this technology (while not taking variable output into account), a surface area of ~15 $km^2$ (0.3-2.4% of suitable area per grid cell) would have to be covered with solar panels. It is clear that solar output is higher towards the south, although implementing high capacities of this technology in grid cell V1-V4 would produce higher transmission and distribution losses.

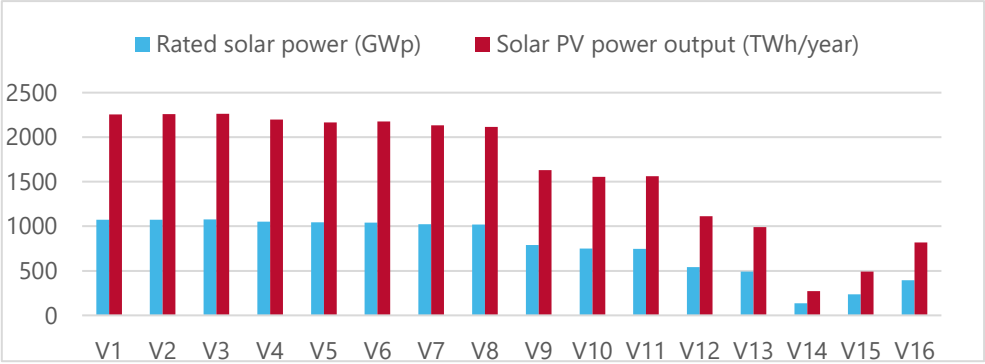


Figure 4.11. Maximum rated solar power ($GW_p$) and power output $E_{PV}$ (TWh/yr) per grid cell. Source: own figure.

Using the power curve together with hourly wind speeds per grid cell, the resulting capacity factors for wind power ($W_{pot}$) between 0.081 (V13) and 0.168 (V2) are significantly lower than for solar power (table 3.3). The corresponding capacities range from 11.4 GW per grid cell (V14) to 41.3 GW per grid cell (V1, 2), which could yield a maximum between 10.7 TWh per grid cell per year (V14) to 54.2 TWh per grid cell per year (V2) (fig. 4.17). These outputs are only 0.7 to 7.5 times higher than UB's projected electricity demand in 2030, because of relatively low average wind speeds (4.2-5.5 m/s). In order to meet demand with this technology, between 630 and 1300 $km^2$ would need to be covered with wind turbines (12-59% of suitable area per grid cell). In the next chapter, the ideal mix between these renewable technologies is determined for the GREEN scenario.

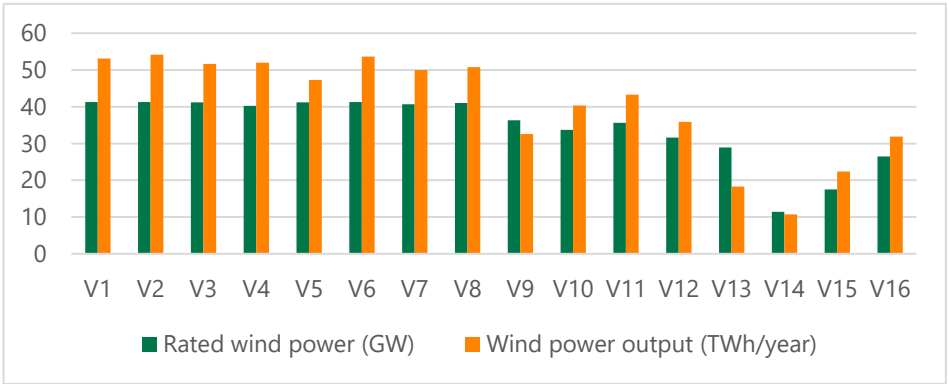


Figure 4.17. Maximum rated wind power (GW) and power output $E_{wind}$ (TWh/yr) per grid cell. Source: own figure.

# 5. Balancing supply and demand

Renewable electricity supply from wind and solar capacity is subjected to weather and seasonal variability. In this chapter *sub-question 4 'How can variable renewable electricity output be compensated in the Ulaanbaatar region?'* is answered by describing the applied methodology and its outcomes.

## 5.1 Methodology

In this study, the following two options are considered for filling the hourly and seasonal electricity gap:

1. Import and export: surplus of renewable electricity at peak hours is exported to other parts of the CES or Russia. At times with lower generation, electricity is imported into Ulaanbaatar. To become more independent of importing electricity, net import from Ulaanbaatar should be zero or lower. As mentioned earlier, the maximum capacity of the grid is estimated to grow to 415 MW in 2030.
2. CHP-4: This plant is a good candidate from existing capacity of filling the electricity gap, as it is relatively new, has ample capacity and also provides heat. The possibility of replacing its fuel by natural gas or co-firing with biomass is explored in the Discussion (section 8.3).

Storage of electricity is not considered in the GREEN scenario as current battery prices are too high to be able to compete with the baseline scenario. EnergyPLAN is used in order to estimate both hourly and seasonal electricity gaps and needed capacities of solar PV, wind power and CHP-4 by simulating electricity supply and demand for the year 2030. This software simulates energy systems on an hourly basis, including electricity, heating, industry and transport (EnergyPLAN, n.d.). The following results from previous research steps are input data in this software:

- Electricity demand in Ulaanbaatar in 2030 (TWh)
- Hourly distribution profiles of $W_{pot}$ and $PV_{pot}$, which function as capacity factors
- The capacity and efficiency of CHP-4 (group 3 CHP) and Salkhit wind farm
- Capacity of transmission lines
- Capacity of new solar PV and wind power

Priority is given to more cost-effective technology options in order to maximize the renewable electricity share, which are determined by calculating the LCOE per technology and per grid cell (eq. 5.1). For installing solar PV and wind power, capital costs, O&M costs and construction time are derived from the IEA's New Policies Scenario assumptions for China in 2020 (table 5.1, IEA, 2016c). These costs are relatively low compared to European or Russian prices or compared to the investment for the Salkhit wind farm (~2400 US$/kW); therefore, these prices are included in the sensitivity analysis (8.1). The grid cell's distance from Ulaanbaatar is not quantified with respect to costs due to losses or installment of new transmission lines. However, if differences between two LCOEs are negligible but one technology is closer to Ulaanbaatar, this is preferred.

(5.1) $$LCOE_{RES} = \frac{I*\alpha+M}{E_{generation}}$$

$LCOE_{RES}$ = Levelized cost of solar PV or wind power (US$/kWh)
I = Total investment costs for power source (US$)
α = Capital recovery factor (-)
M = Yearly operations and maintenance costs (US$/yr)
$E_{generation}$ = Electricity generation by power source per year (kWh/yr)

Table 5.1. Assumptions for costs per renewable capacity built in the GREEN scenario. Source: IEA, 2016,

| Costs for renewable technologies in China, 2020 | | | |
|---|---|---|---|
| Type of renewable | Capital costs (US$/kW) | Operations and maintenance costs (US$/kW) | Construction time (years) |
| Onshore wind power | 1200 | 30 | 1.5 |
| Solar PV (buildings) | 1120 | 14 | 1.0 |
| Solar PV (large-scale) | 1020 | 12 | 1.5 |

## 5.2 Electricity mix

In order to select the best mix of renewable technologies and non-renewable compensation in the GREEN scenario, the individual LCOEs per grid cell are shown in figure 5.1. Solar PV is the cheapest technology in every grid cell compared to wind power, and there is only little variation in PV prices among cells. Roof PV is slightly more expensive due to higher specific capital and O&M costs (table 2.7), but would produce lower transmission and distribution costs. Wind power is most expensive in grid cell 13, since the urbanized area likely distorts wind flows, whereas it is more cost-effective in V2, V6 and V4.

The best option that is relatively cheap and nearby the source of electricity demand, is roof PV in Ulaanbaatar. According to previous calculations, approximately 1727 MW worth of suitable roof area is available in the city in 2030 (fig. 4.12). For wind power, grid cell V10 is closest to UB, while also having a relatively low price of electricity (12.6 cents/kWh). This is the optimal choice for wind power, however, as it is less cost-effective, it should be supplementing solar PV in an ideal electricity mix. To minimize extensive construction of additional transmission lines, it is assumed utility solar PV is also built in grid cell V10 in the GREEN scenario.

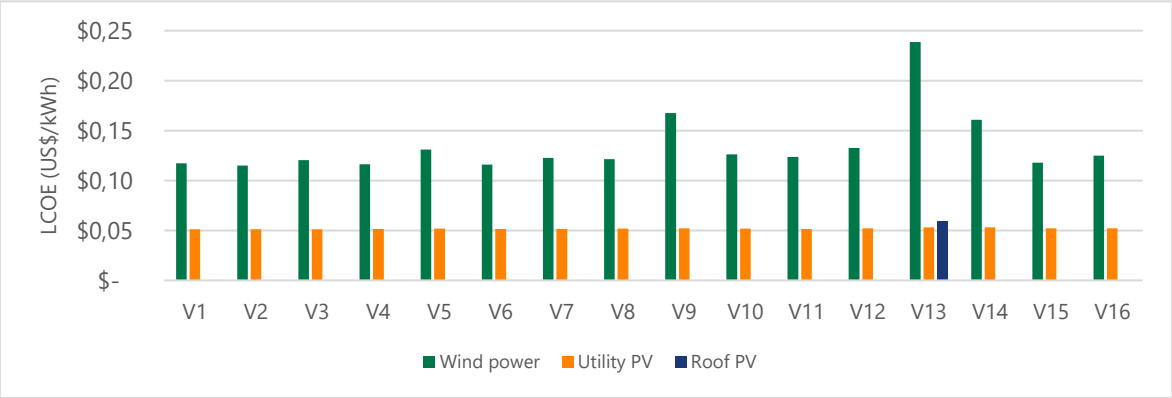


Figure 5.1. Levelized cost of electricity (LCOE) per technology and grid cell for 2000 MW capacity. Source: own figure.

The respective shares of solar PV and wind power to electricity production, combined with the hourly irradiance and wind profiles (in grid cell V10), determine the share of CHP-4 in EnergyPLAN. In table 5.2 various ratios are shown with corresponding total renewable shares and amounts of CHP generation. Actual generation by solar PV and wind power is lower than the estimated value, since peak supply of those technologies often exceeds demand (fig. 5.2). This oversupply is exported until the transmission line's maximum capacity is reached (415 MW), after which renewable production is stopped. To optimize renewable electricity share, a mix of 60% solar PV and 40% wind power is chosen for GREEN, resulting in a maximum share of 76.9% (table 5.2). In this electricity mix, a yearly total of 2.55 TWh by CHP-4 (23.1% of production) is needed to fill variable electricity gaps in 2030. This is caused by limited output of solar PV and wind power during the night (fig. 5.2). During the day, there is high production of renewable electricity supply which surpasses demand and results in net export of 1.09 TWh per year. If in this

scenario CHP-4 is ultimately replaced by hydropower or biomass combustion capacity, 100% renewable electricity share could be achieved. (Lund, 2007).

The resulting electricity mix of 54% solar PV, 23% wind power and 23% CHP-4 is used as power mix in the GREEN scenario (chapter 6).

Table 5.2. EnergyPLAN outputs for various shares of solar PV and wind power in Ulaanbaatar in 2030. Source: own table derived from EnergyPLAN.

| | Electricity shares of solar PV and wind power (%) | | | | | |
|---|---|---|---|---|---|---|
| Total electricity supply (TWh) | 7.51 | 7.52 | 7.54 | 7.13 | 7.31 | 7.22 |
| Share of solar PV (%) | 80 | 70 | 60 | 50 | 40 | 30 |
| Share of wind power (%) | 20 | 30 | 40 | 50 | 60 | 70 |
| Needed capacity solar PV (MW) | 2550 | 2143 | 1873 | 1531 | 1225 | 918 |
| Estimated production solar (TWh) | 5.09 | 4.27 | 3.82 | 3.05 | 2.44 | 1.91 |
| Needed capacity wind power (MW) | 1054 | 1581 | 2109 | 2535 | 3163 | 3690 |
| Estimated production wind (TWh/yr) | 1.27 | 1.91 | 2.54 | 2.18 | 3.8 | 4.45 |
| Capacity CHP-4 (MW) | 705 | 705 | 705 | 705 | 705 | 705 |
| Actual solar generation (TWh) | 3.79 | 3.57 | 3.42 | 2.98 | 2.44 | 1.83 |
| Share actual of estimated (%) | 74 | 84 | 90 | 98 | 100 | 96 |
| Actual wind generation (TWh) | 0.82 | 1.18 | 1.47 | 1.79 | 2.21 | 2.59 |
| Share actual of estimated (%) | 65 | 62 | 58 | 82 | 58 | 58 |
| Needed CHP-4 generation (TWh) | 2.8 | 2.67 | 2.55 | 2.56 | 2.56 | 2.7 |
| Needed import (TWh) | 0.1 | 0.1 | 0.1 | 0.1 | 0.1 | 0.1 |
| Renewable share of electricity supply (%) | 72 | 75 | **77** | 75 | 73 | 69 |

Figure 5.2. Two examples of daily fluctuations in electricity demand and production in 2030 in Ulaanbaatar. Source: own figures made with EnergyPLAN.

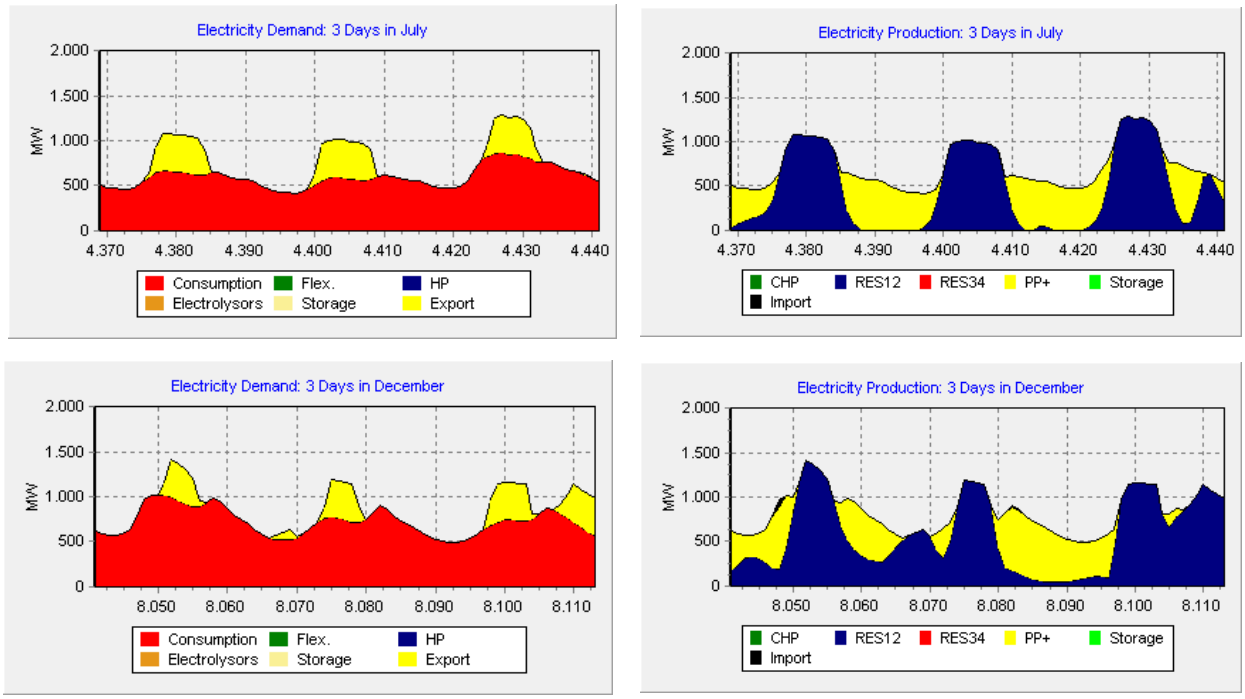

# 6. GREEN scenario

The applied methodology and corresponding outcomes for answering sub-question 5: '*What are the resulting costs and indirect emissions of implementing a high share of renewable electricity, compared to the business-as-usual scenario?*' are described in this chapter. First, the boundary conditions for constructing the GREEN scenario are described, after which the needed additional capacity, emissions and costs are explained.

## 6.1 Methodology

The criteria for the GREEN scenario are described more in detail below:

- Renewable electricity share is maximized by implementing the most cost-effective option, supplemented by less cost-effective options. The previously established mix of 54% solar PV, 23% wind power and 23% CHP-4 is therefore used in this scenario.
- CHP-2 and CHP-3 are phased out completely during the building of wind and solar capacity. According to IEA (2016), this takes approximately 1.5 years. Therefore, it is assumed for this scenario that the solar and wind capacity are fully operational from the year 2020.
- Salkhit wind farm and CHP-4 remain operational, of which the latter only fills variable electricity gaps if necessary (~2.55 TWh in 2030).
- Baganuur CHP is not included in GREEN, since two of the following options may be the case:
  - After 2030, Baganuur could take over from CHP-4 after which it surpassed an age of 40 years.
  - Baganuur is built, but not for electricity supply to Ulaanbaatar. It could function as an electricity-exporting facility or for meeting demand in other parts of Mongolia.
- Import of electricity to Ulaanbaatar is minimized, which both curtails dependency on Russia and decreases indirect emissions from Russian electricity generation. Only imperative imports due to daily or seasonal gaps are accepted in this scenario. This results in Ulaanbaatar to changing from a net importing to net exporting city during this scenario (~1.09 TWh in 2030).

The amount of new capacity that needs to be built in order to achieve the aforementioned electricity mix is determined by including Salkhit and by allocating solar generation to roof and utility PV. Of total needed wind power (1.47 TWh in 2030) Salkhit is already generating ~90 GWh per year (section 3.2.1). Therefore, only 1.41 TWh has to be generated by newly built wind turbines in 2030. This is assumed to be produced by a wind power plant in grid cell 10 with a total capacity of 1988 MW (Wind Power V10). To achieve such a capacity, ~795 x 2.5 MW wind turbines need to be built, occupying a significant surface area of ~250 $km^2$. Total solar PV generation of 3.42 TWh per year in 2030 needs to be allocated to roof PV and utility PV. As mentioned earlier, roof PV is a cheap and convenient option. It is assumed that 80% of all available roofs is covered with solar cells (~17 $km^2$). This results in a roof PV capacity of 1381 MW and expected generation of 2.5 TWh in 2030. The remaining large-scale PV capacity of 482 MW is projected to generate 0.917 TWh in 2030 (Utility PV V10; ~24 $km^2$).

An overview of capacity, load hours and electricity generation per power source is shown in table 6.1. The amount of load hours for CHP-4 is assumed to be the same as in BAU, supplying 4.6 TWh to the CES and 2.55 TWh to UB. The total amount of load hours of this CHP is not reduced in this scenario, since the city's heat demand is assumed to be met by heat supply from this facility. Due to a low capacity factor for wind power and limited exporting capacity resulting in high share of curtailment (40%, table 5.2), the amount of load hours for Wind Power V10 is very low. This could increase in the future by expanding the capacity of the electricity grid (chapter 7). The electricity supply of 7.54 TWh to Ulaanbaatar (table 5.2) exceeds the city's projected demand in 2030, of which the surplus is exported to other parts of the CES or Russia. This export is on top of the excess generation by CHP-4 intended for other parts of the CES.

Table 6.1. Capacity, generation and load hours in the GREEN scenario. Source: own table.

| | 2010 | 2030 | | |
|---|---|---|---|---|
| Name of facility | Capacity (MW) | Capacity (MW) | Load hours (h) | Yearly generation (GWh) |
| CHP-2 | 21.5 | 0 | 0 | 0 |
| CHP-3 | 136 | 0 | 0 | 0 |
| CHP-4 | 580 | 705 | 6525 | 2550 |
| Salkhit | 0 | 49.6 | 1810 | 59 |
| Wind power V10 | 0 | 1834 | 753 | 1411 |
| Roof solar PV | 0 | 1381 | 1812 | 2503 |
| Utility PV V10 | 0 | 482 | 1903 | 917 |
| Total | 738 | 1891 | | 7540 |

In the sections 6.2.1-6.2.3, the projected electricity capacity and generation together with their GHG emissions and costs are discussed for the GREEN scenario. In section 6.3, this scenario is compared to the BAU, taking costs and emissions into account. Total greenhouse gas emissions in the GREEN scenario are calculated similarly as the BAU using equation 6.1. In order to compare the levelized cost of electricity for the scenario as a whole, the same method is used as for BAU by calculating the weighted average of LCOEs per power source (eq. 6.2). LCOEs per power source are compared to previously calculated LCOEs in the BAU scenario in a power curve. Using this curve, the cost-effective measures are distinguished from more expensive measures.

(6.1) $$GHG_{GREEN} = (CO_{2\,direct} + GHG_{other\,direct} + GHG_{construction} + CO_{2\,import})_{GREEN}$$

$GHG_{GREEN}$ = Total yearly greenhouse gas emissions in GREEN scenario (kt $CO_2$-eq)
$CO_{2\,direct}$ = Yearly direct $CO_2$ emissions (kt $CO_2$)
$GHG_{other\,direct}$ = Yearly direct other greenhouse gas emissions (kt $CO_2$-eq)
$GHG_{construction}$ = Yearly GHG emissions from construction or expansion of power plants, wind parks or solar parks (kt $CO_2$-eq)
$CO_{2\,import}$ = Yearly $CO_2$ emission from importing electricity to Ulaanbaatar (kt $CO_2$)

(6.2) $$\mathrm{LCOE}_{\mathrm{GREEN}} = \frac{\sum \alpha_a * I_a + \sum M_a + \sum F_a}{\sum E_a}$$

$LCOE_{GREEN}$ = Average levelized cost of electricity for the GREEN scenario (US$/kWh)
$\alpha$ = Capital recovery factor for power source a (-)
$I_a$ = Total investment costs for power source a (US$)
$M_a$ = Yearly operations and maintenance costs for power source a (US$/yr)
$F_a$ = Yearly fuel costs for power source a (US$/yr)
$E_a$ = Electricity generation per year by power source a (kWh)

## 6.2 Scenario projections

In this section, the alternative scenario (GREEN) is described by using electricity supply, greenhouse gas emissions and costs. An overview of essential parameters is shown in table 6.1.

Table 6.1. Projected parameters for the GREEN scenario 2010-2030 in Ulaanbaatar. Source: own table.

| | | Year | | | | | BAU |
|---|---|---|---|---|---|---|---|
| Parameter (unit) | **Facility** | 2010 | 2015 | 2020 | 2025 | 2030 | 2030 |
| Electric capacity (MW) | CHP-2 | 22 | 22 | 0 | 0 | 0 | 0 |
| | CHP-3 | 136 | 186 | 0 | 0 | 0 | 436 |
| | CHP-4 | 580 | 705 | 705 | 705 | 705 | 705 |
| | Salkhit | 0 | 50 | 50 | 50 | 50 | 50 |
| | Wind power V10 | 0 | 0 | 1988 | 1988 | 1988 | - |
| | Roof solar PV | 0 | 0 | 921 | 1123 | 1381 | - |
| | Utility PV V10 | 0 | 0 | 482 | 482 | 482 | - |
| | Baganuur | - | - | - | - | - | 700 |
| Load hours (h) | CHP-2 | 6307 | 6307 | 0 | 0 | 0 | 0 |
| | CHP-3 | 5515 | 4032 | 0 | 0 | 0 | 6307 |
| | CHP-4 | 5172 | 5674 | 5390 | 6525 | 6525 | 6525 |
| | Salkhit | 0 | 1810 | 1810 | 1810 | 1810 | 1810 |
| | Wind power V10 | 0 | 0 | 502 | 612 | 753 | - |
| | Roof solar PV | 0 | 0 | 1812 | 1812 | 1812 | - |
| | Utility PV V10 | 0 | 0 | 1269 | 1546 | 1903 | - |
| | Baganuur | - | - | - | - | - | 1825 |
| $E_{generation}$ per facility to Ulaanbaatar (GWh) | CHP-2 | 50 | 87 | 0 | 0 | 0 | 0 |
| | CHP-3 | 278 | 478 | 0 | 0 | 0 | 1805 |
| | CHP-4 | 1112 | 2552 | 1700 | 2072 | 2550 | 3020 |
| | Salkhit | 0 | 58 | 39 | 48 | 59 | 59 |
| | Wind power V10 | 0 | 0 | 941 | 1147 | 1411 | - |
| | Roof solar PV | 0 | 0 | 1669 | 2034 | 2503 | - |
| | Utility PV V10 | 0 | 0 | 611 | 745 | 917 | - |
| | Import | 0 | 0 | 67 | 81 | 100 | - |
| | Export | 0 | 0 | -786 | -958 | -1179 | - |
| | Baganuur | - | - | - | - | - | 1477 |
| | **Total** | **1440** | **3175** | **5027** | **6127** | **7540** | **6361** |
| $CO_{2\ direct}$ based on Ulaanbaatar generation (kt) | CHP-2 | 84 | 144 | 0 | 0 | 0 | 0 |
| | CHP-3 | 249 | 429 | 0 | 0 | 0 | 1617 |
| | CHP-4 | 886 | 2034 | 1355 | 1652 | 2032 | 2407 |
| | Salkhit | 0 | 0 | 0 | 0 | 0 | - |
| | Wind power V10 | 0 | 0 | 0 | 0 | 0 | 0 |
| | Roof solar PV | 0 | 0 | 0 | 0 | 0 | - |
| | Utility PV V10 | 0 | 0 | 0 | 0 | 0 | - |
| | Baganuur | - | - | - | - | - | 1313 |
| | **Total** | **1219** | **2607** | **1355** | **1652** | **2032** | **5302** |
| $CO_2$ import | **Total** | **50** | **142** | **35** | **43** | **53** | **53** |

| | | Year | | | | | BAU |
|---|---|---|---|---|---|---|---|
| **Parameter (unit)** | **Facility** | 2010 | 2015 | 2020 | 2025 | 2030 | 2030 |
| $GHG_{other\ direct}$ based on Ulaanbaatar generation (kt $CO_2$-eq) | CHP-2 | 0 | 1 | 0 | 0 | 0 | 0 |
| | CHP-3 | 1 | 3 | 0 | 0 | 0 | 9.4 |
| | CHP-4 | 5 | 12 | 8 | 10 | 12 | 14.1 |
| | Salkhit | 0 | 0 | 0 | 0 | 0 | 0 |
| | Wind power V10 | 0 | 0 | 0 | 0 | 0 | - |
| | Roof solar PV | 0 | 0 | 0 | 0 | 0 | - |
| | Utility PV V10 | 0 | 0 | 0 | 0 | 0 | - |
| | **Total** | **7** | **16** | **8** | **10** | **12** | **23.6** |
| $GHG_{construction}$ (kt $CO_2$-eq) | CHP-2 | 0 | 0 | 0 | 0 | 0 | 0 |
| | CHP-3 | 0 | 0 | 0 | 0 | 0 | 0 |
| | CHP-4 | 0 | 0 | 0 | 0 | 0 | 0 |
| | Salkhit | 0 | 1 | 1 | 1 | 1 | 1 |
| | Wind power V10 | 0 | 0 | 10 | 13 | 16 | - |
| | Roof solar PV | 0 | 0 | 77 | 94 | 115 | - |
| | Utility PV V10 | 0 | 0 | 28 | 34 | 42 | - |
| | **Total** | 0 | 1 | 116 | 141 | 173 | 1 |
| Annual O&M costs per facility (million US$/yr) | CHP-2 | 10 | 10 | 0 | 0 | 0 | 0 |
| | CHP-3 | 12 | 9 | 0 | 0 | 0 | 14 |
| | CHP-4 | 17 | 17 | 18.5 | 18.5 | 18.5 | 18.5 |
| | Salkhit | 0 | 1 | 1 | 1 | 1 | 1.5 |
| | Wind power V10 | 0 | 0 | 60 | 60 | 60 | - |
| | Roof solar PV | 0 | 0 | 13 | 16 | 19 | - |
| | Utility PV V10 | 0 | 0 | 6 | 6 | 6 | - |
| | Import costs | 8 | 22 | 5 | 7 | 8 | - |
| | Baganuur | - | - | - | - | - | 18.4 |
| | **Total** | **46** | **60** | **104** | **107** | **113** | **52.4** |
| Annual fuel costs based on Ulaanbaatar generation (million US$/yr) | CHP-2 | 2 | 3 | 0 | 0 | 0 | **0** |
| | CHP-3 | 6 | 10 | 0 | 0 | 0 | 37 |
| | CHP-4 | 20 | 47 | 31 | 38 | 47 | 56 |
| | Baganuur | - | - | - | - | - | 27 |
| | **Total** | **28** | **60** | **31** | **38** | **47** | **120** |
| LCOE Based on total generation to CES f(US$/kWh) | CHP-2 | 0.11 | 0.11 | 0 | 0 | 0 | 0 |
| | CHP-3 | 0.04 | 0.03 | 0 | 0 | 0 | 0.026 |
| | CHP-4 | 0.03 | 0.02 | 0.02 | 0.02 | 0.02 | 0.02 |
| | Salkhit | 0.00 | 0.09 | 0.09 | 0.09 | 0.154 | 0.154 |
| | Wind power V10 | 0.00 | 0.00 | 0.32 | 0.25 | 0.21 | - |
| | Roof solar PV | 0 | 0 | 0.09 | 0.08 | 0.07 | - |
| | Utility PV V10 | 0 | 0 | 0.08 | 0.07 | 0.06 | - |
| | Baganuur | - | - | - | - | - | 0.157 |

### 6.2.1 Electricity capacity and generation

Figure 6.1 shows the development of electricity generation per power source for the GREEN scenario. As mentioned earlier, most renewable capacity is operational from 2020 onwards. However, since available area for roof PV grows alongside GDP per capita, solar roof PV capacity is projected to increase from 921 MW in 2020 to 1381 MW in 2030. CHP-4's electricity supply to Ulaanbaatar is lower than in the BAU scenario (3 TWh), but it is still considerate (1.1-2.55 TWh). The difference in load hours between Salkhit and Wind power V10 is a result of curtailment of wind power in this scenario due to variable output and limited grid capacity. Import of electricity from 2019 is limited to obligated maximum of 0.1 TWh per year, whereas there is significant exporting of renewable electricity during peak hours (0.8-1.18 TWh per year).

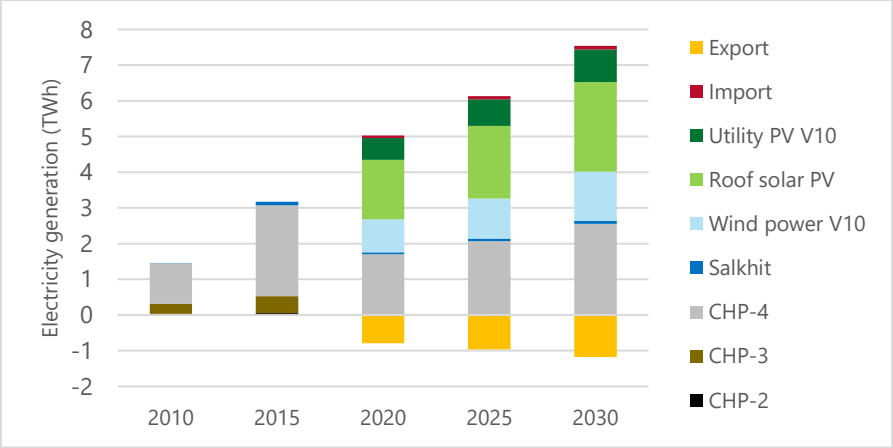


Figure 6.1. Electricity generation in the GREEN scenario 2010-2030 in Ulaanbaatar. Source: own figure.

### 6.2.2 Greenhouse gas emissions

From 2020 onwards, the only direct greenhouse gas emissions are emitted by CHP-4, whereas import of electricity and construction of wind turbines and solar cells emit indirect GHGs (fig. 6.2). Roof solar PV contains the highest share of indirect emissions, increasing from 77 kt/yr in 2020 to 115 kt/yr in 2030. Cumulative emissions increase to 45 Mt $CO_2$-eq in 2030, whereas greenhouse gas intensity drops from 886 to 357 kg $CO_2$-eq/kWh (fig. 6.3). Furthermore, emissions per capita drop from 2.3-1.0 t $CO_2$-eq/cap between 2019 and 2020, after which they increase to 1.23 t $CO_2$-eq/cap in 2030. Lastly, emissions per $GDP_{city}$ decrease from 0.54 kg in 2010 to 0.19 kg $CO_2$-

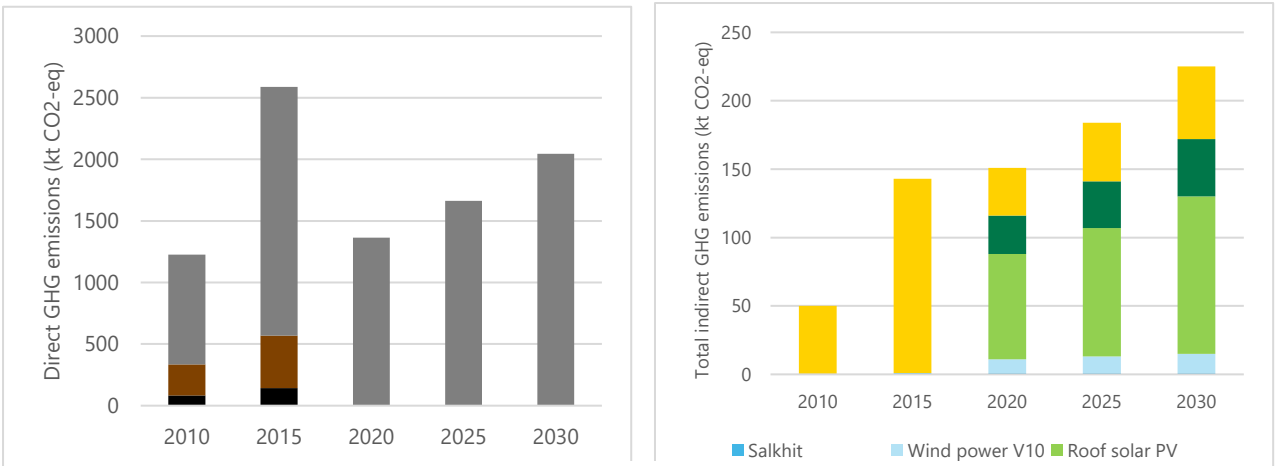


Figure 6.2. Left: Total direct GHG emissions for GREEN 2010-2030. Right: Total indirect GHG emissions for GREEN 2010-2030. Source: own figures.

eq/US$ in 2030 (fig. 6.3). Exporting renewable electricity may lead to indirect GHG reduction elsewhere due to the replacement of fossil-based electricity generation.

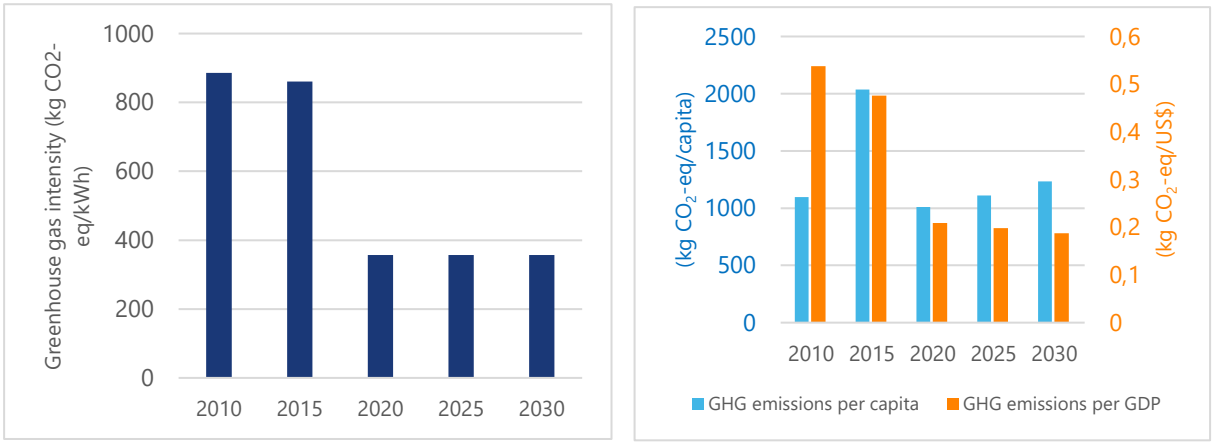


Figure 6.3. Left: Greenhouse gas intensity for GREEN 2010-2030. Right: Emissions per capita and $GDP_{city}$ for GREEN 2010-2030. Source: own figures.

### 6.2.3 Costs

First, the following investment costs are included in the GREEN scenario, some of which are calculated by using table 5.1 (IEA, 2016c):

- Construction of Salkhit wind farm: 122 million US$ in 2010
- Expansion of CHP-4 in 2015: 45 million US$
- Construction of Roof PV: 1.547 billion US$ in 2019.
- Construction of Wind Power V10: 2.386 billion US$ in 2019.
- Construction of Utility PV V10: 492 million US$ in 2019.

Secondly, the same O&M and fuel costs are made by the CHPs as in the BAU scenario until 2020, after which they decrease significantly due to the shutdown of CHP-2 and 3. In 2030, almost half of all yearly costs are made by CHP-4 and the other half by maintenance of renewable capacity. From 2020, import costs are 5-8 million US$, whereas UB also benefits from exporting electricity in this scenario. Total yearly costs (excluding annualized

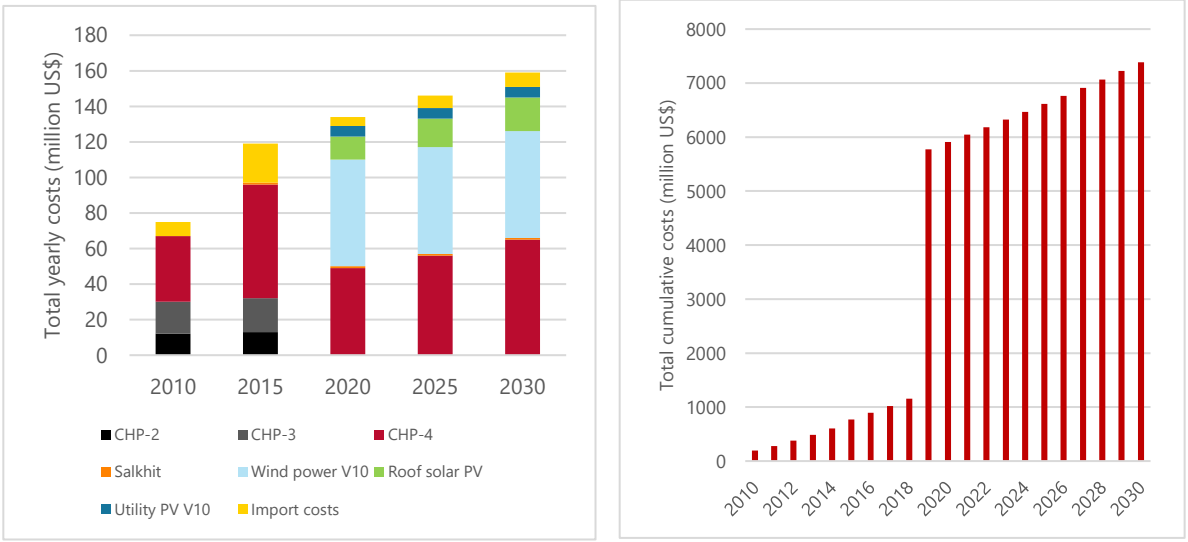


Figure 6.4. Left: Composition of yearly costs. Right: Total cumulative costs. Both for GREEN 2010-2030. Source: own figures.

investments) are projected to increase from 70 to 160 million US$ per year between 2010 and 2030 (fig. 6.4). The LCOEs per technology and GREEN are further described in the next section.

## 6.3 Comparison BAU and GREEN

In this section, the two constructed scenarios are compared with respect to greenhouse gas emissions and costs of electricity. An overview is show in table 6.2.

Table 6.2. Various types of greenhouse gas emissions and costs for BAU and GREEN 2010-2030 and difference in percentage. Source: own table.

| | Scenario | 2010 (base year) | 2015 | 2020 | 2025 | 2030 (target year) |
|---|---|---|---|---|---|---|
| Direct GHG (kt $CO_2$-eq) | **BAU** | 1226 | 2622 | 3583 | 4406 | 5361 |
| | **GREEN** | 1226 | 2622 | 1363 | 1661 | 2044 |
| | | 0% | 0% | -62% | -62% | -62% |
| Indirect GHG (kt $CO_2$-eq) | **BAU** | 50 | 142 | 1 | 1 | 1 |
| | **GREEN** | 50 | 142 | 151 | 184 | 226 |
| | | 0% | 0% | 22294% | 33177% | 34477% |
| Cumulative emissions (kt $CO_2$-eq) | **BAU** | 1276 | 12524 | 28401 | 48798 | 73443 |
| | **GREEN** | 1276 | 12524 | 26356 | 34880 | 45317 |
| | | 0% | 0% | -7% | -29% | -38% |
| Greenhouse gas intensity (g $CO_2$-eq/kWh) | **BAU** | 886 | 871 | 845 | 852 | 843 |
| | **GREEN** | 886 | 871 | 357 | 357 | 357 |
| | | 0% | 0% | -58% | -58% | -58% |
| O&M costs (million US$/yr) | **BAU** | 39 | 38 | 45 | 64 | 52 |
| | **GREEN** | 39 | 38 | 98 | 101 | 105 |
| | | 0% | 0% | 117% | 59% | 100% |
| Fuel costs (million US$/yr) | **BAU** | 28 | 60 | 82 | 99 | 120 |
| | **GREEN** | 28 | 60 | 31 | 38 | 47 |
| | | 0% | 0% | -62% | -62% | -61% |
| Total yearly costs (million US$/yr) | **BAU** | 197 | 165 | 128 | 163 | 173 |
| | **GREEN** | 197 | 165 | 135 | 146 | 160 |
| | | 0% | 0% | 6% | -10% | -7% |
| Cumulative total costs (million US$) | **BAU** | 197 | 768 | 1426 | 5666 | 6480 |
| | **GREEN** | 197 | 768 | 5907 | 6614 | 7383 |
| | | 0% | 0% | 314% | 17% | 14% |
| LCOE (US$cts/kWh) | **BAU** | 3.0 | 3.1 | 2.9 | 5.9 | 5.6 |
| | **GREEN** | 3.0 | 3.0 | 11.1 | 9.3 | 7.8 |
| | | 0% | -2% | 281% | 57% | 38% |

### 6.3.1 Greenhouse gas emissions

Until the year 2019 the source of electricity generation in Ulaanbaatar is the same for both scenarios. From that year renewable capacity will have started to be built in GREEN and from 2020 CHP-2 and 3 will be shut down. In 2021, Baganuur will start operating in BAU, which means the scenarios will diverge even more with respect to emissions. According to GREEN, direct emissions will be 2.0 Mt $CO_2$-eq in 2030, which is 3.3 Mt (-62%) lower than BAU (table 6.2; fig. 6.5). On the other hand, indirect emissions due to construction of wind turbines and solar panels and import of electricity are much higher for GREEN; ~226 kt per year in 2030 (fig. 6.5). Cumulative emissions in GREEN will also start to deviate from BAU from 2020. Cumulative emissions between 2010 and 2030 in GREEN are reduced by 20.8 Mt or 38% compared to BAU (fig. 6.6). Lastly, greenhouse gas intensity in 2030 is reduced by 486 g $CO_2$-eq/kWh (58%) in GREEN compared to the baseline (fig. 6.6).

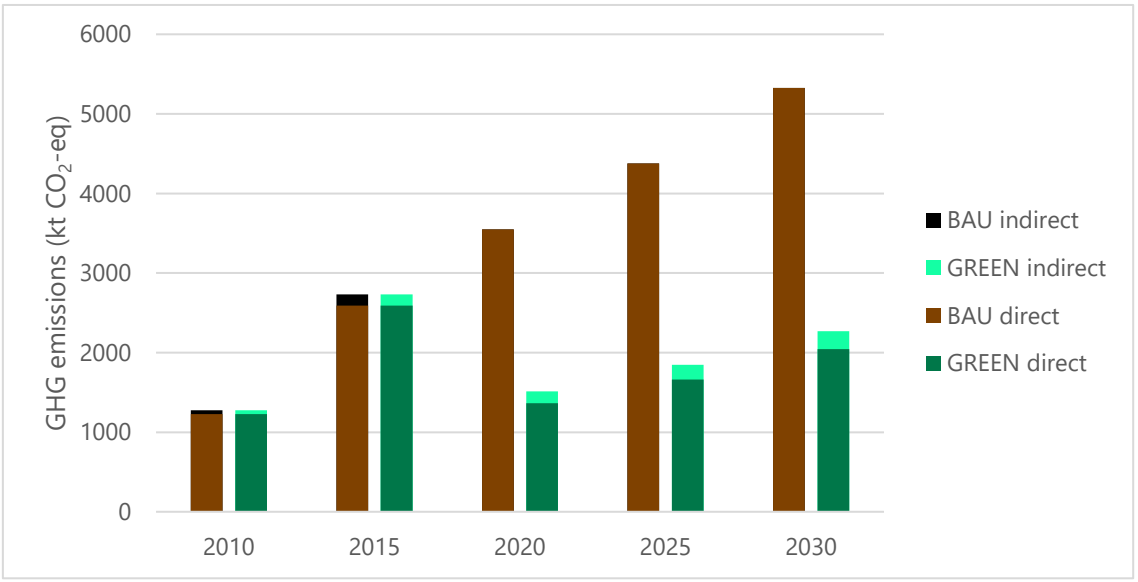


Figure 6.5. Total (in)direct emissions in two different scenarios 2010-2030 in Ulaanbaatar (incl. $N_2O$ and $CH_4$). Source: own figure.

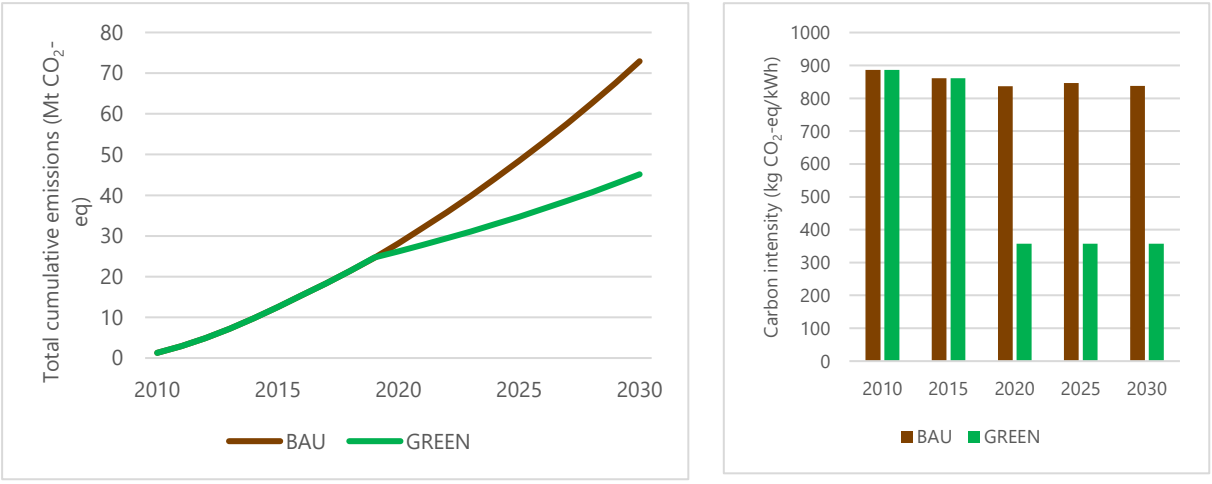


Figure 6.6. Left: Cumulative emissions for two scenarios 2010-2030. Right: greenhouse gas intensity for two scenarios 2010-2030. Source: own figures.

### 6.3.2 Costs

First of all, the sum of investment costs between 2010 and 2030 for GREEN (4.6 billion US$) is 924 million US$ – or 25% higher – than BAU. Especially costs for construction of wind power in V10 and roof PV increases the total investment costs significantly. Additionally, O&M costs in GREEN (105 million US$ in 2030) are two times higher compared to BAU. On the other hand, fuel costs in GREEN are diminished due to closing of CHP-2 and 3 and exclusion of Baganuur, which results in a reduction of 73 million US$ or 61% in 2030. If annualized investments are excluded, the sum of total O&M, fuel and import costs in 2030 are lower in GREEN compared to baseline (-10% in 2030; fig. 6.6). Total cumulative costs between 2010 and 2030 for GREEN are higher with an increase of 903 million US$ - or 14% - compared to baseline (fig. 6.7).

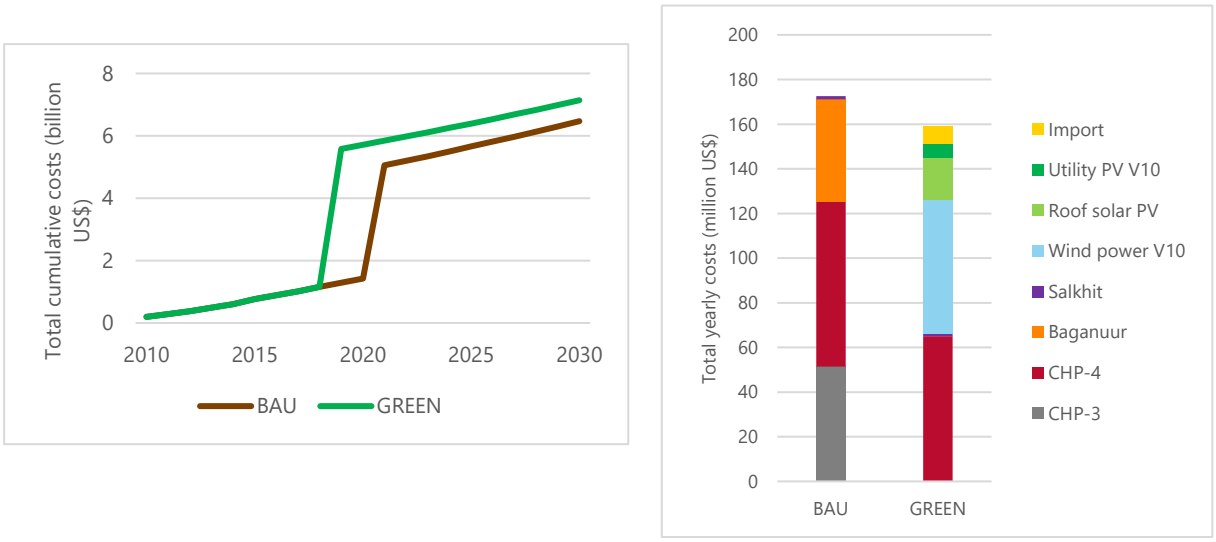


Figure 6.7. Left: Total cumulative costs for two scenarios in Ulaanbaatar 2010-2030. Right: Composition of yearly costs for both scenarios in 2030. Source: own figures.

The cost curve containing each LCOE per technology is shown in figure 6.8. Wind power V10 is the most expensive power source per generated electricity of both scenarios (21 US$cts/kWh), as the capacity factor is very low compared to solar energy and it is curtailed significantly by the grid's low capacity. Baganuur is projected to generate ~2.25 TWh per year to the CES in 2030, which means the 3.5 billion investment is relatively high, resulting in a LCOE of 16 US$cts/kWh. As mentioned earlier, this is expected to decrease as the amount of load hours will increase when other CHPs are closed due to old age. CHPs-3 and 4 are relatively cheap since initial investments are not included and fuel costs of lignite are relatively cheap due to acceptable plant efficiencies. However, solar PV technologies are only slightly more expensive than these CHPs (~3 cents/kWh).

$LCOE_{BAU}$ and $LCOE_{GREEN}$ are calculated using equations 3.7 and 6.2 and their yearly development is shown in figure 6.8. Average $LCOE_{GREEN}$ increases dramatically in 2019, when all major investments for new renewable capacity is projected, after which $LCOE_{GREEN}$ declines steadily to 7.8 cents/kWh in 2030. $LCOE_{BAU}$ also increases due to the Baganuur investment, after it remains stable and slightly decreases to 5.6 cents/kWh in 2030. Thus, in order to achieve the GREEN scenario in 2030, the additional needed levelized cost of electricity is 2.2 cents/kWh compared to baseline. The costs of greenhouse gas abatement in the GREEN scenario compared to baseline is 32 US$/t $CO_2$-eq abated.

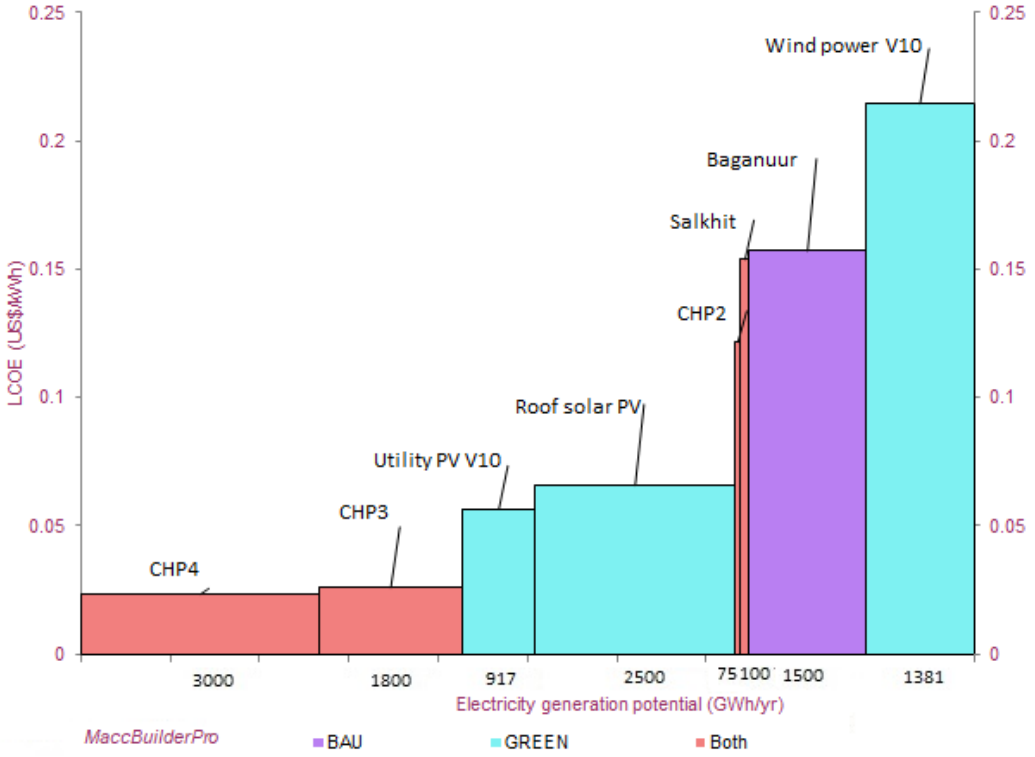


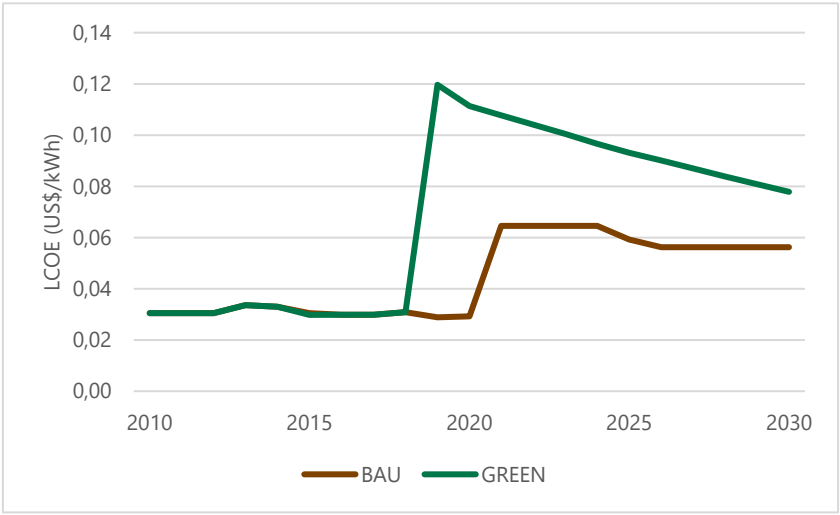


Figure 6.8. Upper: Cost curve containing LCOEs per technology operating in 2030. Lower: $LCOE_{BAU}$ and $LCOE_{GREEN}$ between 2010 and 2030. Source: own figures.

# 7. Barriers and policy

In order to answer the last research sub-question 6. '*What barriers exist to implementing renewable electricity in the Ulaanbaatar region and which policy instruments are needed to overcome them?*', the current policy and legal landscape regarding (renewable) energy in Mongolia is established. Secondly, a set of essential barriers within the current landscape are described for achieving the GREEN scenario together with suggested policies to overcome these.

In order to achieve the GREEN scenario instead of its baseline, various technical, economic and social barriers need to be overcome. The following four barriers are considered most important and are elaborated in this section:

1. Capacity of power grid
2. Unfair competition with aged power plants
3. Investments and subsidy scheme
4. Maintenance and public involvement

First, all acting laws and policies on renewable energy in Mongolia need to be determined. In 2007 the Renewable Energy Law was adopted, which includes a subsidy scheme for renewables (see 3). Formal authorities for executing this law are Parliament, the Government of Mongolia, the State Administrative Authority, the Governors of Aimags (a first-level administrative sub-division) and the Capital city. According to article 7.1 of this law, the city of Ulaanbaatar has some jurisdiction as it has the authority to *''organize implementation of legislation on energy and decisions issued by competent authorities and develop policies on energy supply of their respective territories in cooperation with relevant authorities.'' (*MoE, 2007).

Furthermore, the National Renewable Energy Program was issued in 2005 by the Ministry of Energy (MoE, 2005). This program included policies to stimulate renewable energy in Mongolia and coined two goals: achieving a renewable electricity share of 3-5% in 2010 and a share of 20-25% in 2020. In 2015 a more recent version of renewable policy was adopted in the Mongolia State Policy on Energy 2015-2030 which focuses on 1) energy safety and establishing foundations for a renewable sector (2015-2023) and 2) exporting secondary energy and developing a renewable energy sector (2024-2030) (IEA, 2015). This program does not include any quantitative goals like its predecessor. In order to achieve a high renewable electricity share while bearing these laws and policies in mind, four major barriers with corresponding recommended policies are further described below:

1. Low capacity of (international) power grid

As shown earlier in this study, renewable electricity output by solar PV and wind energy is variable on a daily and seasonal basis. Therefore, a significant capacity of transmission lines is needed to enable import and export of electricity in order to achieve high renewable electricity shares. EnergyPLAN models used in section 3.4.1 require a minimum capacity of ~415 MW with given projected demand and supply in Ulaanbaatar in 2030 for the GREEN scenario. Higher capacities would result in less curtailment of wind and solar electricity generation during the day, which increases renewable share and lowers costs per kWh.

However, the current estimated capacity for import and export from CES to Russia is estimated only 100-180 MW, which causes financial losses due to differences between electricity prices during peak hour and at night (CEE Bankwatch, 2017). Reportedly, various licensed developers have run into problems while implementing renewable capacity in the low-capacity power grid of the CES (Renewable Energy World, 2017). There are plans to improve national interconnectivity of electricity systems, but whether plans are being developed for advancing international transmission lines is currently unknown. In fact, Mongolia could take an active role in improving international power connections, such as joining the Asia Super Grid project, because of its geographical position in Asia, ample energy resources and the will to meet growing electricity demand (Batmunhk, 2018).

This first barrier does not only apply to achieving the GREEN scenario; in order to meet increasing electricity demand and be more reliable in any scenario in the future, the power grid needs be able to absorb more capacity. The Ministry of Energy should take initiative to arrange significant investments for expanding the electricity grid.

2. Unfair competition with aged power plants

It has become clear from section 3.2.3 that existing CHPs in the capital city are operating very cost-effectively compared to any (non-) renewable newly built capacity. CHP-2 and 3 are long overdue considering their respective ages of 53 and 46 years and their initial investment costs are well written off. Additionally, both plants receive their fuel from local lignite mines which assures cheap electricity generation even more. In the meanwhile, these plants have very low efficiencies and contain extremely high specific plant emissions, which cause disastrous consequences to air quality in Ulaanbaatar (Allen, 2013; Amarsaikhan, 2014). Competing with these sources of generation is very hard; new non-renewable capacity like Baganuur, which will be built with similar technology and fuel use, would be ~14 US$cts/kWh more expensive than existing CHPs due to significant needed investments. It is a major challenge for renewable capacity with even higher initial investments and maintenance costs to compete with current suppliers.

A way of resolving this unfair competition and improving the business cases of renewable projects is to establish minimum standards for power plants with respect to efficiency and emissions by law. In the European Union each new or retrofitted industrial plant must include combustion technologies which meet best-available techniques (BAT; EC, 2017). GoM could adopt similar laws to prevent that more subcritical and inefficient will be built in the future. Additionally, the government should issue requirements to existing power plants with respect to efficiency, emissions and age, resulting in the prohibition of CHP-2 and 3 from keeping generating electricity and ensuring that CHP-4 gets replaced as soon as its lifetime is reached.

3. Investments and subsidy scheme

As shown in section 3.4.4, costs per kWh are only slightly higher for GREEN compared to the baseline, but significantly more investments are needed to achieve it. Private (foreign) developers should be stimulated to invest in renewable capacity in Ulaanbaatar and Mongolia in general. Currently, general interest is growing more and more and potential renewable energy projects are lining up, such as the Scaling-up Renewable Energy Program (SREP) including a 10 MW solar-PV project in the Western Region (GoM, 2015). Foreign investors are especially keen because of the beneficial feed-in-tariff (FIT) the GoM has been granting since 2007. Tariffs range between 8.0-9.5 US$cts/kWh for wind power, 15-18 US$cts/kWh for solar PV and 4.5-6.0 US$cts/kWh for hydropower up to 5 MW (IEA, 2007). In comparison, Dutch SDE+ subsidies are around 6.0 €cts/kWh for onshore wind and 9.0 €cts/kWh for solar PV (RES Legal, 2019).

The aforementioned FITs were promised to developers by GoM and any price difference caused by renewable electricity supply is absorbed into the selling prices of other generators connected to the central grid, which increases tariffs for consumers and creates the earlier mentioned problems with limited grid capacity (Renewable Energy World, 2017). Currently, this subsidy scheme is stimulating renewable projects in Mongolia while it should be updated to schemes that better fit the situation in the coming years. GoM has already started exploring other options for alternative subsidy schemes, for instance in the SREP project (Renewable Energy World, 2017). Current and future FITs were not taken into account in the construction of the GREEN scenario, which is further discussed in section 8.2.

4. Maintenance and public involvement

It has become clear from section 3.5.2 that the GREEN scenario includes technologies with significantly higher maintenance costs. These costs may even be higher due to rough weather conditions in Mongolian winter, which is why maintenance of newly built renewable capacity should not be underestimated. Experiences from several

case-studies surrounding implementation of renewable capacity in developing countries in Asia state that regular monitoring of the equipment is important for a project to be successful (Urmee, 2009). For local small-scale projects, involving the public by enabling to their own technology and giving responsibility for day-to-day maintenance to users and local people reduces maintenance costs significantly (Urmee, 2009).

In the case of GREEN scenario, projected roof PV capacity should be (partly) owned by consumers and local companies in order to create ownership and to maximize benefits. These systems should be partly subsidized by GoM, in a way that low-income households could also benefit from this development, without substantially increasing consumers prices. Such a program should include some sort of information campaign in order to increase public acceptance.

# 8. Discussion

This chapter includes the reliability of the methodology applied in this study and its outcomes. First, a sensitivity analysis is performed and discussed. Secondly, additional limitations of this study and theoretical implications of its results are debated.

## 8.1 Sensitivity analysis

A sensitivity analysis is conducted in order to establish the importance of certain parameters to the results of this thesis. This is accomplished by using the one-factor-at-a-time (OFAT) method (Delgarm, 2018). First, the range of uncertainty is determined for high impacting parameters described in chapters 2-6. Secondly, one input variable is moved, while all others are kept at their nominal values. Finally, changes in $GHG_{BAU}$, $GHG_{GREEN}$, $LCOE_{BAU}$ and $LCOE_{GREEN}$ are documented and the moved variable is brought back to its nominal value. This method is repeated for the following variables:

- Capital costs
- O&M costs
- Discount rate
- Coal price
- Electricity demand
- Lifetime of technologies

First of all, the initial investments for existing CHPs are included in this analysis. In order to estimate these costs, a rule-of-thumb is derived from the Baganuur investment, resulting in a cost of capacity of ~5 US$/W. The resulting initial capital costs for building the 2010 capacities of CHP-2, 3 and 4 are therefore estimated at 0.1, 0.7 and 2.9 billion US$, which limits the difference of LCOE between both scenarios to only 0.6 cents/kWh (table 8.2).

Salkhit wind farm demanded a particularly high investment of 2400 US$ per kW. However, this occurred in 2010 and it is assumed that cost of wind power technology has reduced significantly in 2020. Therefore, for this sensitivity analysis the assumed Chinese capitals costs for renewable capacity were changed to Russian prices which are projected to be significantly higher in 2020 (table 8.1; IEA, 2016c). Applying these changes, $LCOE_{GREEN}$ increases to 12 cents/kWh, which enlarges the gap compared to baseline to 6.5 cents/kWh. These investment costs of (non-) renewable capacity have the highest impact on this study's end results and their effect on $LCOE_{BAU}$, $LCOE_{GREEN}$, $LCOE_{BAU}$-$LCOE_{GREEN}$ ($LCOE_{difference}$) and individual LCOE per technology is shown in the error margin in figure 8.1.

Maximizing renewable O&M costs to Russian prices also has some impact, but only results in a slight increase of $LCOE_{GREEN}$ (0.9 cents/kWh). Furthermore, instead of the chosen discount rate (8%), a higher discount rate (15%) causes all sources of electricity with high investment costs to become more expensive, while lower discount rate (5%) does not have major effects on LCOE per technology. Changing the discount rate only results in slight changes to $LCOE_{difference}$, ranging between -0.6 cents/kWh and +0.5 cents/kWh. Altering the lifetime of technologies has similar effect; changing the lifetimes of technologies to their minimum and maximum values (25/60 yr for CHPs, 15/25 yr for wind power and 20/30 yr for solar power) results in changes to $LCOE_{difference}$ of +0.1 and -0.8 US$cts/kWh (table 8.2).

If the minimum price of coal is assumed (37.7 US$, fig. 3.3) instead of the average price (61.3 US$), both scenarios drop in price, but since BAU contains higher fuel consumption, costs of electricity drop to 7.2 cents/kWh in GREEN compared to 4.8 cents/kWh in the baseline. If the maximum coal price is assumed (106.7 US$), baseline costs increase to 7 cents/kWh, only 0.9 cents cheaper than GREEN.

Lastly, if the needed electricity generation is changed to ADB Bear market scenario values which increase to 7.7 TWh in 2030 (error margin in section 2.2.3), the reduction of GHG emissions compared to baseline increases from 3.1 to 4.2 Mt $CO_2$-eq in 2030. Higher electricity demand would therefore reduce more greenhouse gas emissions in the GREEN scenario. Additionally, Wind power V10 would be slightly less curtailed, resulting in $LCOE_{GREEN}$ to reduce slightly to 7.6 US$cts/kWh. This suggests electric capacity in the GREEN scenario is capable of enduring increasing electricity demand beyond 2030.

Table 8.1. Projected Russian prices for renewable capacity in 2020. Source: IEA. 2016

| | Capital costs (US$/kW) | O&M (US$/kW) |
|---|---|---|
| Large-scale solar PV | 1760 | 24 |
| PV buildings | 2300 | 32 |
| Onshore wind | 2040 | 52 |

Table 8.2. Overview of outcomes of OFAT method on LCOE and GHG for both scenarios in the year 2030. Source: own table.

| US$/kWh in 2030 | $LCOE_{BAU}$ | $LCOE_{GREEN}$ | $LCOE_{difference}$ | $\Delta LCOE_{difference}$ |
|---|---|---|---|---|
| *Nominal value* | *0.056* | *0.078* | *0.022* | *0* |
| Inclusion non-renewable capital costs | 0.086 | 0.092 | 0.006 | **-0.016** |
| Increased renewable capital costs | 0.056 | 0.120 | 0.065 | **+0.043** |
| Increased renewable O&M costs | 0.056 | 0.084 | 0.028 | +0.006 |
| Changed discount rate | 0.046-0.081 | 0.062-0.108 | 0.016-0.027 | - 0.006<br>+ 0.005 |
| Changed lifetime of technologies | 0.055-0.060 | 0.069-0.081 | 0.014-0.021 | - 0.008<br>+0.001 |
| Changed coal price | 0.049-0.070 | 0.072-0.079 | 0.023-0.009 | - 0.013<br>+0.001 |

| Mt $CO_2$-eq in 2030 | $GHG_{BAU}$ | $GHG_{GREEN}$ | $\Delta GHG$ |
|---|---|---|---|
| Nominal value | 5.34 | 2.27 | -3.07 |
| Increased electricity demand | 6.48 | 2.27 | -4.2 |

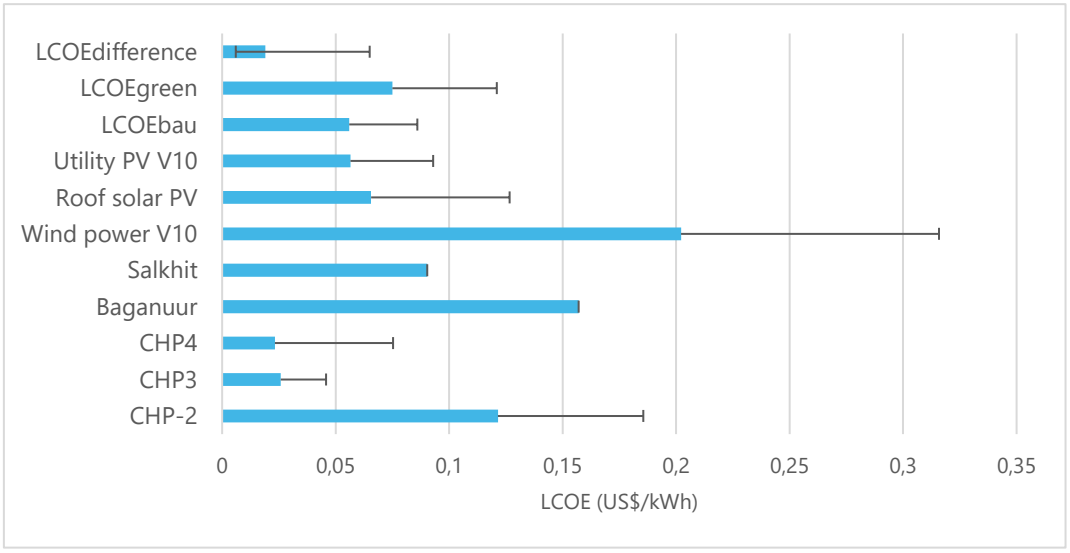


Figure 8.1. Changes in LCOE per technology with increased capital costs. Source: own figure.

## 8.2 Limitations

The applied methodology in this research and its corresponding outcomes contain several limitations. This section first discusses the outcomes of the sensitivity analysis and its consequences to the study's reliability. Secondly, other limitations are discussed, among which necessary assumptions due to limited data availability.

The sensitivity analysis performed in the previous section explores the effect of changing high-impact variables to the end results of this research. This resulted in an error margin of $LCOE_{difference}$ between -72% (-1.3 cents/kWh) and +195% (+4.3 cents/kWh), which mainly depends on (increased) capital costs of technologies. $LCOE_{GREEN}$ causes the largest uncertainty, as Russian prices for renewable technology are considerable higher than Chinese prices. Project developers, which aim at constructing renewable capacity in the Ulaanbaatar area, should take care when purchasing technology to limit investment costs. The error margin could be reduced if more financial specifics were known on existing or future capacity in Mongolia. However, at the time of writing, these specifics are unknown since reliable (scientific) literature is lacking.

Apart from significant parameter sensitivity, the applied methodology has some other limitations. It primarily focuses on renewable electricity rather than supplying heat. Therefore, all the calculated greenhouse gas emissions originate from electricity generation, which is a simplification compared to reality. Introducing renewable heat to the city's infrastructure may complicate the situation. Additionally, determining the minimum amount of load hours by CHP-4 in order to meet UB's heat supply was not included in this study due to time constraints.

Secondly, the current subsidy scheme for renewables in Mongolia (feed-in tariff; chapter 7) is not taken into account while constructing the scenarios. If current FITs for solar power (15 cents/kWh) and wind power (8 cts/kWh) are applied to the GREEN scenario, LCOE for Wind Power V10 is reduced to 13 cents/kWh and $LCOE_{GREEN}$ to -0.5 US$cts/kWh in 2030 due to negative costs of high-share utility- and roof solar PV. This confirms that, according to this scenario, Mongolia's current FITs for solar PV could be lowered to 3-5 US$cts/kWh to be able to compete with existing CHPs. On the other hand, if the low capacity factors calculated with this study are representative for actual performance of wind power in Mongolia, it needs an increase of its current FIT.

Thirdly, due to limited data availability on local statistics regarding electricity generation, some assumptions have been made which could have simplified the results. For instance, at times national indicators were assumed to be the same as at city-level, such as future GDP growth rates and share of electricity imports or losses. In this study this is considered acceptable because of Ulaanbaatar's large contribution to national population, GDP and electricity demand. Additionally, general rules-of-thumb have been used in case specific data was missing, for instance the indirect emissions originating from the construction of wind turbines. In some cases (i.e. O&M costs or share of electricity losses) were assumed to be frozen until 2030. In the case of O&M, costs would probably increase for old power plants until 2030, but no reliable information about these plants could support this. Furthermore, the costs of sustained replacement of capacity that has reached its lifetime, is not included in this study, as most power sources remain operational during the whole length of the scenario or capacity does not need replacing (CHP-2) because of already existing alternatives. Lastly, solar and wind potential is calculated from a one-year data set due to time constraints, which could be more accurate if multiple years are included in the necessary calculations.

This study is internally consistent, because boundary conditions such as discount rate, GDP growth, electricity demand and lifetimes of technologies, are constant for both scenarios. The majority of results are based on (physically) accurate mathematical correlations which ensure viability of the results. In short, this study proposes a transparent method with a public dataset, which should result in similar reliable outcomes among researchers.

## 8.3 Implications

This study has combined a small-scale potential analysis of renewable technology with the ability of these renewables to meet projected electricity demand. This integral approach including both supply and demand-side analyses underlines that this study's results are likely to be feasible and applicable to local context, which is generally not the case in scientific literature. In order to improve this methodology, more detailed modelling of a city's energy system should be conducted, which includes heat supply, precise system boundaries and dense local information rather than general assumptions. Future research could therefore be able to project more accurately how much capacity needs to be built in order for a city to lower its dependency on carbon-based energy supply.

This study has shown that it might be possible for a developing city like Ulaanbaatar to transition to maximum renewable electricity before 2030 without excessive increases in costs, which could reduce greenhouse gas emissions significantly. The existing subsidy scheme in combination with projected net exporting of electricity may cause the GREEN scenario to be more cost-effective than the business-as-usual scenario. If lignite-fired electricity generation were to be replaced by, for instance, natural gas (using a 60% efficiency and emission factor of 15.3 t C/TJ; IPCC, 1996), CHP-4 would emit ~860 kton $CO_2$ in 2030, which is an additional 58% reduction compared to projected GREEN emissions. Therefore, it is important for Ulaanbaatar to search for feasible non-variable alternatives like hydropower, biomass or geothermal power plants in order to provide reliable electricity baseloads.

In the case of Ulaanbaatar, it is especially important to decrease its non-renewable share, because of adverse effects on air quality. However, it is important to proceed with care, because previous reports have already proven that increasing renewable capacity cannot be done without improving local grid's electricity capacity. Therefore, (local) government has the prime responsibility to oversee the integrality of the energy system and only to grant licenses to renewable projects if the grid is able to absorb increased variable output. At last, it is recommended to implement aforementioned policy measures like setting standards for power plants and stimulating private ownership of renewable capacity.

# 9. Conclusions

While renewable energy goals on global and national level, such as the European 20-20-20 targets or the Dutch National Climate Accord, are gaining more and more attention, it has become increasingly important how to achieve these goals by implementing renewables on a regional or local scale. Therefore, it is vital to develop methodologies for zooming in on current and future local energy demand in combination with determining potential of renewable capacity. Only then it is possible to project future costs and avoided emissions more precisely on a local scale. This study aims to unite electricity demand and supply-side analyses in combination with a thorough local potential analysis of wind and solar power. This research uses Ulaanbaatar as a case-study in order to answer the following sub-questions and general research question below.

*Sub-question 1: What is the projected electricity demand of the Ulaanbaatar region until 2030?*

In this study it is assumed needed electricity generation depends on electricity intensity, gross domestic product, losses and imports. Ulaanbaatar's gross domestic product ($GDP_{city}$) is expected to increase from 2.4 billion US$ in 2010 to 12.1 billion US$ in 2030. Resultingly, the city's electricity demand is projected to increase from 1.44 TWh in 2010 to 6.36 TWh in 2030.

*Sub-question 2: What is the needed capacity and are the costs and emissions in the business-as-usual scenario in order to meet projected electricity demand until 2030?*

In the business-as-usual scenario, current capacity is expected to remain operational until 2030, with the exception of the closure of CHP-2 in 2026. New CHP Baganuur (700 MW) will start operation in 2021 in order to meet increasing demand. Electricity will cost approximately 0.056 US$/kWh or 6.5 billion US$ between 2010 and 2030, in which CHP-3 and 4 are the cheapest sources of supply. According to this scenario, electricity generation results in total yearly greenhouse gas emissions of 5.4 Mt $CO_2$-eq in 2030 and cumulative emissions of 73 Mt $CO_2$-eq between 2010 and 2030. Electricity generation will contain a greenhouse gas intensity of 843 g $CO_2$-eq/kWh in 2030.

*Sub-question 3: What is the deployment potential of renewable electricity sources in the Ulaanbaatar region?*

The southern part of the researched area surrounding Ulaanbaatar is highly suitable for wind power (88-90%) and solar power capacity (84-90%), whereas the northern part closer to the city is less suitable (56-78% for wind and 34-66% for solar power), due to the occurrence of permafrost, protected or urbanized areas, forests, croplands, water bodies and relief. Global in-plane irradiance on panels facing south varies between 242 W/m$^2$ in the south and 230 W/m$^2$ in the north, resulting in an average capacity factor of 0.237. The average wind speed at 80 meters altitude is estimated to be 5.33 m/s, resulting in a lower capacity factor between 0.081 near the city and 0.168 towards the south. Rated maximum power ranges from 11.4 GW (10.7 TWh/yr) to 41.3 GW (53.6 TWh/yr) per grid cell for wind power and from 134 $GW_p$ (271 TWh/yr) to 1077 $GW_p$ (2264 TWh/yr) for large-scale solar PV. Estimated suitable rooftop area per person will be 11.7 m$^2$ per person in 2030, which could yield a maximum yearly power output of 3.5 TWh using roof solar PV. Thus, total renewable potential for solar and wind power exceeds projected demand in Ulaanbaatar by far.

*Sub-question 4: How can variable renewable electricity output be compensated in the Ulaanbaatar region?*

Exporting peak hour renewable supply and importing at lower generation periods is a viable option for achieving high renewable electricity shares in the GREEN scenario. However, maximum capacity of the city's electricity grid puts a major restraint on the extent of net-export of electricity, which is projected to be limited to 1.09 TWh/yr in 2030. In the GREEN scenario, CHP-4 will fill the remaining electricity gaps to a total of 23% (2.55 TWh/yr) in 2030.

Greenhouse gas emissions by this plant could be reduced with 58% if natural gas would replace lignite-fired generation and by 100% if it is replaced by a hydropower or biomass plant.

*Sub-question 5: What are the resulting costs and indirect emissions of implementing a high share of renewable electricity, compared to the business-as-usual scenario?*

The maximum renewable electricity share in GREEN is estimated to be 77% in Ulaanbaatar in 2030 (54% solar and 23% wind power). New needed capacity includes 1988 MW wind power, 1381 MW roof solar PV and 482 MW utility PV, which are projected to generate 1.41 TWh, 2.50 TWh and 0.92 TWh respectively in 2030. The share of renewable electricity could increase even more if the grid capacity would be improved significantly. Levelized cost of electricity in the GREEN scenario is estimated to be 38% more expensive compared to baseline (0.078 US$/kWh or 7.1 billion US$), mainly due to investments in new renewable capacity. The estimated total reduction of greenhouse gas emissions between 2010 and 2030 is 28.1 Mt $CO_2$-eq or 38% compared to baseline., of which direct emissions by CHP-4 and indirect emissions by renewable capacity construction are major contributors in the GREEN scenario. Greenhouse gas intensity in 2030 is reduced by 486 g $CO_2$-eq/kWh compared to the baseline.

*Sub-question 6: What barriers exist to implementing renewable electricity in the Ulaanbaatar region and which policy instruments are needed to overcome them?*

There are four major barriers which prevent achieving high renewable electricity shares in Ulaanbaatar until 2030: low capacity of the power grid, unfair competition with old CHPs, high initial investment cost and maintenance and public ownership. In order to face these challenges, the (inter) national transmission grid needs to be expanded and standards for power suppliers should be established. Additionally, the current feed-in tariff scheme needs to be updated and unnecessary maintenance costs prevented by involving the public and stimulating private ownership. To summarize, the main research question of this thesis is answered:

**What is the renewable electricity potential in a developing city and what are the costs, emissions and barriers of achieving a high renewable electricity share before 2030?**

The investigated research area surrounding Ulaanbaatar has enormous renewable potential due to extremely low population density: 35 GW/grid cell for wind power to 781 $GW_p$/grid cell for solar energy. Potential is higher towards the south due to lower occurrence of permafrost, protected or urbanized areas, forests, croplands, water bodies and relief and higher wind speeds and solar irradiation. Capacity factors in the Ulaanbaatar area for wind and solar power are 0.149 and 0.237, resulting in a yield of 40.5 TWh/yr/grid cell and 1625 TWh/yr/grid cell respectively, which exceeds projected electricity demand by far. If balancing of supply and demand is taken into account, a share of 77% renewable electricity can be achieved, which contains solar and wind power of which the latter is significantly curtailed by limited grid capacity. The costs of achieving this share before 2030 is ~2.16 US$cts/kWh or 0.9 billion US$, compared to business-as-usual, which reduces cumulative emissions by 54% between 2019 and 2030. Besides improving grid capacity, various challenges arise in order to achieve maximum renewable share, such as establishing standards for combustion plants, updating the subsidy scheme and involving the public.

These results may be similar to other developing cities surrounded by area with moderate population density, vegetation and relief, such as cities in North Africa, the Middle-East, South America or China. These cities are likely to have enough renewable potential to meet their demand in the future and to achieve significant renewable electricity shares before 2030. However, comparable challenges might arise as well with respect to variable electricity output, grid capacity and searching for adequate subsidy schemes. Additionally, cities situated in more densely populated areas may face additional challenges such as competition with agriculture, infrastructure and the building sector.

# 10. References


Adiyasuren, E., Damba, U. O., & Tsedensodnom, B. (2013). Comparison of power generation from solar panel with various climate condition and selection of best tilt angles in Ulaanbaatar. In Strategic Technology (IFOST), *2013 8th International Forum* on (Vol. 2, pp. 519-521). IEEE.

Allen, R. W., Gombojav, E., Barkhasragchaa, B., Byambaa, T., Lkhasuren, O., Amram, O., ... & Janes, C. R. (2013). An assessment of air pollution and its attributable mortality in Ulaanbaatar, Mongolia. *Air Quality, Atmosphere & Health*, *6*(1), 137-150.

Amarsaikhan, D., Battsengel, V., Nergui, B., Ganzorig, M., & Bolor, G. (2014). *A study on air pollution in Ulaanbaatar city, Mongolia. Journal of Geoscience and Environment Protection,* 2(02), 123.

Amirnekooei, K., Ardehali, M. M., & Sadri, A. (2012). Integrated resource planning for Iran: Development of reference energy system, forecast, and long-term energy-environment plan. *Energy, 46*(1), 374-385.

Andrews, J., & Jelley, N. (2017). Energy science: principles, technologies, and impacts. *Oxford University Press*.

Antvorskov, S. (2008). Introduction to integration of renewable energy in demand controlled hybrid ventilation systems for residential buildings. *Building and Environment*, 43(8), 1350-1353.

Arino, O., Ramos Perez, J. J., Kalogirou, V., Bontemps, S., Defourny, P., & Van Bogaert, E. (2012). Global land cover map for 2009 (GlobCover 2009). *ESA & UCL*.

Arvesen, A., & Hertwich, E. G. (2012). Assessing the life cycle environmental impacts of wind power: A review of present knowledge and research needs. *Renewable and Sustainable Energy Reviews, 16*(8), 5994-6006.

Asia Foundation (2014). *Ulaanbaatar 2020 Master Plan and development approaches for 2030. Technical summary*. https://asiafoundation.org/resources/pdfs/UBMasterPlanTechnicalSummary.pdf

Asian Development Bank (2013). Technical Assistance Consultant's Report. *E. Gen Consultants Ltd. Bangladesh in association with MVV decon GmbH, Germany, and Mon-Energy Consult, Mongolia*

Asian Development Bank (2018) *Asian Development Outlook 2018. How technology affects jobs.* https://www.adb.org/sites/default/files/publication/411666/ado2018.pdf

Batmunkh, S., & Battogtokh, Z. (2007). The exhausting pollutants from coal combustion of Fourth Thermal Power Plant of Ulaanbaatar. *Strategic Technology, 2007*. IFOST 2007. International Forum on (pp. 158-161). IEEE.

Batmunkh, S., Stennikov, V., Bat-Erdene, B., & Erdenebaatar, A. (2018). Mongolia's potential in international cooperation in the Asian energy space. *E3S Web of Conferences* (Vol. 27, p. 01006). EDP Sciences.

Blok, K., & Nieuwlaar, E. (2009). *Introduction to energy analysis*. Chapter 12. Taylor & Francis.

Bogdanov, D., & Breyer, C. (2015). Eurasian Super Grid for 100% Renewable Energy power supply: Generation and storage technologies in the cost optimal mix. *In Proceedings of the ISES Solar World Congress*.

Borgford-Parnell, N. (2011). Synergies of scale: A vision of Mongolia and China's common energy future. *Energy policy, 39*(5), 2764-2771.

Branker, K., Pathak, M. J. M., & Pearce, J. M. (2011). A review of solar photovoltaic levelized cost of electricity. *Renewable and sustainable energy reviews, 15*(9), 4470-4482.

Breyer, C., Bogdanov, D., Komoto, K., Ehara, T., Song, J., & Enebish, N. (2015). North-East Asian super grid: renewable energy mix and economics. *Japanese Journal of Applied Physics, 54*(8S1), 08KJ01.

Brundtland, G., Khalid, M., Agnelli, S., Al-Athel, S., Chidzero, B., Fadika, L., ... & Singh, M. (1987). Our *common future (\'brundtland report\')*.

Byrne, J., Taminiau, J., Kurdgelashvili, L., & Kim, K. N. (2015). A review of the solar city concept and methods to assess rooftop solar electric potential, with an illustrative application to the city of Seoul. *Renewable and Sustainable Energy Reviews, 41*, 830-844.

CEE Bankwatch Network (2017). *Mongolia's energy sector: time for a rethink*.

Climate Change Project Implementing Unit (2017). *Mongolia's National Inventory Report – 2017 Annex to Initial Biennial Update Report to UNFCCC*. https://unfccc.int/files/national_reports/non-annex_i_parties/ica/technical_analysis_of_burs/application/pdf/mongolia-bur1-1-nir.pdf

Climate-data.org (n.d). *Climate Ulaanbaatar*. https://en.climate-data.org/asia/mongolia/ulaanbaatar/ulaanbaatar-490/#climate-graph

The Conversation (2012). *Fuji can't function without oil: cheap renewables could reduce the risk*. https://theconversation.com/fiji-cant-function-without-oil-cheap-renewables-could-reduce-the-risk-5354

Crijns-Graus (2016). Renewable energy: past trends and future growth in 2 degrees scenarios. *CPESE 2016*: 8-10 September 2016, Kitakyushu, Japan.

Davy, P. K., Gunchin, G., Markwitz, A., Trompetter, W. J., Barry, B. J., Shagjjamba, D., & Lodoysamba, S. (2011). Air particulate matter pollution in Ulaanbaatar, Mongolia: determination of composition, source contributions and source locations. *Atmospheric Pollution Research, 2*(2), 126-137.

Delgarm, N., Sajadi, B., Azarbad, K., & Delgarm, S. (2018). Sensitivity analysis of building energy performance: A simulation-based approach using OFAT and variance-based sensitivity analysis methods. *Journal of Building Engineering, 15*, 181-193.

Detert, N., & Kotani, K. (2013). Real options approach to renewable energy investments in Mongolia. *Energy Policy, 56*, 136-150.

Dhakal, S. (2010). GHG emissions from urbanization and opportunities for urban carbon mitigation. *Current Opinion in Environmental Sustainability, 2*(4), 277-283.

Dorj, P. (2015). Geothermal development in Mongolia: country update. In *Proceedings, World Geothermal Congress*.

Duffie, J. A., & Beckman, W. A. (2013). *Solar engineering of thermal processes*. John Wiley & Sons.

Earth Resources Observation and Science (EROS) Center (n.d.) USGS EROS Archive - Digital Elevation - Global 30 Arc-Second Elevation (GTOPO30). https://www.usgs.gov/centers/eros/science/usgs-eros-archive-digital-elevation-global-30-arc-second-elevation-gtopo30?qt-science_center_objects=0#qt-science_center_objects

Economic Research Institution (2017). *Report Coal Market Study*. https://www.eri.mn/download/NUURS.pdf

Elliott, D., Schwartz, M., Scott, G., Haymes, S., Heimiller, D., & George, R. (2001). Wind energy resource atlas of Mongolia (No. NREL/TP-500-28972). *National Renewable Energy Lab*., Golden, CO (US).

EnergyPLAN (n.d.) Advanced energy system analysis computer model. *Sustainable Energy Planning Research group at Aalborg University.* https://www.energyplan.eu/

Enkhtuul, T., & Undarmaa, C. (2013). Statistical study and analysis on electricity consumption of the city of Ulaanbaatar. *In Strategic Technology* (IFOST), 2013 8th International Forum on (Vol. 2, pp. 640-643). IEEE.

European Commission (2017). Commissions implementing decision (EU) 2017/1442 of 31 Juli 2018 establishing best available techniques (BAT) conclusions, under Directive 2010/75/EU of the European Parliament and of the Council, for large combustion plants. https://eur-lex.europa.eu/legal-content/EN/TXT/PDF/?uri=CELEX:32017D1442&from=EN

Farukh, M. A., Hayasaka, H., & Mishigdorj, O. (2009). Recent tendency of Mongolian wildland fire incidence: analysis using MODIS hotspot and weather data. *Journal of Natural Disaster Science, 31*(1), 23-33.

Feng, Y. Y., Chen, S. Q., & Zhang, L. X. (2013). System dynamics modeling for urban energy consumption and CO2 emissions: A case study of Beijing, China. *Ecological Modelling, 252*, 44-52.

Ganchimeg, G., & Havrland, B. (2011). Economic analysis of household energy consumption: the case of herders in Mongolia. *AGRICULTURA TROPICA ET SUBTROPICA, 44*, 4.

Global Modeling and Assimilation Office (GMAO) (2008a), tavg1_2d_slv_Nx: MERRA 2D IAU Diagnostic, Single Level Meteorology, Time Average 1-hourly V5.2.0, Greenbelt, MD, USA, Goddard Earth Sciences Data and Information Services Center (GES DISC), 10.5067/B6DQZQLSFDLH. https://disc.gsfc.nasa.gov/datasets/MAT1NXSLV_V5.2.0/summary

Global Modeling and Assimilation Office (GMAO) (2008b), tavg1_2d_rad_Nx: MERRA 2D IAU Diagnostic, Radiation Surface and TOA, Time Average 1-hourly V5.2.0, Greenbelt, MD, USA, Goddard Earth Sciences Data and Information Services Center (GES DISC), 10.5067/RI9VTUQN74XJ. https://disc.gsfc.nasa.gov/datasets/MAT1NXRAD_V5.2.0/summary

Global Wind Atlas (n.d.) *Map of Mongolia*. https://globalwindatlas.info/en/area/Mongolia?print=true

Government of Mongolia (2015). *SCALING-UP RENEWABLE ENERGY PROGRAMME (SREP) - Investment Plan for Mongolia*. https://www.climateinvestmentfunds.org/sites/cif_enc/files/srep_ip_mongolia_final_14_dec_2015-latest.pdf

Government of Mongolia, Ministry of Energy (2017). *Energy sector of Mongolia, Policy and Strategies*.

Greenhouse Gas Protocol (2013). *Global Protocol for Community-Scale Greenhouse Gas Emission Inventories (GPC)*. http://ghgprotocol.org/sites/default/files/standards/GHGP_GPC_0.pdf

Griggs, D., Stafford-Smith, M., Gaffney, O., Rockström, J., Öhman, M. C., Shyamsundar, P., ... & Noble, I. (2013). Policy: Sustainable development goals for people and planet. *Nature, 495*(7441), 305.

Grossmann, W. D., Grossmann, I., & Steininger, K. W. (2013). Distributed solar electricity generation across large geographic areas, Part I: A method to optimize site selection, generation and storage. *Renewable and Sustainable Energy Reviews, 25*, 831-843.

Gruber, S. (2012). Derivation and analysis of a high-resolution estimate of global permafrost zonation. *The Cryosphere, 6*(1), 221.

Guttikunda, S. (2008). Urban air pollution analysis for Ulaanbaatar, Mongolia. *The World Bank Consultant Report*, Washington DC USA

Guttikunda, S. K., Lodoysamba, S., Bulgansaikhan, B., & Dashdondog, B. (2013). Particulate pollution in Ulaanbaatar, Mongolia. *Air Quality, Atmosphere & Health, 6*(3), 589-601.

Hahn, J. S., Yoon, Y. S., Yoon, K. S., Lee, T. Y., & Kim, H. S. (2012). A study on development potential of shallow geothermal energy as space heating and cooling sources in Mongolia. *Transactions of the Korea Society of Geothermal Energy Engineers, 8*(2), 36-47.

Hallgren, W., Gunturu, U. B., & Schlosser, A. (2014). The potential wind power resource in Australia: a new perspective. *PloS one, 9*(7), e99608.

Harris et al., 2014: Updated high-resolution grids of monthly climatic observations – CRU TS3.10: The Climatic Research Unit (CRU) Time Series (TS) Version 3.10 Dataset, *Int. J. Climatology, 34*(3), 623-642, doi: 10.1002/joc3711; updated from previous version of CRU TS3.xx

He, G., & Kammen, D. M. (2016). Where, when and how much solar is available? A provincial-scale solar resource assessment for China. *Renewable Energy, 85*, 74-82.

Helm, D. (2005). Economic instruments and environmental policy. *Economic and social review, 36*(3), 205-228.

Hofierka, J., & Kaňuk, J. (2009). Assessment of photovoltaic potential in urban areas using open-source solar radiation tools. *Renewable energy, 34*(10), 2206-2214.

HOMER (n.d.). HOMER pro 3.13. Capital recovery factor. https://www.homerenergy.com/products/pro/docs/latest/capital_recovery_factor.html

Hoogwijk, M. M. (2004). *On the global and regional potential of renewable energy sources* (Doctoral dissertation).

Hu, J. (2018). *Working Document: Cost supply curve and efficient portfolio for wind and PV development in Taiwan*.

Huang, Y. A., Weber, C. L., & Matthews, H. S. (2009). *Categorization of scope 3 emissions for streamlined enterprise carbon footprinting.*

Huang, Y. K., Luvsan, M. E., Gombojav, E., Ochir, C., Bulgan, J., & Chan, C. C. (2013). Land use patterns and SO2 and NO2 pollution in Ulaanbaatar, Mongolia. *Environmental research, 124*, 1-6.

International Energy Agency (2007). Mongolia renewable energy feed-in tariff. https://www.iea.org/policiesandmeasures/pams/mongolia/name-169879-en.php

International Energy Agency (2015). Mongolia State Policy on Energy 2015-2030. https://www.iea.org/policiesandmeasures/pams/mongolia/name-169880-en.php?s=dHlwZT1yZSZzdGF0dXM9T2s,&return=PG5hdiBpZD0iYnJlYWRjcnVtYiI-PGEgaHJlZj0iLyI-SG9tZTwvYT4gJnJhcXVvOyA8YSBocmVmPSIvcG9saWNpZXNhbmRtZWFzdXJlcy8iPlBvbGljaWVzIGFuZCBNZWFzdXJlczwvYT4gJnJhcXVvOyA8YSBocmVmPSIvcG9saWNpZXNhbmRtZWFzdXJlcy9yZW5ld2FibGVlbmVyZ3kvIj5SZW5ld2FibGUgRW5lcmd5PC9hPjwvbmF2Pg,,

International Energy Agency (2016a). *Extended Energy Balance 2016.*

International Energy Agency (2016b). *Indicators 2016.*

International Energy Agency (2016c) *World Energy Outlook 2016*. https://webstore.iea.org/world-energy-outlook-2016

International Energy Agency (2017a) *Renewable energy*. http://www.iea.org/about/faqs/renewableenergy/

International Energy Agency (2017b) *Scenarios and projections*. https://www.iea.org/publications/scenariosandprojections/

International Energy Agency ETSAP (2010). *Combined Heat and Power*. https://iea-etsap.org/E-TechDS/PDF/E04-CHP-GS-gct_ADfinal.pdf

International Futures (n.d.). *Country Profile Mongolia*. www.ifs.du.edu/ifs/frm_CountryProfile.aspx?Country=MN

International Monetary Fund (n.d.) *IMF DataMapper*. https://www.imf.org/external/datamapper/NGDP_RPCH@WEO/MNG

International Renewable Energy Agency (IRENA) (2012). *RENEWABLE ENERGY TECHNOLOGIES: COST ANALYSIS SERIES*. https://www.irena.org/documentdownloads/publications/re_technologies_cost_analysis-wind_power.pdf

IPCC (1996). *Revised 1996 IPCC Guidelines for National Greenhouse Gas Inventories: Workbook*.

IPCC (2006). *2006 IPCC guidelines for national greenhouse gas inventories* (Vol. 5). Hayama, Japan: Institute for Global Environmental Strategies.

IPCC (2011). Renewable energy sources and climate change mitigation: Special report of the intergovernmental panel on climate change. *Cambridge University Press.*

IPCC (2014a). *Chapter 7 Energy Systems. Climate Change 2014: Mitigation of Climate Change. Contribution of Working Group III to the Fifth Assessment Report of the Intergovernmental Panel on Climate Change.*

IPCC (2014b) *Chapter 2 Observations: Atmosphere and Surface. Climate Change 2014: the Physical Science Basis. Contribution of Working Group I to the Fifth Assessment Report of the Intergovernmental Panel on Climate Change*

Jerez, S., Thais, F., Tobin, I., Wild, M., Colette, A., Yiou, P., & Vautard, R. (2015). The CLIMIX model: a tool to create and evaluate spatially-resolved scenarios of photovoltaic and wind power development. *Renewable and sustainable energy reviews, 42*, 1-15.

JICA (2013). Japanese ODA Loan, Ex-ante evaluation. *Ulaanbaatar Thermal Power Plant No.4 Optimization Project*. https://www.jica.go.jp/english/our_work/evaluation/oda_loan/economic_cooperation/c8h0vm000001rdjt-att/mongolia_131115_01.pdf

Joint Crediting System (n.d.) *Additional information on calculating the conservative emission factor of Mongolia.* https://www.jcm.go.jp/mn-jp/methodologies/44/attached_document1

Kalashnikov, V., Gulidov, R., & Ognev, A. (2011). Energy sector of the Russian Far East: Current status and scenarios for the future. *Energy Policy, 39*(11), 6760-6780.

Kale, R. V., & Pohekar, S. D. (2014). Electricity demand and supply scenarios for Maharashtra (India) for 2030: An application of long range energy alternatives planning. *Energy Policy, 72*, 1-13.

Kamata, T., Reichert, J. A., Tsevegmid, T., Kim, Y., & Sedgewick, B. (2010). Mongolia: enhancing policies and practices for ger area development in Ulaanbaatar. *The World Bank: Washington, DC, USA*.

Kammen, D. M., & Sunter, D. A. (2016). City-integrated renewable energy for urban sustainability. *Science, 352*(6288), 922-928.

Kaygusuz, K. (2012). Energy for sustainable development: A case of developing countries. *Renewable and Sustainable Energy Reviews, 16*(2), 1116-1126.

Keohane, N. O., Revesz, R. L., & Stavins, R. N. (1998). The choice of regulatory instruments in environmental policy. *Harv. Envtl. L. Rev., 22*, 313.

Komoto, K., Enebish, N., & Song, J. (2013, June). Very large scale PV systems for North-East Asia: Preliminary project proposals for VLS-PV in the Mongolian Gobi desert. In Photovoltaic Specialists Conference (PVSC), 2013 *IEEE 39th* (pp. 2376-2379). IEEE.

Liodakis, E. G. (2011). The Nuclear Alternative: Energy Production within Ulaanbaatar, Mongolia. In *AIP Conference Proceedings* (Vol. 1342, No. 1, pp. 91-101). AIP.

Lkhagvadorj, I., & Tseesuren, B. (2005). Geothermal energy resources, present utilization and future developments in Mongolia. In *World Geothermal Congress* (WGC-2005), Antalya, Turkey (pp. 24-29).

Lund, H. (2007). Renewable energy strategies for sustainable development. *Energy, 32*(6), 912-919.

Luvsan, M. E., Shie, R. H., Purevdorj, T., Badarch, L., Baldorj, B., & Chan, C. C. (2012). The influence of emission sources and meteorological conditions on SO2 pollution in Mongolia. *Atmospheric Environment, 61*, 542-549.

Maatallah, T., El Alimi, S., & Nassrallah, S. B. (2011). Performance modeling and investigation of fixed, single and dual-axis tracking photovoltaic panel in Monastir city, Tunisia. *Renewable and Sustainable Energy Reviews, 15*(8), 4053-4066.

McPherson, M., & Karney, B. (2014). Long-term scenario alternatives and their implications: LEAP model application of Panama' s electricity sector. *Energy Policy, 68*, 146-157.

McPherson, M., Sotiropoulos-Michalakakos, T., Harvey, L. D., & Karney, B. (2017). An open-access web-based tool to access global, hourly wind and solar PV generation time-series derived from the MERRA reanalysis dataset. *Energies, 10*(7), 1007.

Millward-Hopkins, J. T., Tomlin, A. S., Ma, L., Ingham, D. B., & Pourkashanian, M. (2013). Assessing the potential of urban wind energy in a major UK city using an analytical model. Renewable energy, 60, 701-710.

Ministry of Energy (2005). *National Renewable Energy Program.* https://policy.asiapacificenergy.org/sites/default/files/National%20Renewable%20Energy%20Program%20%28EN%29.pdf

Ministry of Energy (2007). *Energy Law, Law of Mongolia*. http://energy.gov.mn/laws/show/id/203

Mondal, M. A. H., & Denich, M. (2010). Assessment of renewable energy resources potential for electricity generation in Bangladesh. *Renewable and Sustainable Energy Reviews, 14*(8), 2401-2413.

Mongolian Statistical Information Service (n.d.) http://www.1212.mn/

Mott Macdonald (n.d.). *Salkhit wind farm site, Mongolia*. https://www.mottmac.com/article/2321/salkhit-wind-farm-mongolia

NASA (n.d.). *How to calculate and plot wind speed using MERRA-2 wind component data using Python*. https://disc.gsfc.nasa.gov/information/howto?title=How%20to%20calculate%20and%20plot%20wind%20speed%20using%20MERRA-2%20wind%20component%20data%20using%20Python

National Statistical Office of Mongolia (2016). *2015 population and housing by-census of Mongolia: national report.*

Nie, S., Huang, C. Z., Huang, G. H., (2016). Planning renewable energy in electric power system for sustainable development under uncertainty–a case study of Beijing. *Applied energy, 162*, 772-786.

Nizami, A. S., Shahzad, K., Rehan, M., (2017). Developing waste biorefinery in Makkah: a way forward to convert urban waste into renewable energy. *Applied Energy, 186*, 189-196.

NREL (2016), *An Improved Global Wind Resource Estimate for Integrated Assessment Model*. https://www.nrel.gov/docs/fy17osti/65323.pdf

Pacca, S., & Horvath, A. (2002). Greenhouse gas emissions from building and operating electric power plants in the Upper Colorado River Basin. *Environmental Science & Technology, 36*(14), 3194-3200.

Painuly, J. P. (2001). Barriers to renewable energy penetration; a framework for analysis. *Renewable energy, 24*(1), 73-89.

Perwez, U., Sohail, A., Hassan, S. F., & Zia, U. (2015). The long-term forecast of Pakistan's electricity supply and demand: An application of long range energy alternatives planning. *Energy, 93*, 2423-2435.

Phdungsilp, A. (2010). Integrated energy and carbon modeling with a decision support system: Policy scenarios for low-carbon city development in Bangkok. *Energy Policy, 38*(9), 4808-4817.

Qu, Y., An, J., He, Y., & Zheng, J. (2016). An overview of emissions of SO2 and NOx and the long-range transport of oxidized sulfur and nitrogen pollutants in East Asia. *Journal of Environmental Sciences, 44*, 13-25.

Reich, N. H., Alsema, E. A., Van Sark, W. G. J. H. M., Turkenburg, W. C., & Sinke, W. C. (2011). Greenhouse gas emissions associated with photovoltaic electricity from crystalline silicon modules under various energy supply options. *Progress in Photovoltaics: Research and Applications, 19*(5), 603-613.

Reindl, D. T., Beckman, W. A., & Duffie, J. A. (1990). Evaluation of hourly tilted surface radiation models. *Solar energy, 45*(1), 9-17.

Renewable Energy World (2017). *Investors Keen to Support Mongolia's Renewable Energy Goals* by Gordon Feller. https://www.renewableenergyworld.com/articles/2017/12/investors-keen-to-support-mongolia-s-renewable-energy-goals.html#gref

RES Legal (2019). *Premium tariff (SDE+)* - Updated: 09.01.2019 - Author: Stijn Anciaux. http://www.res-legal.eu/search-by-country/netherlands/single/s/res-e/t/promotion/aid/premium-tariff-sde/lastp/171/

Ridley, B, Boland, J. and Lauret, P. (2010), Modelling of diffuse solar fraction with multiple predictors, *Renewable Energy 35* (2010): 478-483.

Runing, T. (2002). The possibility of houses supplied with renewable energy in cold clinate regions. *Acta Energiae Solaris Sinica*, 23, 340-343.

Ryu, H., Dorjragchaa, S., Kim, Y., & Kim, K. (2014). Electricity-generation mix considering energy security and carbon emission mitigation: Case of Korea and Mongolia. *Energy, 64*, 1071-1079.

Schoemaker, P. J. (1995). Scenario planning: a tool for strategic thinking. *Sloan management review, 36*(2), 25.

Shilendans (2015a) *Glass account information – UVS AIMAG THERMAL POWER PLANT # 2 IPO* http://www.shilendans.gov.mn/org/5895?form=2242548&year=2017&month=12&group=0&task=5870

Shilendans (2015b) *Glass account information – Thermal Power plant 3 state property committee*. http://www.shilendans.gov.mn/org/5184?form=123700&year=2016&month=12&group=0&task=500

Shilendans (2015c). *Glass account information – Thermal Power plant 4 state property committee*. https://www.shilendans.gov.mn/org/5185?form=2838248&year=2018&month=12&group=0&task=501

Slootweg, J. G., De Haan, S. W. H., Polinder, H., & Kling, W. L. (2003). General model for representing variable speed wind turbines in power system dynamics simulations. *IEEE Transactions on power systems, 18*(1), 144-151.

Sohn, B., Choi, J. H., & Min, K. C. (2015). Heating performance of geothermal heat pump system applied in cold climate region (Mongolia). *Korean Journal of Air-Conditioning and Refrigeration Engineering, 27*(1), 31-38.

Sovacool, B. K. (2012). Deploying off-grid technology to eradicate energy poverty. *Science, 338*(6103), 47-48.

Sovacool, B. K. (2012). Design principles for renewable energy programs in developing countries. *Energy & Environmental Science, 5*(11), 9157-9162.

Sovacool, B. K., & D'Agostino, A. L. (2012). A comparative analysis of solar home system programmes in China, Laos, Mongolia and Papua New Guinea. *Progress in Development Studies, 12*(4), 315-335.

Sovacool, B. K., & Dworkin, M. (2012). Overcoming the global injustices of energy poverty. *Environment: Science and Policy for Sustainable Development, 54*(5), 14-28.

Sovacool, B. K., D'Agostino, A. L., & Bambawale, M. J. (2011). Gers gone wired: lessons from the renewable energy and rural electricity access project (REAP) in Mongolia. *Energy for Sustainable Development, 15*(1), 32-40.

Sovacool, B., D'Agostino, A. L., & Bambawale, M. J. (2011). Gers just want to have fun: evaluating the renewable energy and Rural Electricity Access Project (REAP) in Mongolia. *Lee Kuan Yew School of Public Policy Energy Governance Case Study# 01*.

Statistical Department of Ulaanbaatar (SDU) (n.d.). http://ubstat.mn/JobTables.aspx

Sterner, T., & Coria, J. (2013). *Policy instruments for environmental and natural resource management*. Routledge.

Sumiya, B. (2016). Energy poverty in context of climate change: What are the possible impacts of improved modern energy access on adaptation capacity of communities?. *International Journal of Environmental Science and Development, 7*(1), 73.

Sun, R., Zhang, T., & Liang, J. (2011). Evaluation and application of wind power integration capacity in power grid. Dianli Xitong Zidonghua. *Automation of Electric Power Systems, 35*(4), 70-76.

TACC (2018). *The cost of electricity in Moscow will rise from January 1, 2019*. https://tass.ru/moskva/5928047

The Wind Power (n.d.). Online Access. https://www.thewindpower.net/windfarm_en_15972_salkhit.php

Toshiki, K., Giang, P. Q., Serrona, K. R. B., Sekikawa, T., Yu, J. S., Choijil, B., & Kunikane, S. (2015). Effects of introducing energy recovery processes to the municipal solid waste management system in Ulaanbaatar, Mongolia. *Journal of Environmental Sciences, 28*, 178-186.

UNEP (2009). *World Database on Protected Areas (WDPA).* Annual release.

United Nations (2017a) *The Sustainable Development Goals Report 2017*

United Nations (2017b) *World Population Prospects. The 2017 Revision, Volume 1: Comprehensive Tables. Department of Economic and Social Affairs – Population Division*. New York, 2017. https://population.un.org/wpp/Publications/Files/WPP2017_Volume-I_Comprehensive-Tables.pdf

United Nations Framework Convention on Climate Change (2018). *Third National Communication of Mongolia.* https://www4.unfccc.int/sites/SubmissionsStaging/NationalReports/Documents/06593841_Mongolia-NC3-2-Mongolia%20TNC%202018%20print%20version.pdf

United Nations Framework Convention on Climate Change (2017). CDM-MR-FORM - *Monitoring report form (Version 05.1).* www.koreacdm.com

United States Environmental Protection Agency (n.d). *Particulate Matter (PM) Basics*. https://www.epa.gov/pm-pollution/particulate-matter-pm-basics#PM

University of Oxford (2018). *The development of natural gas demand in the Russian electricity and heat sectors.* https://www.oxfordenergy.org/wpcms/wp-content/uploads/2018/08/The-Development-of-Natural-Gas-Demand-in-the-Russian-Electricity-and-Heat-Sector-NG-136.pdf

UNPD (2017) *World population prospects 2017.* https://esa.un.org/unpd/wpp/Graphs/Probabilistic/POP/TOT/

Urmee, T., Harries, D., & Schlapfer, A. (2009). Issues related to rural electrification using renewable energy in developing countries of Asia and Pacific. *Renewable Energy, 34*(2), 354-357.

van der Wiel, K., Stoop, L.P., van Zuijlen, B.R.H., (2019). Meteorological conditions leading to extreme low variable renewable energy production and extreme high energy shortfall. *Renewable and Sustainable Energy Reviews, 111*, (pp. 261-275) (15 p.).

Verbruggen, A., Dewallef, P., Quoilin, S., & Wiggin, M. (2013). Unveiling the mystery of Combined Heat & Power (cogeneration). *Energy, 61*, 575-582.

Verschuren, P., Doorewaard, H., & Mellion, M. J. (2010). Designing a research project (Vol. 2). *The Hague: Eleven International publishing house*.

Weisser, D. (2007). A guide to life-cycle greenhouse gas (GHG) emissions from electric supply technologies. *Energy, 32*(9), 1543-1559.

Wind Power Program (n.d.). *14. Wind turbine power ouput variation with steady wind speed.* http://www.wind-power-program.com/turbine_characteristics.htm

Winkler, H., Borchers, M., Hughes, A., Visagie, E., & Heinrich, G. (2017). Policies and scenarios for Cape Town's energy future: Options for sustainable city energy development. *Journal of Energy in Southern Africa, 17*(1), 28-41.

World Bank (2017). *Global economic prospects.* http://data.worldbank.org/data-catalog/global-economic-prospects

World Bank (2017): *Indicators (population, CO2 emission, land-surface area).* https://data.worldbank.org/indicator

World Bank (n.d.). *Total greenhouse gas emissions (kt of CO2 equivalent*). https://data.worldbank.org/indicator/EN.ATM.GHGT.KT.CE?locations=MN

World Energy Resource Atlas of Mongolia (2001). *National Renewable Energy Laboratory*.

Worldbank (2017). *The World Bank, Solar resource data: Solargis.* https://solargis.com/maps-and-gis-data/download/mongolia/

Yang, D. (2016). Solar radiation on inclined surfaces: Corrections and benchmarks. *Solar Energy, 136*, 288-302.

Yu, S., Wei, Y. M., Guo, H., & Ding, L. (2014). Carbon emission coefficient measurement of the coal-to-power energy chain in China. *Applied Energy, 114*, 290-300.

Zhuang, J., Liang, Z., Lin, T., & De Guzman, F. (2007). Theory and practice in the choice of social discount rate for cost-benefit analysis: a survey (No. 94). *ERD working paper series*.

# 11. Acknowledgments

I have been writing this thesis for the better part of a year – with some breaks in between – and I feel fulfilled now that it has come to an end. I would like to thank my supervisor Wina Graus for supporting me during the design, research and completion phase. I could not have done this without her!

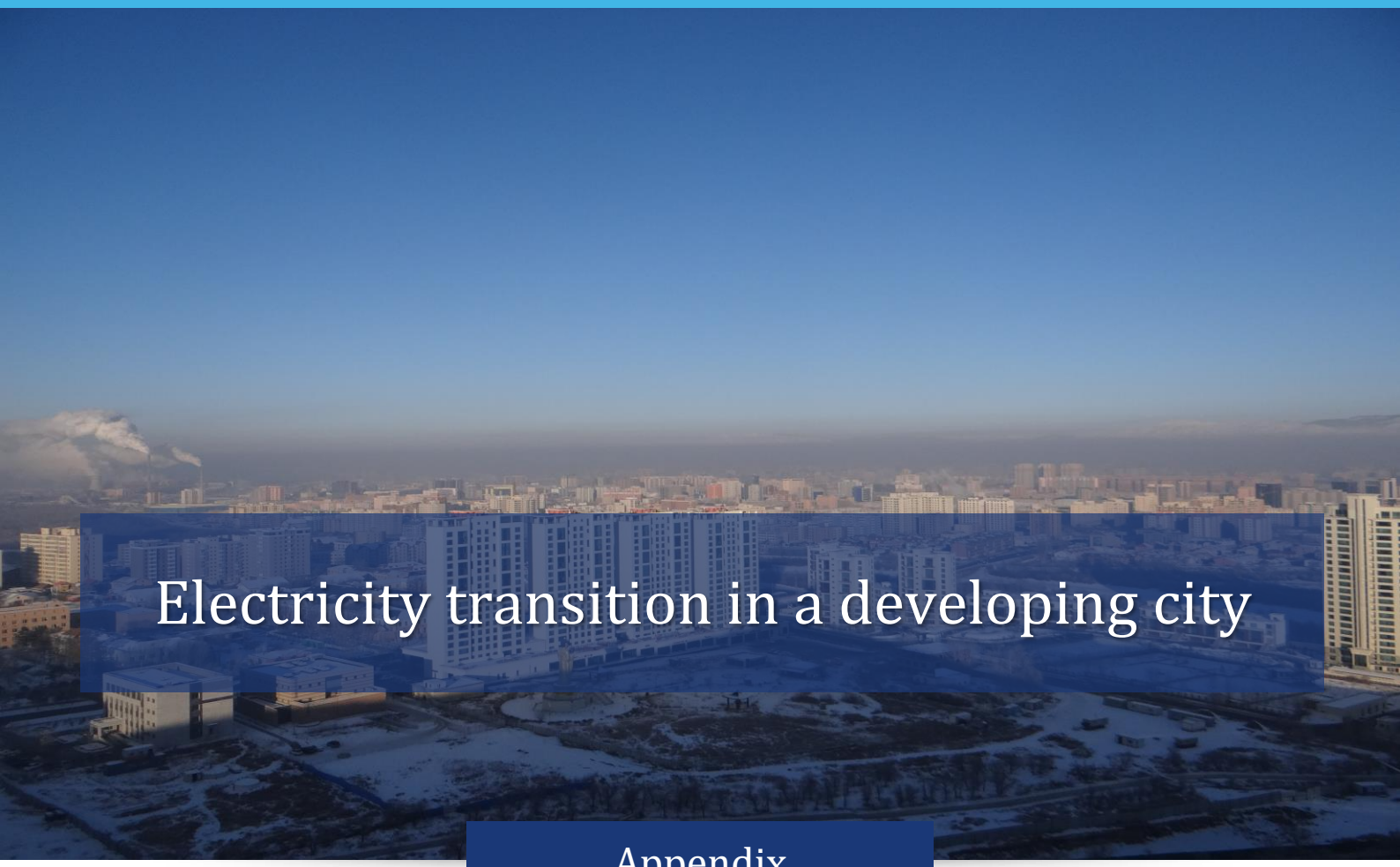

# Electricity transition in a developing city

## Appendix

## Appendix I: Supplementing table

Universiteit Utrecht

## Detailed scenario comparison

| | | 2010 | 2011 | 2012 | 2013 | 2014 | 2015 | 2016 | 2017 | 2018 | 2019 | 2020 | 2021 | 2022 | 2023 | 2024 | 2025 | 2026 | 2027 | 2028 | 2029 | 2030 |
|---|---|---|---|---|---|---|---|---|---|---|---|---|---|---|---|---|---|---|---|---|---|---|
| Direct GHG | **BAU** | 1226 | 1551 | 1882 | 2182 | 2460 | 2622 | 2799 | 2806 | 2920 | 3140 | 3583 | 3761 | 3908 | 4067 | 4252 | 4406 | 4527 | 4713 | 4913 | 5129 | 5361 |
| | **GREEN** | 1226 | 1551 | 1882 | 2182 | 2460 | 2622 | 2799 | 2806 | 2920 | 3140 | 1363 | 1415 | 1470 | 1530 | 1600 | 1661 | 1726 | 1797 | 1874 | 1956 | 2044 |
| | **Difference** | 0 | 0 | 0 | 0 | 0 | 0 | 0 | 0 | 0 | 0 | -2220 | -2346 | -2438 | -2537 | -2653 | -2745 | -2801 | -2916 | -3039 | -3173 | -3316 |
| | | | | | | | | | | | | | | | | | | | | | | |
| Indirect GHG | **BAU** | 50 | 63 | 98 | 116 | 133 | 142 | 152 | 152 | 158 | 166 | 1 | 1 | 1 | 1 | 1 | 1 | 1 | 1 | 1 | 1 | 1 |
| | **GREEN** | 50 | 63 | 98 | 116 | 133 | 142 | 152 | 152 | 158 | 192 | 151 | 156 | 162 | 169 | 177 | 184 | 191 | 199 | 207 | 216 | 226 |
| | | 0 | 0 | 0 | 0 | 0 | 0 | 0 | 0 | 0 | 25 | 150 | 156 | 162 | 169 | 176 | 183 | 190 | 198 | 207 | 216 | 225 |
| | | | | | | | | | | | | | | | | | | | | | | |
| Total emissions | **BAU** | 1276 | 1613 | 1980 | 2298 | 2593 | 2764 | 2951 | 2958 | 3078 | 3307 | 3583 | 3762 | 3908 | 4068 | 4253 | 4406 | 4528 | 4714 | 4914 | 5129 | 5361 |
| | **GREEN** | 1276 | 1613 | 1980 | 2298 | 2593 | 2764 | 2951 | 2958 | 3078 | 3332 | 1514 | 1571 | 1632 | 1699 | 1776 | 1845 | 1917 | 1996 | 2081 | 2172 | 2270 |
| | | 0 | 0 | 0 | 0 | 0 | 0 | 0 | 0 | 0 | 25 | -2070 | -2191 | -2276 | -2369 | -2477 | -2562 | -2610 | -2718 | -2833 | -2957 | -3091 |
| | | | | | | | | | | | | | | | | | | | | | | |
| Cumulative emissions | **BAU** | 1276 | 2889 | 4869 | 7166 | 9760 | 12524 | 15475 | 18432 | 21511 | 24817 | 28401 | 32163 | 36071 | 40138 | 44391 | 48798 | 53325 | 58039 | 62953 | 68082 | 73443 |
| | **GREEN** | 1276 | 2889 | 4869 | 7166 | 9760 | 12524 | 15475 | 18432 | 21511 | 24843 | 26356 | 27928 | 29560 | 31259 | 33035 | 34880 | 36798 | 38794 | 40874 | 43046 | 45317 |
| | | 0 | 0 | 0 | 0 | 0 | 0 | 0 | 0 | 0 | 25 | -2044 | -4235 | -6511 | -8879 | -11356 | -13918 | -16528 | -19246 | -22078 | -25036 | -28127 |
| | | | | | | | | | | | | | | | | | | | | | | |
| GHG intensity | **BAU** | 886 | 886 | 895 | 884 | 869 | 871 | 871 | 871 | 871 | 888 | 845 | 854 | 854 | 854 | 854 | 852 | 843 | 843 | 843 | 843 | 843 |
| | **GREEN** | 886 | 886 | 895 | 884 | 869 | 871 | 871 | 871 | 871 | 895 | 357 | 357 | 357 | 357 | 357 | 357 | 357 | 357 | 357 | 357 | 357 |
| | | 0 | 0 | 0 | 0 | 0 | 0 | 0 | 0 | 0 | 7 | -488 | -498 | -498 | -498 | -498 | -496 | -486 | -486 | -486 | -486 | -486 |
| | | | | | | | | | | | | | | | | | | | | | | |
| Investment | **BAU** | 122 | 0 | 0 | 0 | 0 | 45 | 0 | 0 | 0 | 0.08 | 0 | 3500 | 0 | 0 | 0 | 0 | 0 | 0 | 0 | 0 | 0 |
| | **GREEN** | 122 | 0 | 0 | 0 | 0 | 45 | 0 | 0 | 0 | 4424 | 0 | 0 | 0 | 0 | 0 | 0 | 0 | 0 | 0 | 0 | 0 |

| | | | | | | | | | | | | | | | | | | | | | |
|---|---|---|---|---|---|---|---|---|---|---|---|---|---|---|---|---|---|---|---|---|---|
| | | 0 | 0 | 0 | 0 | 0 | 0 | 0 | 0 | 0 | 4424 | 0 | -3500 | 0 | 0 | 0 | 0 | 0 | 0 | 0 | 0 | 0 |
| | | | | | | | | | | | | | | | | | | | | | | |
| O&M | **BAU** | 39 | 39 | 39 | 40 | 40 | 38 | 38 | 38 | 43 | 45 | 45 | 54 | 54 | 54 | 54 | 64 | 52 | 52 | 52 | 52 | 52 |
| | **GREEN** | 39 | 39 | 39 | 40 | 40 | 38 | 38 | 38 | 43 | 94 | 98 | 99 | 99 | 100 | 101 | 101 | 102 | 102 | 103 | 104 | 105 |
| | | 0 | 0 | 0 | 0 | 0 | 0 | 0 | 0 | 0 | 49 | 53 | 44 | 45 | 45 | 46 | 38 | 49 | 50 | 51 | 52 | 52 |
| | | | | | | | | | | | | | | | | | | | | | | |
| Fuel | **BAU** | 28 | 36 | 43 | 50 | 56 | 60 | 64 | 64 | 67 | 72 | 82 | 85 | 88 | 91 | 96 | 99 | 102 | 106 | 110 | 115 | 120 |
| | **GREEN** | 28 | 36 | 43 | 50 | 56 | 60 | 64 | 64 | 67 | 72 | 31 | 32 | 34 | 35 | 37 | 38 | 40 | 41 | 43 | 45 | 47 |
| | | 0 | 0 | 0 | 0 | 0 | 0 | 0 | 0 | 0 | 0 | -51 | -52 | -54 | -56 | -59 | -61 | -62 | -64 | -67 | -70 | -73 |
| | | | | | | | | | | | | | | | | | | | | | | |
| Total costs | **BAU** | 197 | 84 | 97 | 108 | 117 | 165 | 126 | 126 | 135 | 143 | 128 | 3639 | 142 | 146 | 150 | 163 | 154 | 158 | 163 | 167 | 173 |
| | **GREEN** | 197 | 84 | 97 | 108 | 117 | 165 | 126 | 126 | 135 | 4617 | 135 | 137 | 139 | 141 | 144 | 146 | 148 | 151 | 154 | 157 | 160 |
| | | 0 | 0 | 0 | 0 | 0 | 0 | 0 | 0 | 0 | 4473 | 8 | -3502 | -3 | -5 | -6 | -17 | -6 | -7 | -9 | -11 | -13 |
| | | | | | | | | | | | | | | | | | | | | | | |
| Cumulative | **BAU** | 197 | 281 | 378 | 486 | 603 | 768 | 894 | 1021 | 1155 | 1299 | 1426 | 5065 | 5207 | 5353 | 5503 | 5666 | 5820 | 5978 | 6140 | 6308 | 6480 |
| | **GREEN** | 197 | 281 | 378 | 486 | 603 | 768 | 894 | 1021 | 1155 | 5772 | 5907 | 6044 | 6183 | 6324 | 6468 | 6614 | 6762 | 6913 | 7067 | 7223 | 7383 |
| | | 0 | 0 | 0 | 0 | 0 | 0 | 0 | 0 | 0 | 4473 | 4481 | 979 | 976 | 971 | 965 | 948 | 942 | 935 | 926 | 916 | 903 |
| | | | | | | | | | | | | | | | | | | | | | | |
| LCOE | **BAU** | 0.03 | 0.03 | 0.03 | 0.03 | 0.03 | 0.03 | 0.03 | 0.03 | 0.03 | 0.03 | 0.03 | 0.06 | 0.06 | 0.06 | 0.06 | 0.06 | 0.06 | 0.06 | 0.06 | 0.06 | 0.056 |
| | **GREEN** | 0.03 | 0.03 | 0.03 | 0.03 | 0.03 | 0.03 | 0.03 | 0.03 | 0.03 | 0.12 | 0.11 | 0.11 | 0.10 | 0.10 | 0.10 | 0.09 | 0.09 | 0.09 | 0.08 | 0.08 | 0.078 |
| | | 0.00 | 0.00 | 0.00 | 0.00 | 0.00 | 0.00 | 0.00 | 0.00 | 0.00 | 0.09 | 0.08 | 0.04 | 0.04 | 0.04 | 0.03 | 0.03 | 0.03 | 0.03 | 0.03 | 0.02 | 0.0216 |